THE UNIVERSITY OF CALGARY

A SMALL GAS TURBINE EQUIPPED WITH A SECOND GENERATION PULSE COMBUSTOR

BY

MATTHEW J. O'BLENES

A THESIS

SUBMITTED TO THE FACULTY OF GRADUATE STUDIES

IN PARTIAL FULFILLMENT OF THE REQUIREMENTS FOR THE

DEGREE OF MASTER OF SCIENCE

DEPARTMENT OF MECHANICAL ENGINEERING

CALGARY, ALBERTA

MARCH, 1987

ISBN 0-315-36013-5

THE UNIVERSITY OF CALGARY

FACULTY OF GRADUATE STUDIES

The undersigned certify that they have read, and recommend to the Faculty of Graduate Studies for acceptance, a thesis entitled "A Small Gas Turbine Equipped with a Second Generation Pulse Combustor", submitted by Matthew J. O'Blenes in partial fulfillment of the requirements for the degree of Master of Science.

J. A. C. Kentfield.

Dr. J.A.C. Kentfield, Supervisor
Department of Mechanical Engineering

Richard D. Rowe

Dr. R.D. Rowe
Department of Mechanical Engineering

I. Wierzba

Dr. I. Wierzba
Department of Mechanical Engineering

P. R. Bishnoi

Dr. P.R. Bishnoi
Department of Chemical and Petroleum Engineering

March 19, 1987

ABSTRACT

The work described in this report concerns the application of pulse combustion to a gas turbine cycle. A laboratory gas turbine was operated with an unsteady-flow pulse-combustion chamber substituted for a conventional, steady flow, combustion chamber. This work is the logical continuation of, what is believed to be, the first practical application of a valveless pulse combustor to a gas turbine.

A pulse combustor produces a net stagnation pressure gain across itself, whereas a conventional combustor produces a stagnation pressure loss. The expected benefits of this pressure gain, for the gas turbine cycle, provides the incentive for such work.

Earlier work has shown that a pulse combustor is capable of self sustaining operation as part of a gas turbine, while producing such a pressure gain. The present work consisted of the development of the pulse combustion system for this gas turbine. This required the redesign and resizing of the combustor components, followed by the construction of a new unit to be operated on the gas turbine. The main goals of this redesign were to address excessive energy loss characteristics of the combustion system used in the earlier work and to establish a more optimally dimensioned unit. This new unit is referred to as the Second Generation Pulse Combustion System.

The results show that the second generation system provides superior performance to that of the "first application" system. The combustor pressure gain was more than doubled and the fuel consumption was reduced by roughly 20%. The present system can now provide a gas

generator performance that is superior, over the majority of the operating range, to that produced by the conventional combustor it replaces.

It is suggested in future work that the second generation system be fine tuned for optimum performance. This can be carried out by adjusting physical parameters to which the system appears to be sensitive. To improve component durability, specific design changes are suggested. Also, the use of better instrumentation is recommended for the gas turbine unit. This will allow a more comprehensive comparison to be carried out between pulse and conventional combustion, as applied to a gas turbine. Such work will help to show how the benefits of pulse combustion can be best utilized for the gas turbine cycle.

ACKNOWLEDGEMENTS

The author sincerely thanks his supervisor, Dr. J.A.C. Kentfield, for the expert assistance and guidance provided in carrying out the work reported here.

Appreciation is extended to the technicians involved in the construction and experimentation. The guidance of R. Gustafson, instrumentation skills of A. Moehrle, and the drafting work of N. Vogt contributed greatly to this work. A special thanks goes to B. Crews who carried out component fabrication and helped to provide many practical design solutions. The author would also like to thank Miss W. Gebert for her assistance in typing this report.

Funding for this research has been generously provided by the Natural Sciences and Engineering Research Council of Canada in the form of operating grant A-7928 made available to the project supervisor.

TABLE OF CONTENTS

PAGE

LIST OF FIGURES

LIST OF TABLES

NOMENCLATURE

SYMBOL	DEFINITION
$\dot{m}$	Mass flow rate
N	Turbine rotor speed
P	Pressure
ΔP	Change in pressure
T	Temperature
X	Distance between ejector opening and combustor inlet
Y	Secondary flow duct extension
η	Gas generator performance
CC	Conventional Combustor
FGPC	First Generation Pulse Combustor
SGPC	Second Generation Pulse Combustor
ISGPC	Insulated Second Generation Pulse Combustor

SUBSCRIPTS

1,2,3,4	Stations within the gas turbine (figures 2.2, 5.6 & 5.7)
a	Air
amb	Ambient conditions
cc	Conventional combustor
f	Fuel
in	Inlet
max	Maximum
o	Stagnation condition
out	Outlet
pc	Second generation pulse combustor

This thesis is dedicated to my Father as an expression of my respect and gratitude

1. INTRODUCTION

1.1 BACKGROUND

The name "Pulse Combustor" is descriptive of the operational characteristics of such a device. Pulse combustors operate internally in a non-steady manner and can be arranged to produce a quasi-steady gas inflow and outflow.

Such devices have been considered for numerous applications for nearly a century. Several units have been described in the work of Marzouk [13], Cronje [4], Yerneni [19], and Olorunmaiye [14], to name a few. Pulse combustors exist essentially in one of two categories; valved and valveless types. Perhaps the most well known example of a pulse combustor is that used to propel the V-1 flying bomb (known as the "Buzz Bomb") during World War II; this engine was of the valved type and is illustrated in figure 1.1.

The application of particular interest in this work is that of pulse combustion within the gas turbine cycle. A considerable amount of theoretical and experimental work has been carried out in the past decade, by Kentfield [7,8,9,10,11] and associates, concerning this application. This work has concentrated on developing valveless type pulse combustion devices with the purpose of improving their performance and versatility, and the ultimate aim of application. Development has been carried out on a numerical simulation of pulse combustor operation [4,13,14,16,17] using a technique called the "Method of Characteristics", which is applied to conservation equations. The dynamic coupling of combustors was carried out with the aim of reducing

noise levels and overall size [15,18]. Investigations have been made demonstrating the ability of a pulse combustor to operate using various fuels [6,16]. With respect to the present study, the development of a fluidic device called a "thrust augmenter flow rectifier" [4,7,13] and the work carried out by Yerneni [19] in the practical application of pulse combustion to a gas turbine, are of special importance.

Valveless pulse combustors have also been developed by others as explained in the work of Olorunmaiye [14] and Cronje [4]. Of special interest is the work carried out by the joint efforts of the SNECMA Engine Company of France and the Hiller Aircraft Corporation (US) during the 1950's and 60's [4,12]. The valveless pulse combustor used in the present investigation is based on a unit developed by Lockwood [12] from a SNECMA configuration. The valveless pulse combustor has the advantage, over that of the valved type, in that it contains no moving parts. Lockwood discusses both types and points out that the high pressure (up to 4 bar internal pressure) valved combustors have a short valve life.

Figure 1.2 (extracted from reference 19) shows how the unsteady operation of a valveless pulse combustor takes place. This combustor operates in a cyclic fashion. First, there is ignition of an air fuel mixture. This sends pressure waves, along with expanding combustion products, toward the open ends of the inlet and tail pipe. The waves reflect at both ends resulting in a negative pressure inside the combustor. A wave reflects at the inlet end first, since the inlet pipe is shorter than the tailpipe, and a fresh air charge is drawn in. At

the same time the negative pressure allows fuel to enter via injection nozzles. A recompression wave from the tail pipe end then arrives back at the combustion chamber along with a portion of the exhaust gases present in the exhaust pipe, combustion occures again, and the cycle is repeated. The result is a "pumping" effect that produces a net flow of gases from the inlet to the tailpipe outlet, driven by combustion energy. This gas movement results in a higher average stagnation pressure at the outlet than at the inlet. Boundary conditions dictate that the inlet stagnation pressure is equal to the atmospheric pressure. This is a self sustaining cycle. A separate ignition source is necessary only during start up. Subsequent ignition is due to residual combustion products from the previous cycle.

Although pulse combustion is not used extensively in commercial applications, there are some modern examples of its use in central and portable air heating, and water heating. Lennox markets a home heating unit called the "Lennox Pulse Furnace", which it claims (in agreement with the Canadian Gas Association) to be substantially more efficient than conventional models. Lockwood [12] tested a pulse driven water heater in the early 1960's which was developed and used to a limited degree in Canada. He confirmed a claimed 95% energy efficiency, which was considerably higher then that of more commonly used, steady flow units. Both the furnace and water heater application used a valved type pulse combustor. Problems with valve durability, mentioned earlier, are not significant since these units operate under modest load conditions [1,12].

One reason for the sparse commercial application may be that of certain understanding barriers of pulse combustion. Lockwood [12]

points out that the fluid dynamics is very difficult to analyze and model, and that the most widely used fundamentals in fluid dynamics relate to steady flow.

In practice, noise levels associated with unsteady flows are a problem affecting application. Adams [1], who reported the results of field trials of the Lennox Pulse Furnace, discusses the fact that sound levels are higher than those of steady flow furnaces. He states that this could be a determining factor on its marketplace success. In the prior application of pulse combustion to a gas turbine [19], noise levels were also found to be higher then those for a comparable steady flow system.

1.2 PULSE COMBUSTION AS APPLIED TO A GAS TURBINE

1.2.1 Incentive for Application

As stated above, a pulse combustor is capable of producing a net stagnation pressure gain across itself. Figure 1.3 (extracted from reference 19) shows, in a qualitative way, how pressure gain heat addition would affect the gas turbine cycle. Heat addition, with pressure loss, which occures in steady flow combustors, is shown in this temperature-entropy diagram for comparison. There is a greater turbine temperature drop, and hence a greater work output, for the pressure gain case. Yerneni [19] derives, from simple theory, an expression for thermal efficiency, and shows how this efficiency is affected by a pressure gain or loss. Figure 1.4, taken from this work, shows the effects for a given turbine-inlet temperature ratio. His results also show that the advantages of pressure gain are greatest for low cycle-temperature ratios.

1.2.2 First Application of a Valveless Pulse Combustor to a Gas Turbine

What is believed to be the first practical application of Pulse Combustion to a gas turbine cycle was carried out in the recent work by Yerneni [19]. The pulse combustor used in his work is that of the valveless type referred to in section 1.1. This unit is described in detail in section 2.1.1. With the use of an additional plenum, the combustor was attached to a laboratory compressor-turbine gas generator unit in place of a conventional steady flow combustion chamber. The pulse combustor and attachments, described by Yerneni [19], will be referred to as the First Generation Pulse Combustion System in this report. This unit operated as part of the gas turbine with self sustaining combustion, and produced a slight (less than 1%) stagnation pressure gain. The test results showed that this application, for a given load, resulted in an approximately 30% greater fuel consumption than the same engine when equiped with the conventional combustor. This difference in performance was attributed mainly to the crude pulse combustor plenum design features, which allowed large heat losses to occur to the ambient. It was suggested that for future work design changes be made to address this problem.

1.3 OBJECTIVES OF STUDY

The overall objective of the present study is to continue the practical work carried out by Yerneni [19], with the aim of obtaining a substantial improvement in performance over that of the crude first

application. To meet this objective the following was to be carried out:

1. Design and construct a new pulse combustion system that had lower energy losses than the first generation system. The new design was to be based on a second generation system which was conceptually described by Yerneni [19] and is shown in figure 3.1.

2. Choose a pulse combustor size that better matches the existing compressor-turbine unit. The pulse combustor used in the first generation system was believed to be too large.

3. Operate the new combustion system as part of the gas turbine. Make comparisons of gas turbine performance for this case with those of two other cases: the first generation pulse combustor and the conventional combustor applications.

1.4 ORGANIZATION OF THE TEXT

Chapter 2 of this presentation is concerned with the first application of pulse combustion to the gas turbine cycle [19]. This is intended to familarize the reader briefly with the features of the system and how well it performed. It helps to explain why the system was developed in the way shown in chapter 3, which describes the design process for the second generation system.

Chapter 4 presents the physical design features of this new system, in which the geometric flexibility of the configuration was seen as an important advantage compared with a geometrically inflexible design.

Chapter 5 covers the experimental system operation. The performance parameters are listed and descriptions of the proceedures, apparatus and

operational problems are provided. In addition, changes in configuration, which were carried out during the course of the test work, are described and justified.

Chapter 6 contains the results, analysis and discussion. Performance comparisons between conventional combustion and pulse combustion, as applied to a gas turbine, are also presented. Explanations of behaviour traits are given where applicable.

Finally, in chapter 7, conclusions are presented from the overall results, and recommendations for future work are listed.

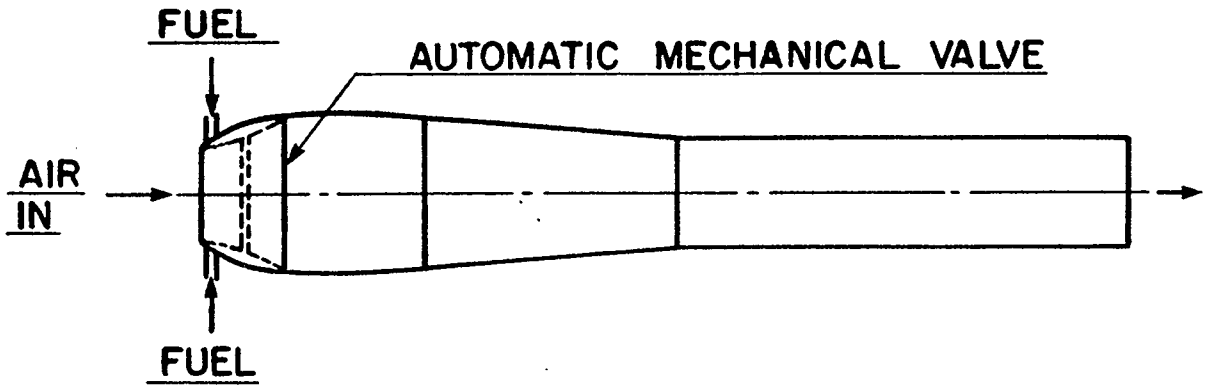

FIGURE 1.1 V-1 SCHMIDT PULSE JET [19]

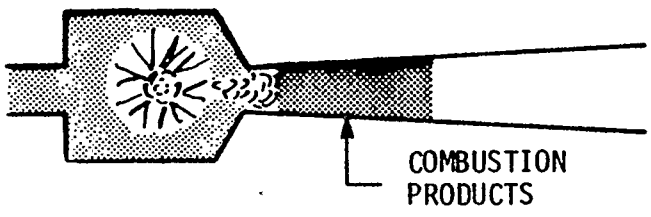

1. IGNITION AND COMBUSTION

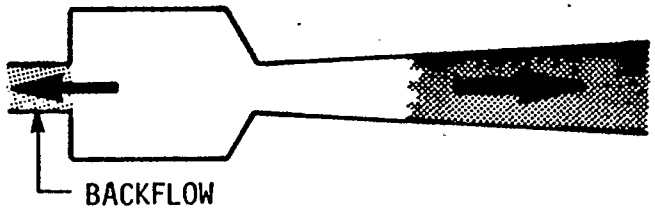

2. EXPANSION

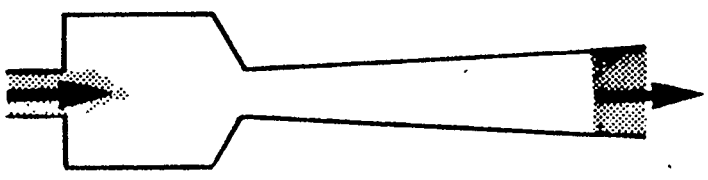

3. PURGE AND RECHARGE

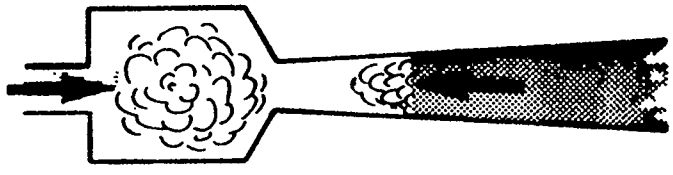

4. RECHARGE AND CHARGE COMPRESSION

FIGURE 1.2 **PHASES OF OPERATION OF A RESONANT COMBUSTOR [19]**

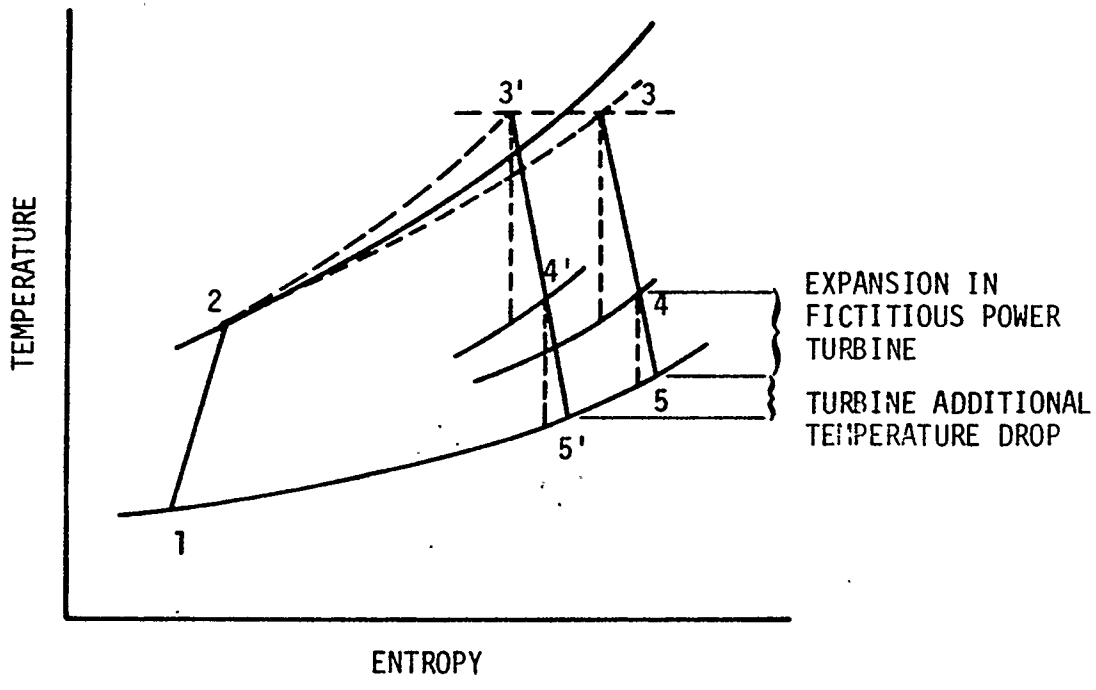

FIGURE 1.3 ADVANTAGE OF COMBUSTION DRIVEN PRESSURE-GAIN (DIAGRAMMATIC)[19]

CYCLE 1-2-3-4-5 : PRESSURE LOSS DURING HEAT-ADDITION
CYCLE 1-2-3'-4'-5' : PRESSURE GAIN DURING HEAT-ADDITION

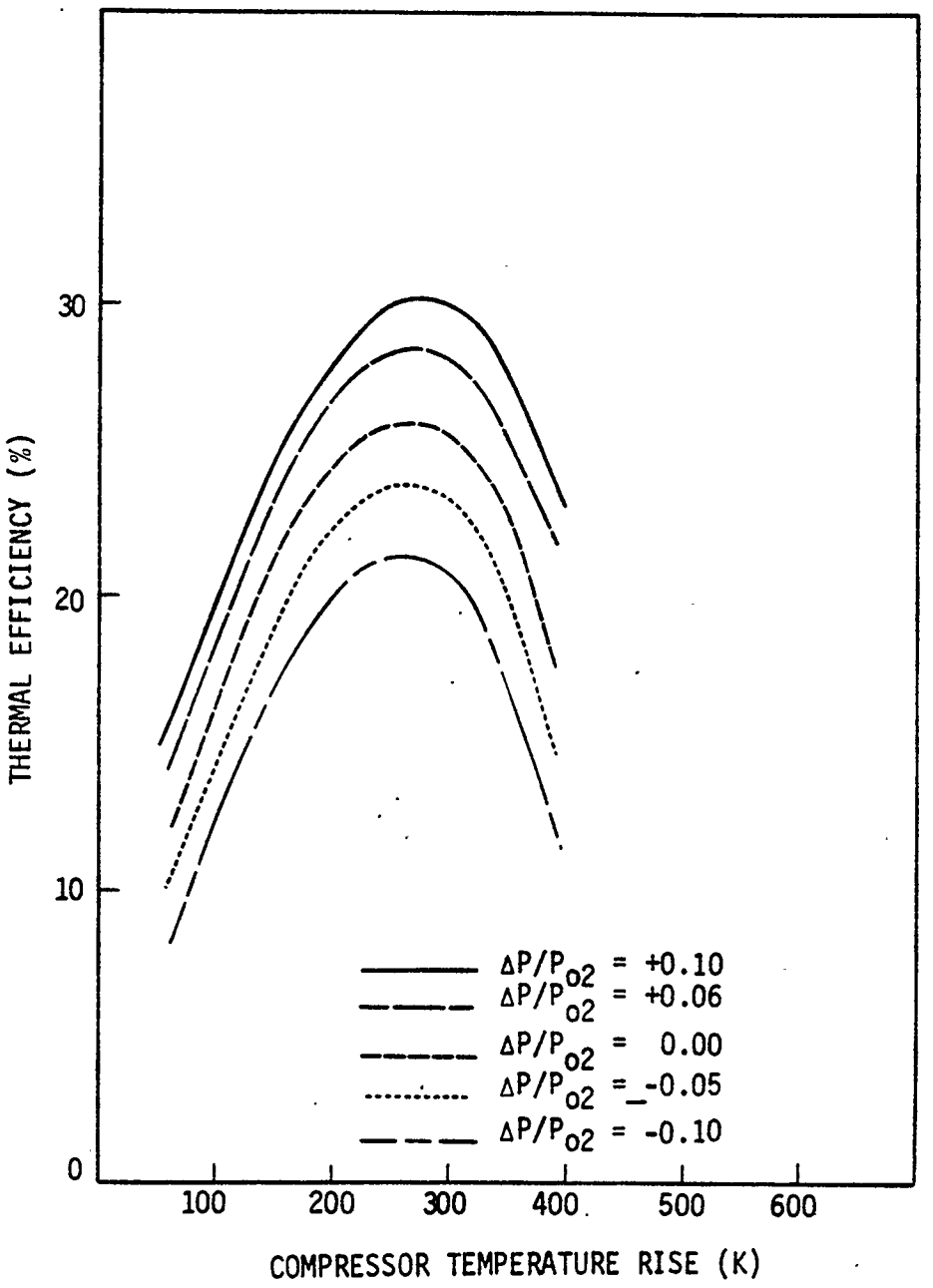

FIGURE 1.4 EFFECT OF COMBUSTOR PRESSURE LOSS/GAIN ON THERMAL EFFICIENCY OF GAS TURBINE CYCLE AT 900 K TURBINE INLET TEMPERATURE AND 288 K COMPRESSOR INLET TEMPERATURE (TURBINE ISENTROPIC EFFECIENCY = COMPRESSOR ISENTROPIC EFFICIENCY = 85%, MECHANICAL EFFECIENCY = 98%) [19]

CHAPTER 2

FAMILIARIZATION WITH THE FIRST GENERATION SYSTEM

2.1 FEATURES OF THE SYSTEM

2.1.1 The HILLER HH-M1 Type Valveless Pulse Combustor

Figure 2.1 displays a detailed drawing of the model Hiller HH-M1 type valveless pulse combustor used within the First Generation Pulse Combustion System which was operated by Yerneni [19] as part of a gas turbine cycle. A sketch of this gas turbine setup is shown in figure 2.2. This system, which was used in place of a conventional combustor, consists of the basic pulse combustor with an air inlet plenum, a rectifier, secondary flow ducts and an outlet combining chamber added to allow connection to the turbo-machine. The sketch in figure 2.3 [10] displays the rectifier and secondary flow ducts in another view. The purpose of this secondary flow system is to redirect combustion gases that flow out of the pulse combustor inlet to the combining zone at the tailpipe exhaust, during the expansion part of the combustor cycle (figure 1.2). This zone is connected directly to the turbine inlet. Note that the air inlet plenum, shown again in figure 2.4, isolates the air inlet zone from the ambient. This allows the compressor outlet air to be received and, after passing through the combustion system, flow through the turbine.

2.1.2 The Cussons Gas Generator Unit

The radial flow compressor and turbine unit which was connected to the First Generation Pulse Combustor, was that of the Cussons P9000 laboratory gas generator. The "original equipment" steady flow

combustor, shown in figure 5.7 (section 5), was replaced by Yerneni with the pulse combustion system previously described [19]. Much of the original instrumentation was retained. A detailed description of the test rig is given in reference 19.

2.2 REVIEW TESTS MADE BY AUTHOR

2.2.1 Comparison of New Data with Previous Work

The gas generator unit, with the pulse combustion system attached, was operated by the author. The setup was left unchanged from that used by Yerneni; only necessary mechanical repairs were made. This work allowed the author to become familiar with the operation of this unit, and to check that all of the associated equipment was working properly before further development was to be carried out.

An important measure of performance is the fuel consumption. Figure 2.5 compares this consumption found by the author to that reported by Yerneni for the back pressure 0 load setting over the turbine rotor speed range. "Back pressure 0" means that the butterfly valve located in the turbine exhaust duct, as shown in figure 5.7, was left open. This implies that the only back pressure imposed on the turbine was due to exhaust duct inherent pressure losses (including the kinetic component, since no exhaust diffuser was provided). The fuel flow was roughly 10% higher for the most recent tests. Figure 2.6 shows that the air consumption was also greater, in this case, by about 5%. It is believed that mechanical deterioration of the combustion system was the reason for this poor performance. The secondary flow duct work

was found to have several leaks which allowed the loss of gases to the ambient. This would explain the higher air mass flow rate measured at the compressor intake.

2.2.2 Modification of Original Inlet and Outlet Chambers

In order to obtain a significant amount of test data, comprehensive rebuilding of the combustion system would have been necessary. This was not carried out because it was felt that such time would be better spent on the design and construction of the proposed Second Generation Pulse Combustion System. Two modifications were, however, made to the system and additional tests were completed. The air inlet plenum (figure 2.4) and the combining chamber (figure 2.2) were enlarged by 50% and 100% respectively. This was carried out by bolting steel extensions to the existing equipment. Results produced by Cronje [4] for the combustion system (shown in figure 2.3) operated in isolation indicated that the combining chamber size and shape affects the thrust performance. It is believed that such effects may occur with the gas generator application.

Results from tests with the extensions added proved to be inconclusive. It was apparent that the mechanical problems had progressed and the overall performance had continually worsened. The believed importance of the inlet plenum and combining chamber volumes were, however, kept in mind in the development of the Second Generation Pulse Combustion System described in chapter 4.

2.2.3 Qualitative Considerations

As stated above, the condition of the First Generation Combustion

System continually worsened over the test period. However, some necessary repairs were made. It was important to study the nature of these repairs so that design changes could be made to the proposed second generation system, to hopefully reduce such problems for the work described here.

The secondary flow ducts (figure 2.3) showed metal cracking and connection flange problems. The ducts are rectangular in cross section. Cracks occured in the corners and near the flanges. The ductwork was removed and welding repairs were carried out. However, subsequent tests showed further cracking problems.

The remaining problems that occurred were associated with the combustor fuel chamber, which can be seen in figure 2.1. Before any testing could be carried out, it was necessary to remove the fuel chamber nozzles and clean out lodged carbon particles that had caused partial clogging. Also, significant cracks were found near the nozzles on the surface exposed to hot gases which extended into the fuel cavity. These cracks were welded before reassembly.

The repeated problem of metal failure at high temperature points of the combustor, reported by Yerneni, did not occur during the test runs carried out by the writer. This was because the gas generator unit was not operated at a high load condition. The turbine was not back pressured (ie., by use of the butterfly valve), thereby avoiding to some extent the higher combustion chamber temperatures associated with high loads.

2.4 COMPARISON OF PREDICTED AND EXPERIMENTALLY OBTAINED PERFORMANCES

Figure 2.7 shows the actual performance results of the pulse combustor operated in isolation. The pressure gain curve was established experimentally by Cronje [4] knowing the thrust, fuel flow, calorific value of the fuel, heat loss, and the inlet and outlet temperatures. This information provides an approximate prediction of the behaviour of the pulse combustor for operation within the gas turbine. The maximum pressure gain attainable with this combustor, while operating in isolation, is approximately 6%. In comparison, the same unit used as part of the first generation system is capable of a maximum of only about 0.4% gain while operating within the gas turbine [19]. Figure 2.7 shows that the actual fuel consumption range for the gas generator is relatively narrow compared to the overall flow range for the isolated combustor. Directly comparing these two ranges is not truely valid when it is considered that, when operated within the gas generator, the combustor receives inlet air at a temperature and pressure that is greater than ambient conditions (because of the compressor). A corrected fuel flow range is shown (figure 2.7) that takes this into account. This correction is an application of the equation of state for gases. Effectively it predicts that because of these higher inlet conditions, the combustor is capable of a greater maximum fuel consumption for operation within the gas turbine.

What is referred to as the "optimum fuel flow range" is also shown in figure 2.7. If the combustor was to operate in this maximum pressure gain range, when incorporated in the gas generator, the gain would be

expected to be about twice that of the present system. If a smaller pulse combustor was used with the present turbo-machine, operation within this optimum range could be achieved. This is true assuming that pulse combustors have the same performance characteristics regardless of their size. Curves in figure 2.8 (extracted from reference 9) show that this is not true over a significant combustor size range. The specific fuel consumption increases and the maximum specific thrust, which is proportional to pressure gain, decreases with combustor size. This indicates that smaller combustors produce a correspondingly lower pressure gain. The reasons for this influence of size on performance are detailed in reference 9. The effects of combustor size were taken into consideration when developing the second generation system, described in section 3.

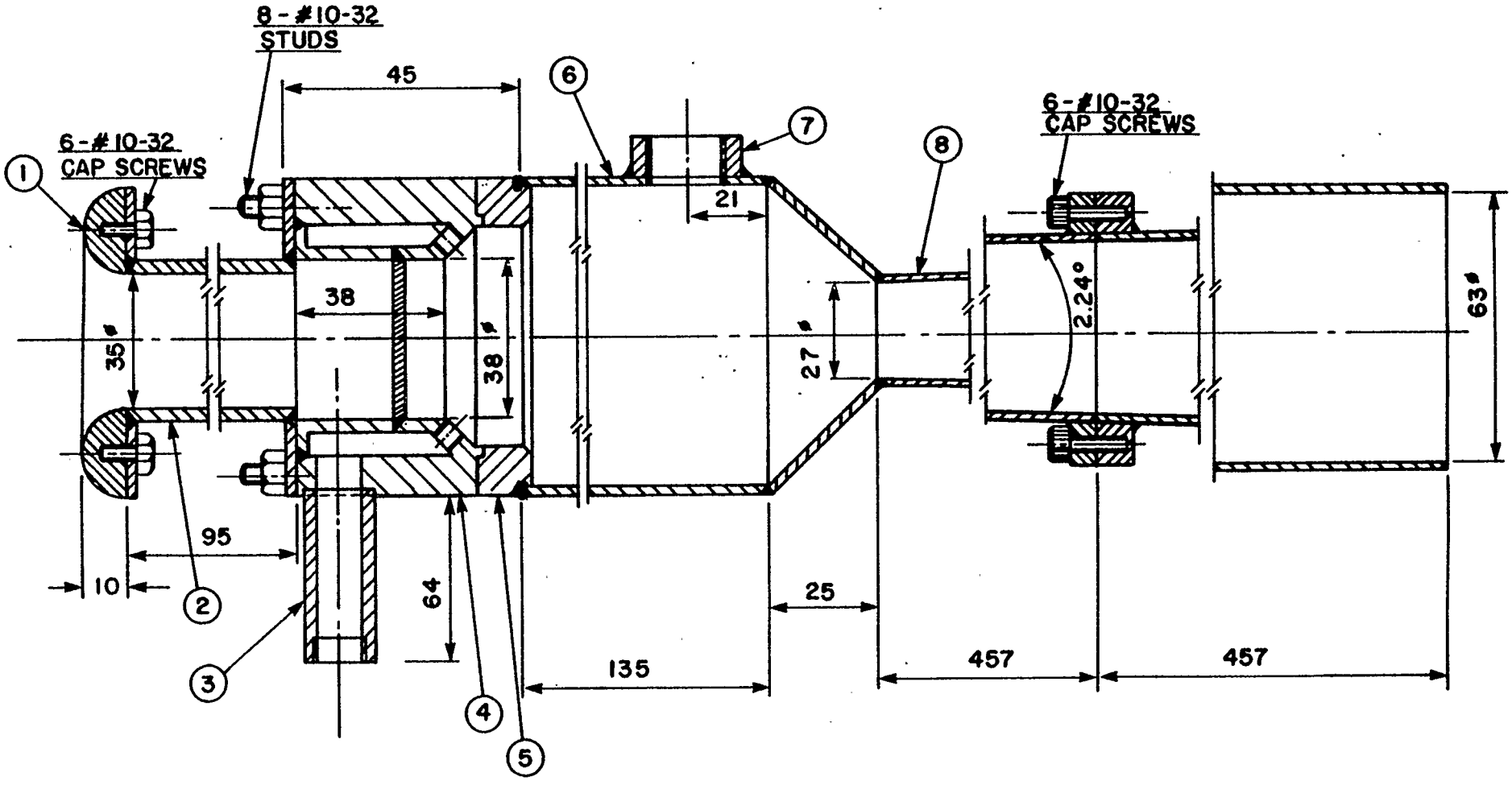

FIGURE 2.1 CONSTRUCTIONAL DETAILS OF PULSE COMBUSTOR [19]

1-INLET BELLMOUTH, 2-INLET PIPE, 3-FUEL INLET
4-FUEL CHAMBER, 5-COMBUSTION CHAMBER REINFORCING
RING, 6-COMBUSTION CHAMBER, 7-SPARK-PLUG BOSS
8-TAILPIPE

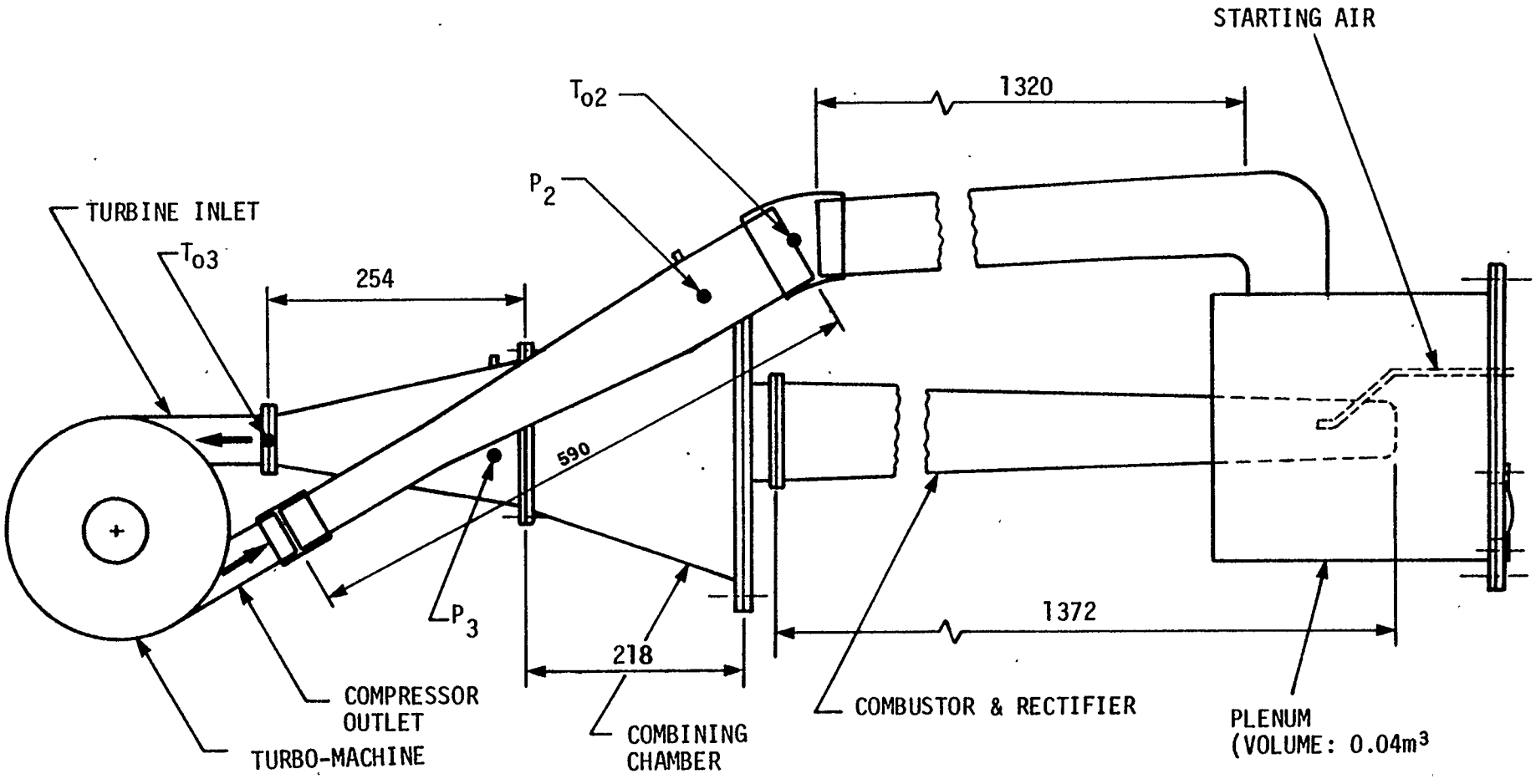

FIGURE 2.2 **PULSE, PRESSURE-GAIN, COMBUSTOR INSTALLATION ON CUSSONS P.9000 GAS GENERATOR [19] (dimensions in mm)**

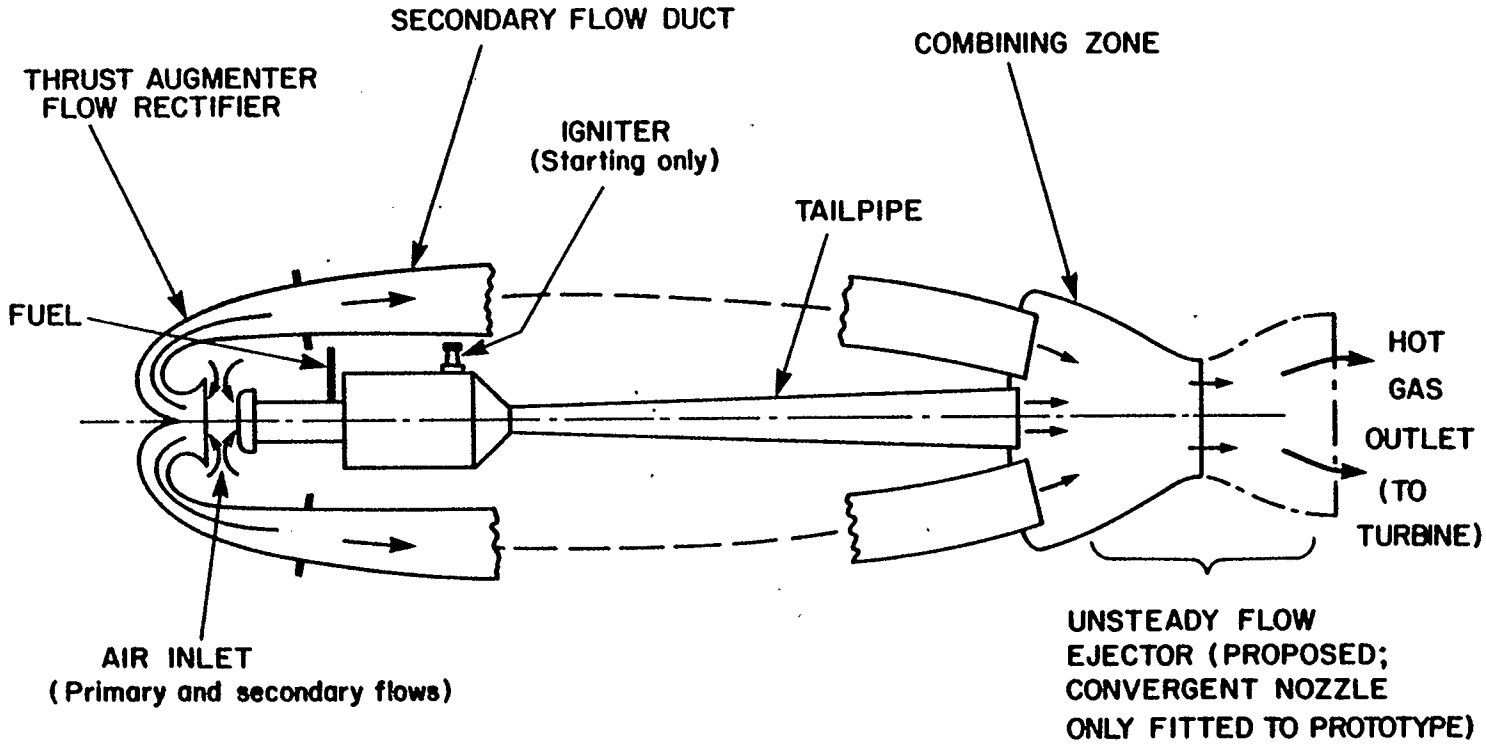

FIGURE 2.3 DIAGRAMMATIC ILLUSTRATION OF PROTOTYPE PULSE COMBUSTOR WITH SECONDARY FLOW [10]

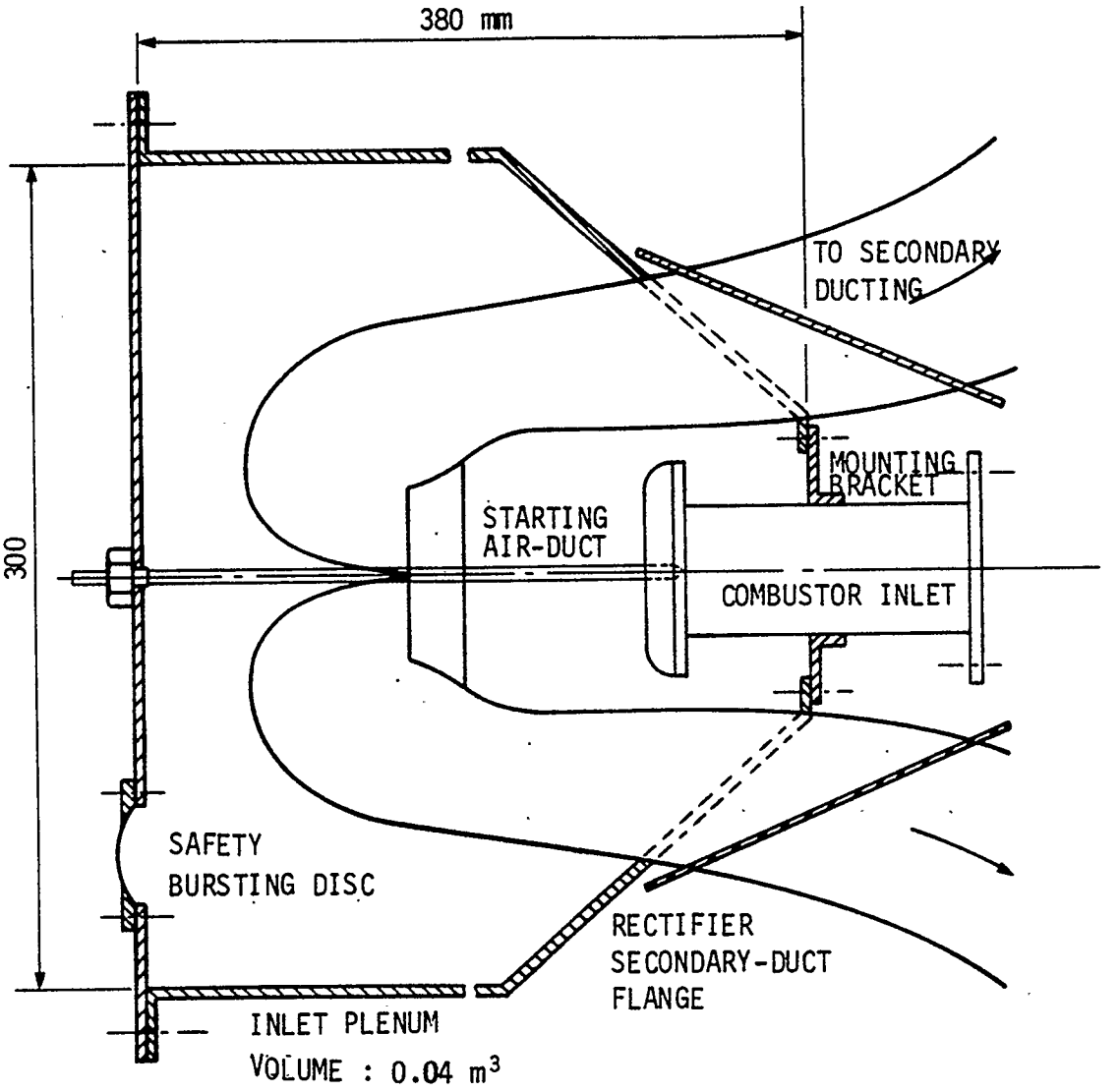

FIGURE 2.4 DETAILS OF PULSED COMBUSTOR INLET PLENUM [19]

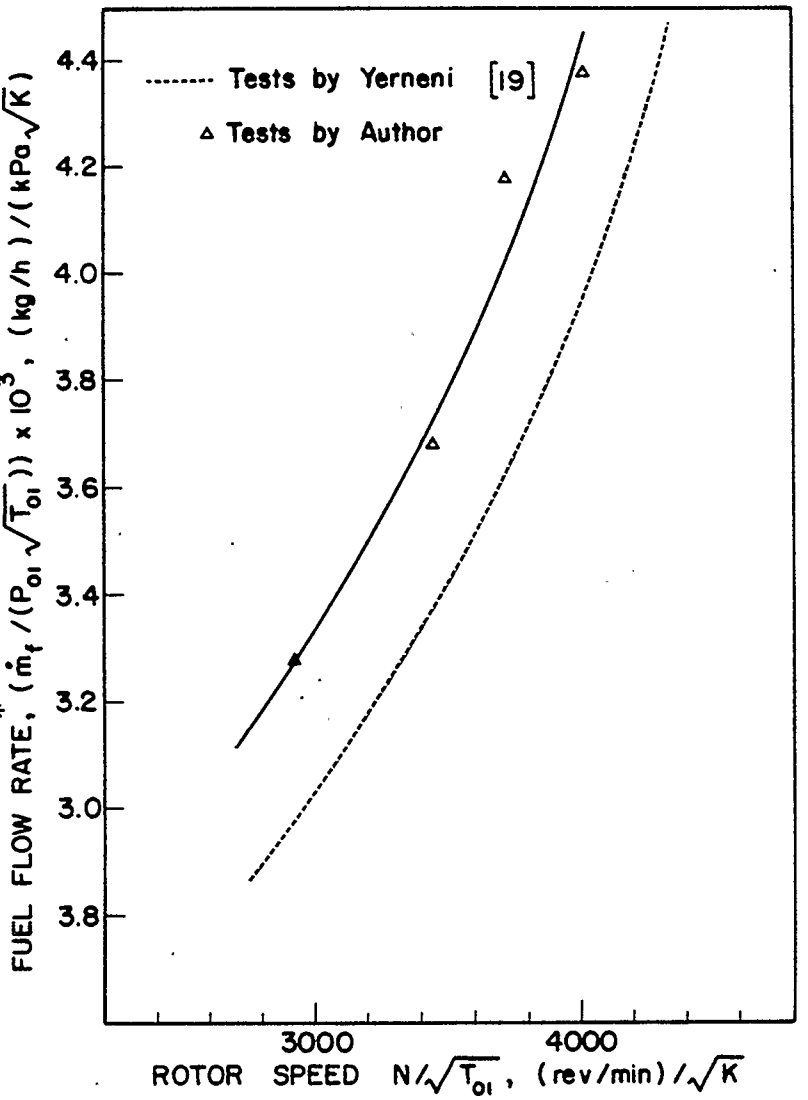

FIGURE 2.5 COMPARISON OF FUEL FLOW RATES FOR FIRST GENERATION COMBUSTION SYSTEM OPERATED ON GAS TURBINE

* Note: To obtain flow rate divide the number shown by 10^3

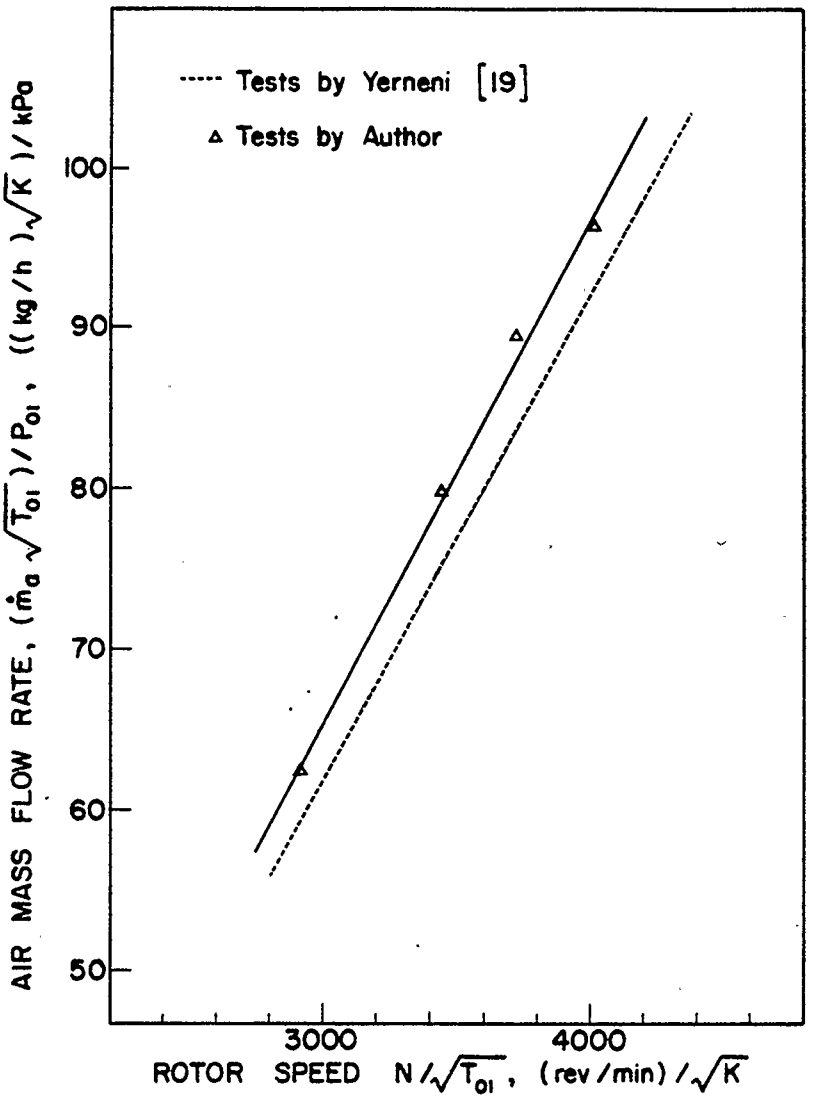

FIGURE 2.6 COMPARISON OF AIR MASS FLOW RATES FOR FIRST GENERATION COMBUSTION SYSTEM OPERATED ON GAS TURBINE

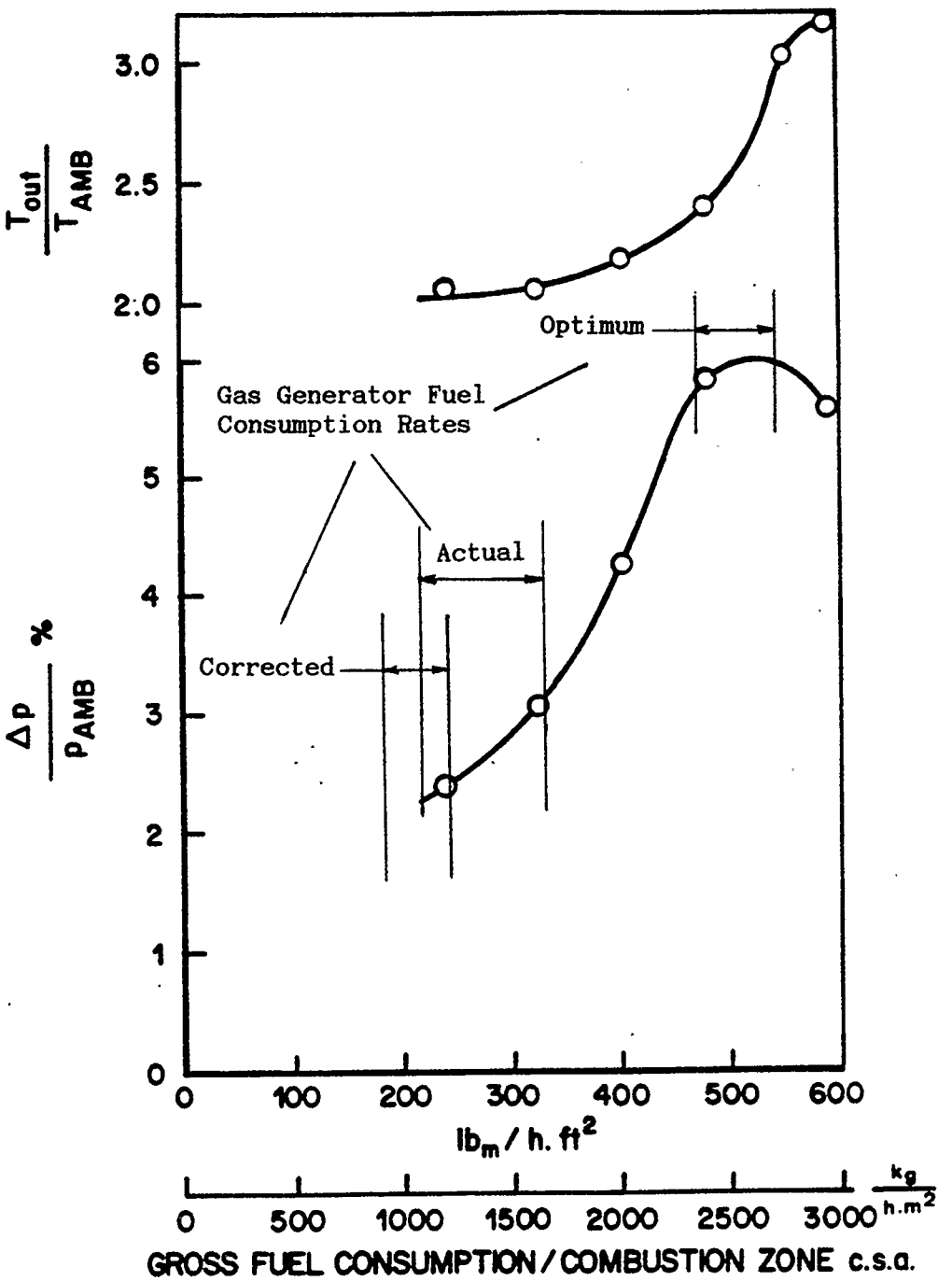

FIGURE 2.7 STAGNATION PRESSURE-GAIN PERFORMANCE OF PULSED COMBUSTOR UNIT WITH THRUST-AUGMENTER FLOW-RECTIFIER [9]
NOTE: TEST DATA UNCORRECTED FOR AMBIENT CONDITIONS, ALL TESTS CARRIED OUT AT 1096m ALTITUDE. AMBIENT TEMPERATURE = 292 - 298 K, AMBIENT PRESSURE = 88.0 - 88.7 kPa.

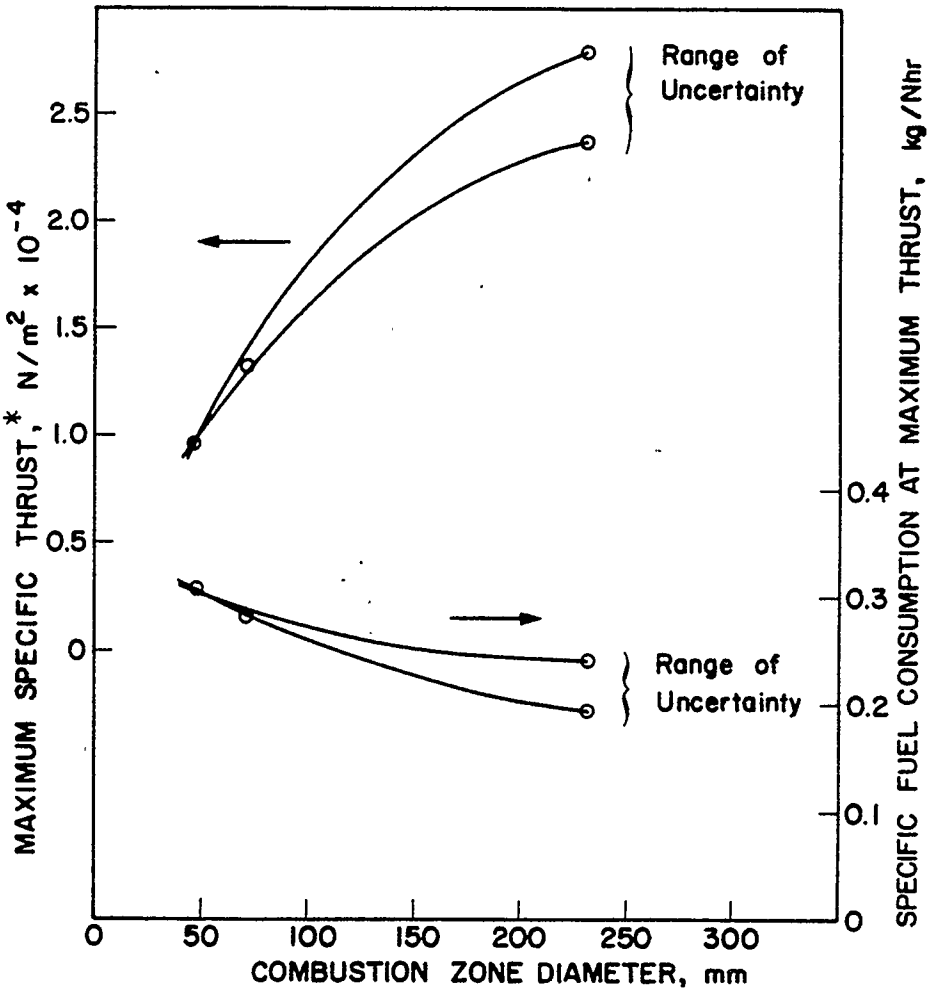

FIGURE 2.8 THE EFFECT OF PULSE COMBUSTOR SIZE ON PERFORMANCE FOR THE VALVELESS HILLER HH-M1 TYPE UNIT [9]

* Note: The Ordinate Numbers Shown are $N/m^2 \times 10^{-4}$

CHAPTER 3

DEVELOPMENT OF THE COMBUSTION SYSTEM

3.1 STATEMENT OF DEVELOPMENT AIMS

As seen in section 1.3, the development of the Pulse Combustion system was a logical continuation of the work carried out by Yerneni [19]. The following suggestions made by Yerneni were implemented during the course of the design work:

First, change the configuration of the combustor flow system to provide convective cooling of the primary zone (combustion chamber and tailpipe) to reduce heat loss to the ambient. As seen in section 2.1.2, Yerneni's prototype combustion system had this area exposed. Figure 3.1 shows a schematic of a "Second Generation System" which was suggested by Kentfield and Yerneni [11]. This design provides cooling of the primary zone by directing the secondary flow over it. The actual combustion system design described in section 4 follows this concept closely.

Secondly, reduce pressure losses in two areas; the duct work connecting the combustion system to the compressor-turbine unit and in the secondary flow ducting of the combustor.

Thirdly, rematch the compressor-turbine unit to the second generation combustion system to attain optimum performance. This suggestion was carried out by attempting to determine the optimum size of the pulse combustor required for this system (addressed in section 3.2).

Fourthly, place thermocouples on the highest temperature components of the pulse combustor because of the combustion chamber burn-out

problems experienced by Yerneni with the first generation unit. Related to this problem, it was also suggested that a more oxidation resistant stainless steel, such as "310-SS", be used for the high temperature areas.

An important feature which must be implicit to the redesigned system is flexibility in geometry. The secondary flow ducting as well as the inlet and outlet chambers were to be designed to be variable in length and volume respectively. Experiments carried out on pulse combustion systems by Cronje [4] display the sensitivity of performance to variations of configuration. Figure 3.2 shows an example of how the shape of the exit combining chamber strongly influences performance.

The design of the basic combustor, excluding secondary flow ducts and attachments, was retained. The Hiller HH-M1 type combustor configuration (figure 2.1) was optimized for maximum performance, over a period of many years, by a number of other workers [4,9,12,13,14].

3.2 CHOICE OF PULSE COMBUSTOR SIZE FOR THE COMPRESSOR-TURBINE UNIT

3.2.1 Performance Matching the Combustor with the Compressor-turbine unit

As shown in section 2.4, the first generation pulse combustor, while connected to the gas turbine, operated in a small section of its overall performance range (figure 2.7). Also, this section corresponded to relatively low fuel consumption rates. If the combustor were to operate higher up in its range for this application, the predicted pressure gain and temperature ratio would be higher. For reasons stated

in section 1.2.1, it is beneficial to increase the pressure gain. Also, a pulse combustor operating at a higher temperature ratio would better match the characteristics of the existing compressor-turbine unit. If a smaller pulse combustor were operated in the existing system, all else being equal, it would be required to operate high up in the performance range. The benefits of greater pressure gain could thus be achieved.

The above argument is true assuming that a smaller combustor will have similar performance characteristics to that of the larger unit used by Yerneni. Reference 9 shows that smaller combustors have greater specific fuel consumptions (refer to section 2.4). Therefore, when downsizing, there is a trade off between the improvement realized in forcing the combustor to operate higher in its performance range (for increased pressure gain) and the reduction in thrust performance due to the smaller size. This idea can be illustrated graphically in figure 3.3. There is an optimum combustor size for this particular compressor-turbine unit that will provide the best performance. The following section addresses this problem.

3.2.2 Assumptions used in the Choice of Combustor Size

In an attempt to better match the performance characteristics of the compressor-turbine unit to those of a pulse combustor, a prediction of the pressure gain and fuel consumption characteristics for various size combustors can be made using the following information: The experimental "pressure gain" curve for the existing combustor shown in figure 2.7; the experimental "maximum specific thrust" and "specific fuel consumption at maximum thrust" versus combustor size curves (figure

2.8); and the following relationships:

$$\text{Maximum Pressure Gain} = \frac{\Delta P_{max}}{P_{in}} \propto \left[\frac{1}{\text{Specific Fuel Flow at Maximum Thrust}} \right]^2 \qquad (3.1)$$

$$\text{Maximum Fuel Flow} = \left[\text{Maximum Specific Thrust} \right] \times \left[\text{Specific Fuel Flow at Maximum Thrust} \right] \qquad (3.2)$$

Equation 3.1 represents a simplification of an expression given by Kentfield, Rehman, and Marzouk [10]. "P_{in}" represents the combustor inlet pressure, which is equal to ambient pressure for atmospheric operation (isolated combustor).

It should be kept in mind that the predicted fuel flow at maximum pressure gain is assumed to occur at about 60% of maximum fuel flow for all combustors as it does for the existing one. The results are shown in table 3.1 for a range of combustor sizes. The combustor size choice was made by comparing the expected gas turbine fuel consumption at maximum load to the predicted fuel consumption of a pulse combustor at maximum pressure gain under similar conditions. All of the information concerning the pulse combustor performance is for ambient inlet conditions. It is, therefore, necessary to apply a correction factor to the combustor fuel flow values. This takes into account the fact that the inlet temperature and pressure is higher for the combustor when connected to the turbo-machine. These "corrected" values were then compared to the expected gas turbine fuel consumption rate. An implicit assumption of this comparison was that the second generation system,

applied to the gas turbine, will have a comparable fuel consumption to that of the conventional combustion system.

Test results for the gas turbine operating with the conventional combustion chamber attached, showed that at maximum turbine rotor speed and load back pressure setting 2 (maximum), the fuel consumption was approximately 6.5 kg/hr. The combustor size (chamber diameter) chosen for use on the system was, therefore, 2.4 inches. This combustor was estimated, in table 3.1, to consume 8.5 kg/hr when operating within the gas turbine at maximum pressure gain. It was decided to use a size that appeared to be slightly large, because it was known that an oversize combustor will operate on the gas turbine, as established by Yerneni [19]. It is unknown how an undersized combustor would behave in such an application. The severe durability problems of the first generation system, due to high operating temperatures, also had to be considered. Smaller combustors will be more highly loaded for this application; this may decrease the durability of such units.

Once the desired combustor fuel chamber size was known, all of the remaining dimensions were easily found by linearly scaling all of the linear dimensions of an existing unit. Figure 3.4 presents these combustor dimensions, for a unit of the Hiller HH-M1 type, normalized with respect to the combustion chamber diameter.

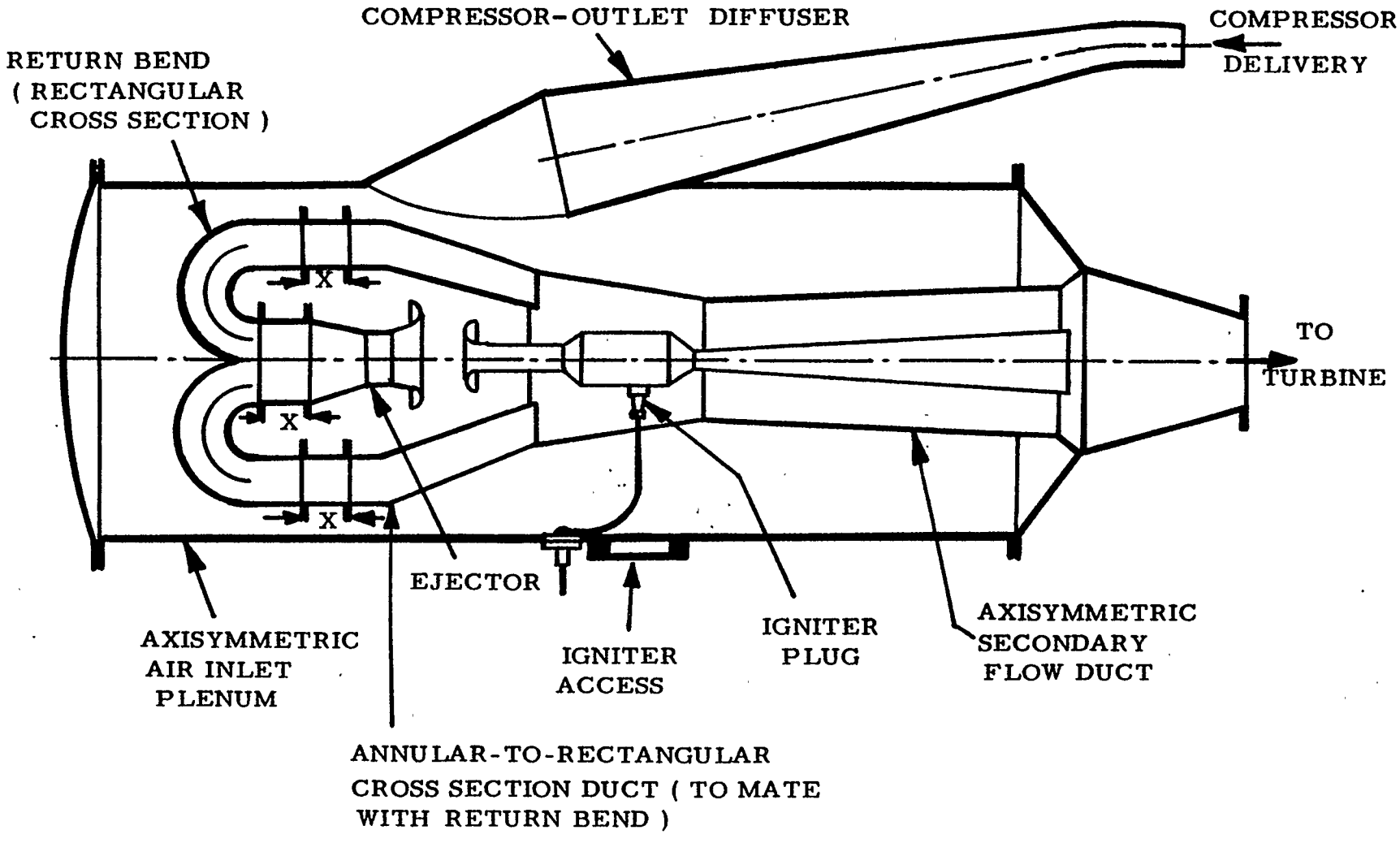

FIGURE 3.1 PROPOSED SECOND GENERATION PULSE, PRESSURE GAIN, COMBUSTOR FOR CUSSONS P.9000 GAS GENERATOR [19]. X INDICATES EQUAL, REPLACEABLE, LENGTHS OF RECTANGULAR CROSS-SECTION DUCTING FOR TUNING SECONDARY FLOW PATH LENGTH

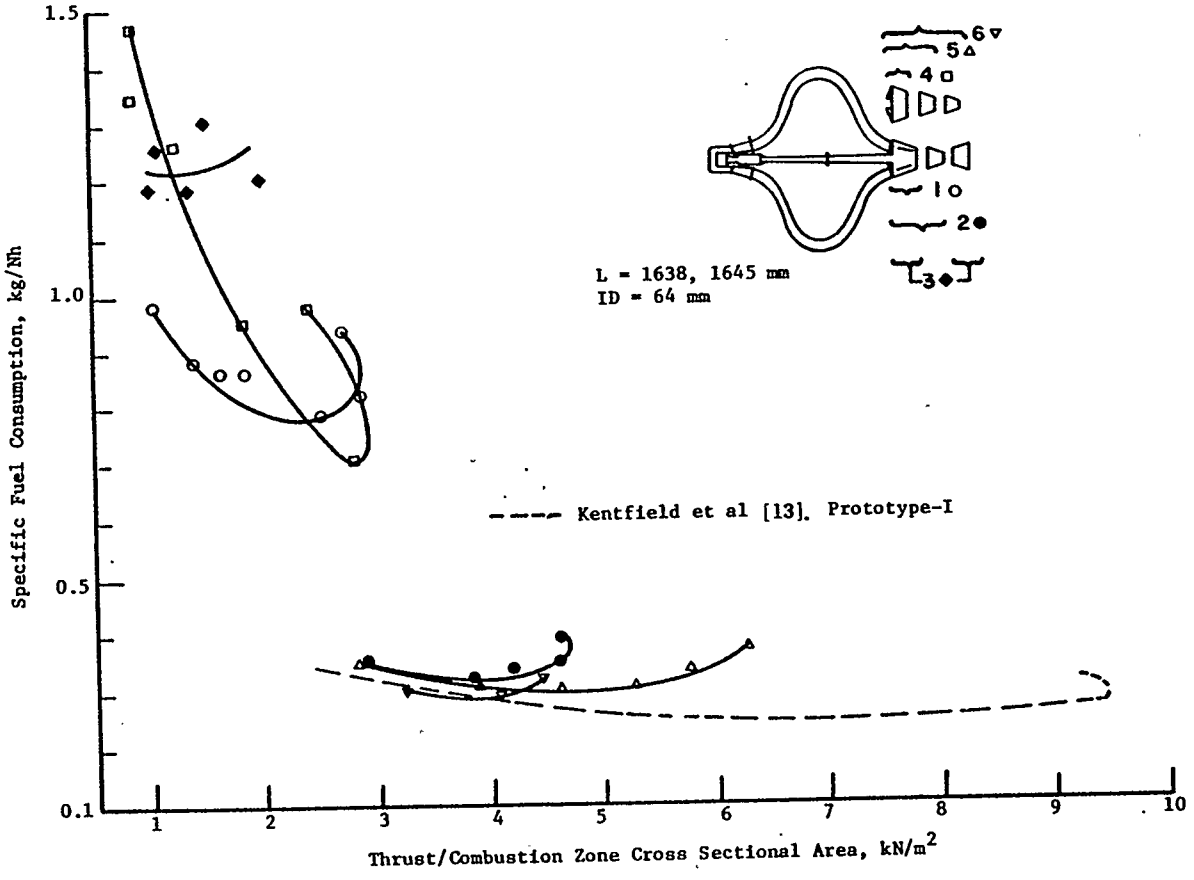

FIGURE 3.2 PERFORMANCE OF PRESSURE GAIN PULSE COMBUSTOR WITH SECONDARY FLOW SYSTEM [4]

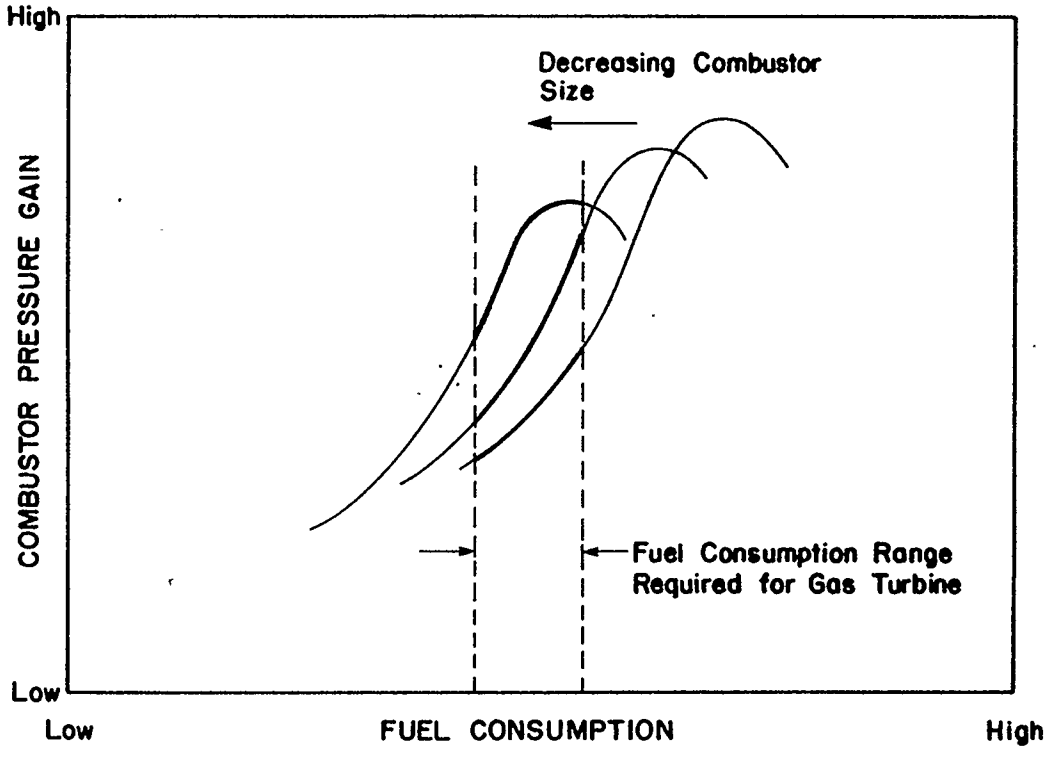

FIGURE 3.3 THE EFFECT OF PULSE COMBUSTOR DOWNSIZING ON PRESSURE GAIN PERFORMANCE

Combustion Chamber Inside Diameter:		Maximum Specific Thrust:	Specific Fuel Consumption at Maximum Thrust:	Maximum Fuel Flow:		Fuel Flow at Max Pressure Gain:		Maximum Pressure Gain:
						Actual¦	Corrected+	
inches	mm	*kN/m^2	kg/(Nh)	$kg/(m^2h)$	kg/h	kg/h	kg/h	%
2.875	73.0	13.6	0.278	3900	16.3	10.0	14.1	6.0
2.80	71.1	13.3	0.280	3730	14.8	9.1	12.8	5.9
2.60	66.0	12.5	0.285	3560	12.2	7.5	10.6	5.7
2.40	61.0	11.6	0.291	3370	9.8	6.0	8.5	5.5
2.20	55.9	10.6	0.295	3130	7.7	4.7	6.6	5.3
2.00	50.8	9.6	0.300	2870	5.8	3.6	5.1	5.1

TABLE 3.1 PREDICTION OF PRESSURE GAIN AND FUEL CONSUMPTION CHARACTERISTICS FOR VARIOUS SIZE PULSE COMBUSTORS

NOTES:

* kN/m^2 represents "Thrust/Combustion Chamber Inside X-sectional Area"
¦ Combustor operated with ambient intake conditions
+ Combustor inlet conditions corresponding to gas-turbine compressor discharge conditions

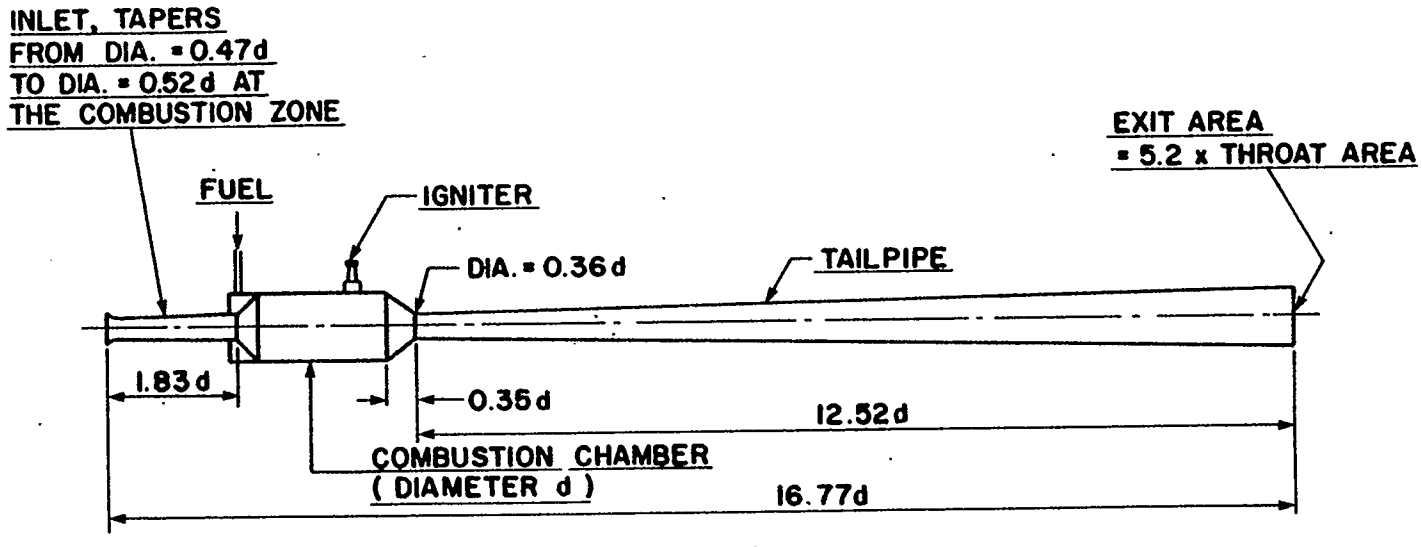

FIGURE 3.5 PROPORTIONS OF THE HILLER HH-M1 VALVELESS PULSE COMBUSTOR [18]

CHAPTER 4

THE REDESIGNED COMBUSTION SYSTEM

4.1 PHYSICAL CHARACTERISTICS

A new combustion system, based on the "second generation combustor" suggested by Kentfield and Yerneni [11], was designed in detail, to meet the aims listed in section 3.1 of this report. An assembly drawing of this unit is shown in figure 4.1.

The overall configuration of this system was designed, as suggested by Yerneni (and, earlier, by Kentfield, Rehman and Cronje [9]), to minimize heat losses to the ambient. The Primary Zone, which consists of the Combustion Chamber and its Tail Pipe, is surrounded by the Secondary Flow Duct. The flow of gases in the duct provide convective cooling of this zone. Also, the Air Inlet Plenum completely surrounds the Combustor and the secondary flow system. This was intended to provide yet lower energy losses than the system used by Yerneni, shown in figure 2.3. This system had the secondary and primary flow systems exposed to the ambient.

The connection between the Compressor and the Air Inlet Plenum was designed as a diffuser in order to reduce flow pressure losses. The Secondary Flow Return Bend was also designed to keep flow losses to a minimum (refer to section 4.2.2).

For reasons suggested in section 3.1, flexibility in geometry was built into the system with the use of flanged joints. These joints were placed on the Secondary Flow Return Bend in the Air Inlet Plenum so that the flow path length and chamber volume could be adjusted. This

variable geometry was provided to allow the performance to be somewhat optimized.

4.2 JUSTIFICATION OF DESIGN DETAILS

4.2.1 The Pulse Combustion Chamber

The Pulse Combustion Chamber to be used in the redesigned combustion system was of the Hiller HH-M1 type, as displayed in figure 2.1. Certain design details used on previous units were changed in an attempt to address some of the durability problems experienced by Yerneni.

To reduce the "burn-out" problems [19] of the combustion chamber and the divergent part of the tail-pipe close to the combustion chamber, two changes were made.

First of all, the convergent part of the combustion chamber and a part of the adjacent section of the tailpipe were fabricated as a single machined stainless steel component. As shown in figure 4.2, the wall thicknesses along with the outside transition zone radius were made larger than those of the fabricated sheetmetal sections used on previous models.

Secondly, the material used for fabrication of the remainder of the combustion chamber and tailpipe, with exception of the fuel chamber, was a type 310 stainless steel. This type has greater yield and ultimate strengths as well as higher heat resistance than the type 316 stainless steel used in previous combustors. A summary of these properties are listed in table A.1 of the appendix. In addition, table A.2 displays test results carried out by the American Iron and Steel Insitute which

show that the type 310 stainless steel has consistently greater high temperature rupture resistance than the type 316.

Further, the problem of fuel chamber cracking near the fuel nozzles, referred to in section 2.2.3, was addressed by increasing the chamber wall thickness in that area.

4.2.2 The Flow Rectifier-Thrust Augmenter

Figure 4.3 shows both the previous and the latest Flow Rectifier-Thrust Augmenter configurations. On the assembly drawing, figure 4.1, this section consists of the Ejector and the Secondary Flow Return Bend. A curve showing the cross sectional area as a function of the duct length, used for the Prototype I design, is shown in figure 4.4 (extracted from reference 4). This design, made by Kentfield, provides the best thrust performance of any to date. The cross sectional area design of the latest Augmenter is based on this curve with a scaling factor applied to the path length. This factor, equal to 0.835, is the same as the length scale factor that was applied to the pulse combustor of the first generation system to provide the dimensions of the pulse combustor used in this second generation system. Note that the vane bend radii are larger for the present augmenter. This should reduce flow losses in this area.

4.2.3 The Axisymmetric Secondary Flow Duct

The Axisymmetric Secondary Flow Duct can be seen in the assembly drawing displayed in figure 4.1. The flow area versus length design of this duct is based on that of the Prototype I design by Kentfield [13].

As with the Flow Rectifier-Thrust Augmenter, described above, a scaling factor of 0.835 was applied to this design.

Because of the inherent shape of the pulse combustion chamber and its tailpipe, it is difficult to construct an axisymmetric flow duct that has a cross sectional flow area that varies along its length in a smooth way. To methodically follow a chosen area versus duct length curve, a complicated shape would be required. Another way to achieve a similar effect would be to use a simple secondary flow duct shape and to shroud the pulse combustor at various locations along its length. This would yield the desired cross-sectional area versus axial-station schedule.

It was felt that, for this initial design, neither one of these alternatives were desirable, largely because of their complexity. A relatively simple and easy to fabricate secondary flow duct shape was chosen.

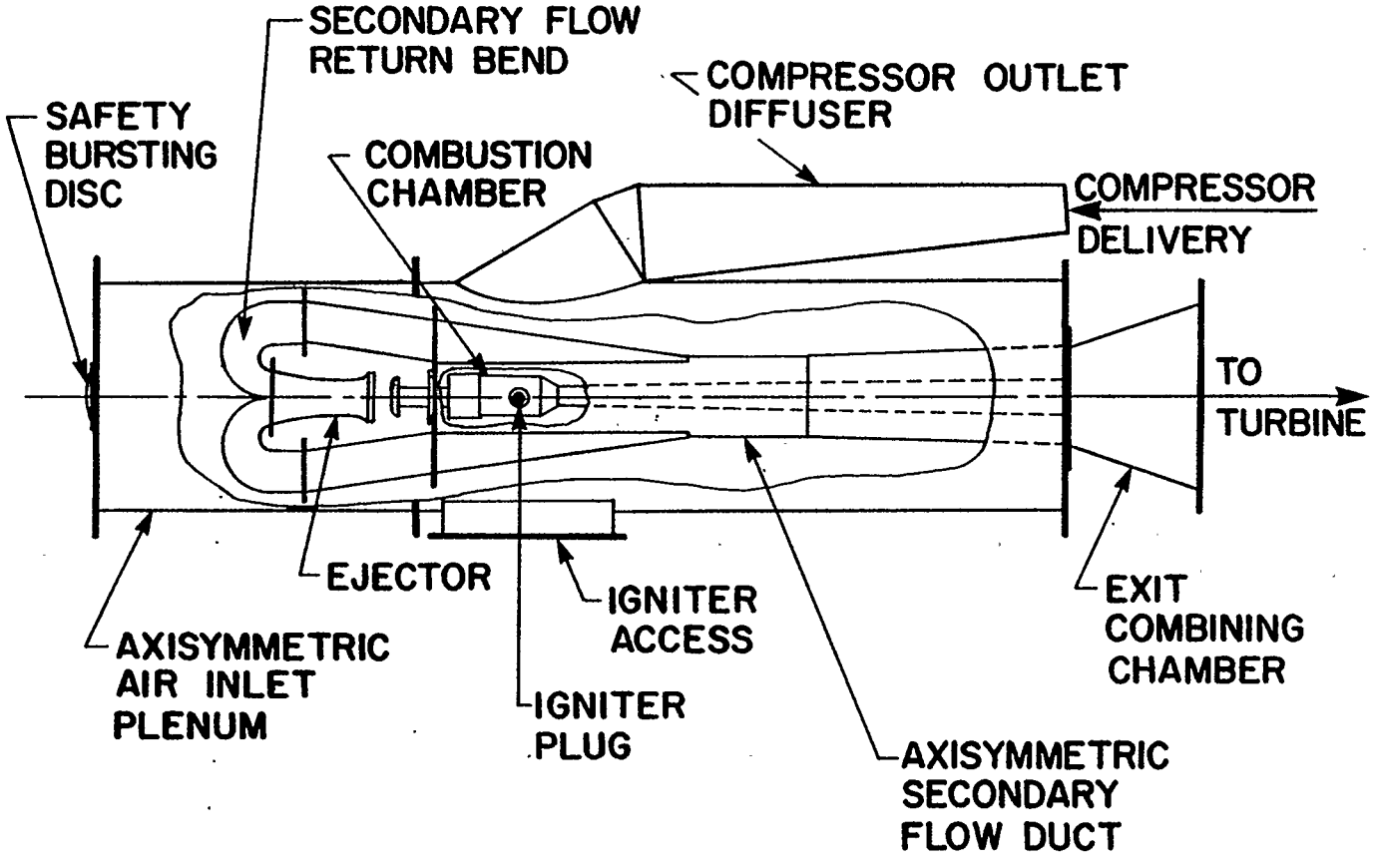

FIGURE 4.1 ACTUAL SECOND GENERATION PULSE COMBUSTION SYSTEM

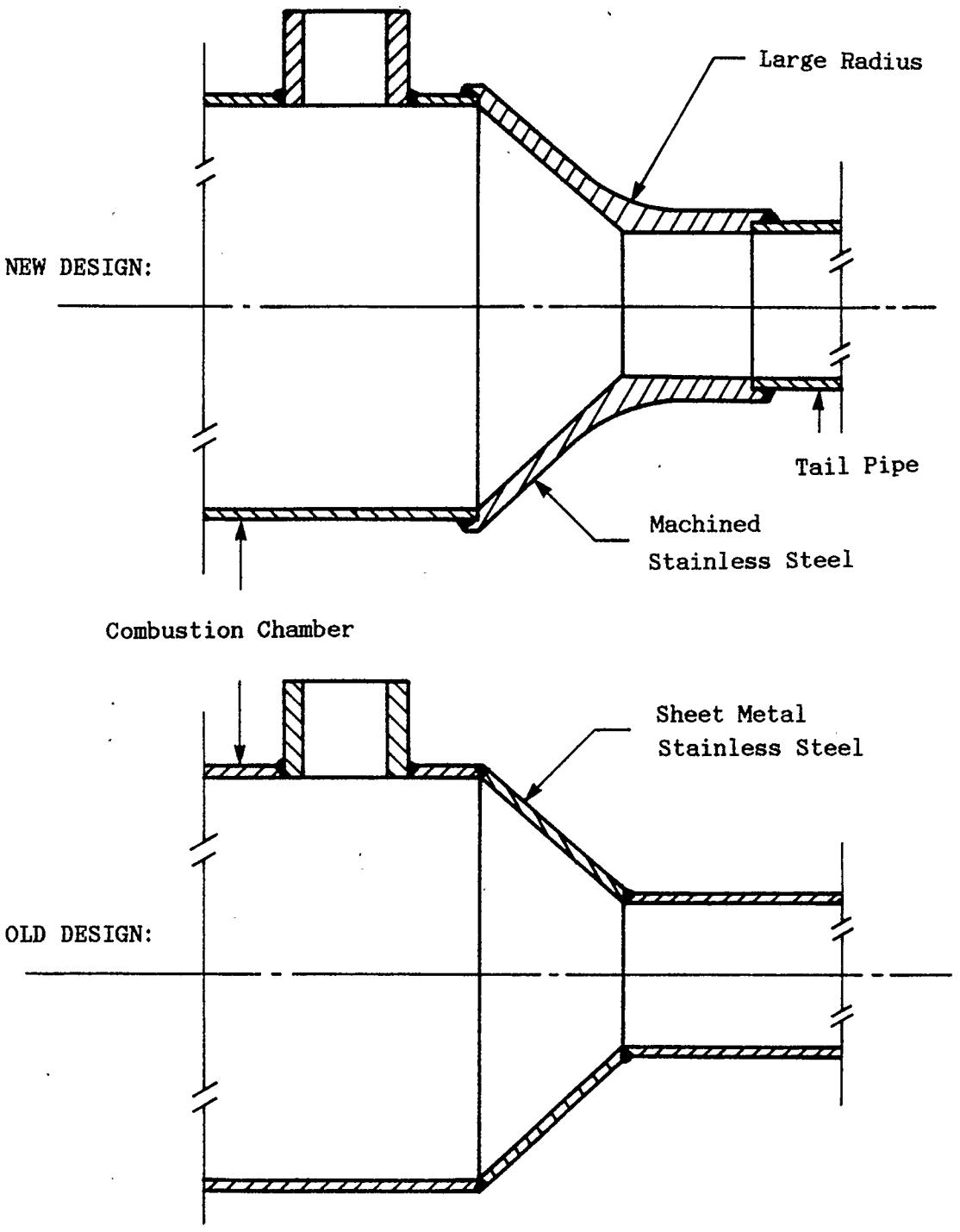

FIGURE 4.2 DESIGN CHANGE OF POOR DURABILITY AREA OF PULSE COMBUSTOR

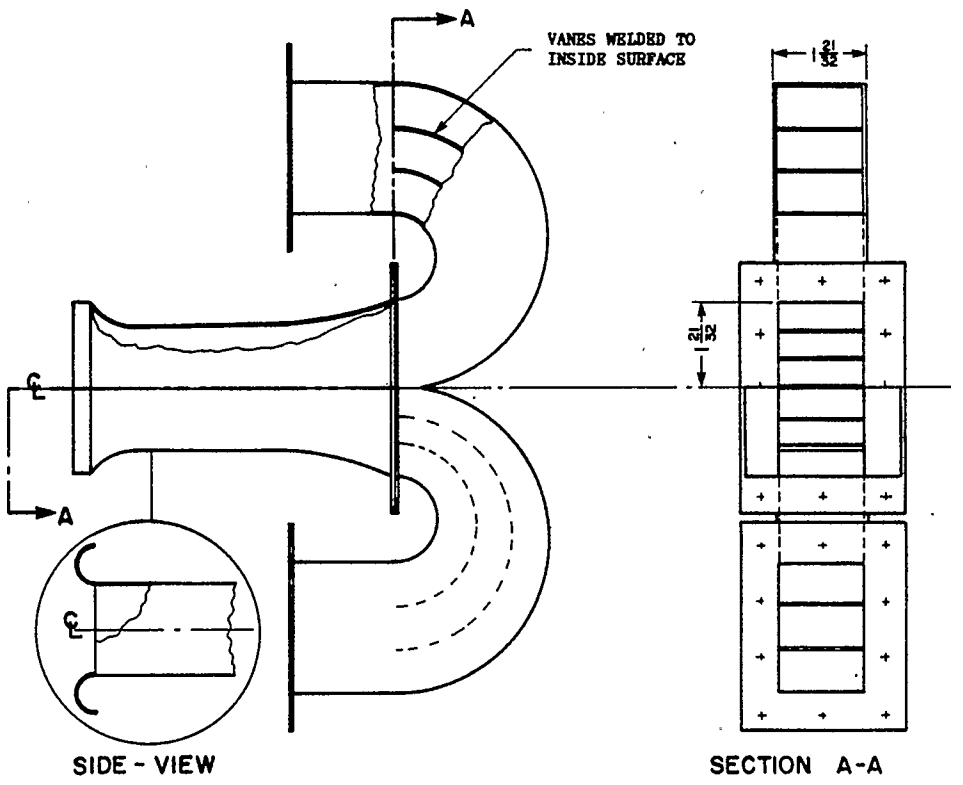

Present Augmenter for Second Generation Pulse Combustion System

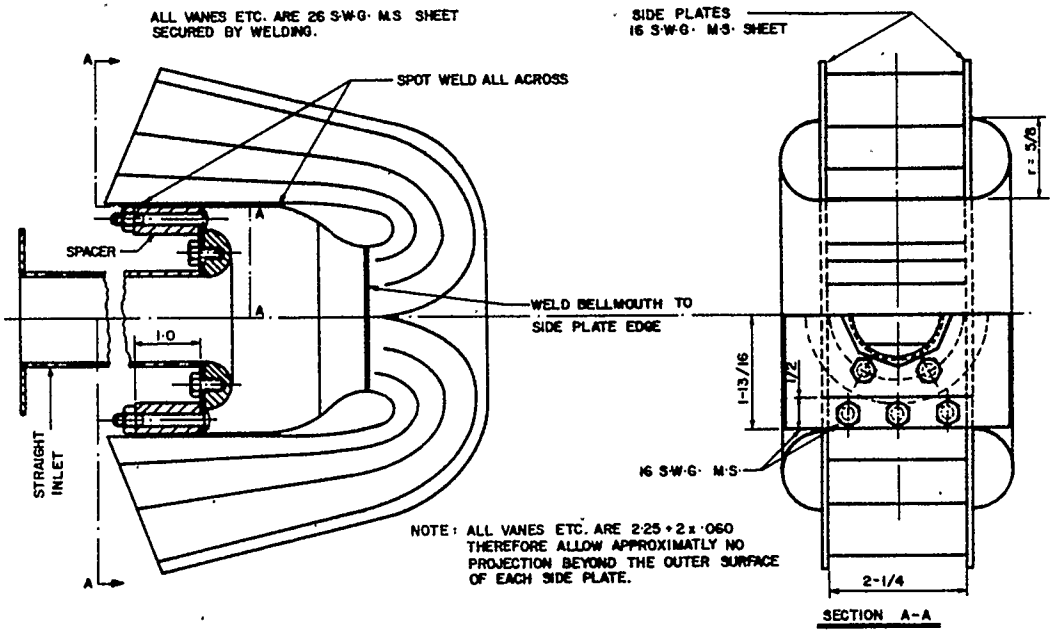

Previous Augmenter Used in First Generation Pulse Combustion System (Prototype 1 Design) [13]

FIGURE 4.3 COMPARISON OF FLOW RECTIFIER THRUST AUGMENTERS

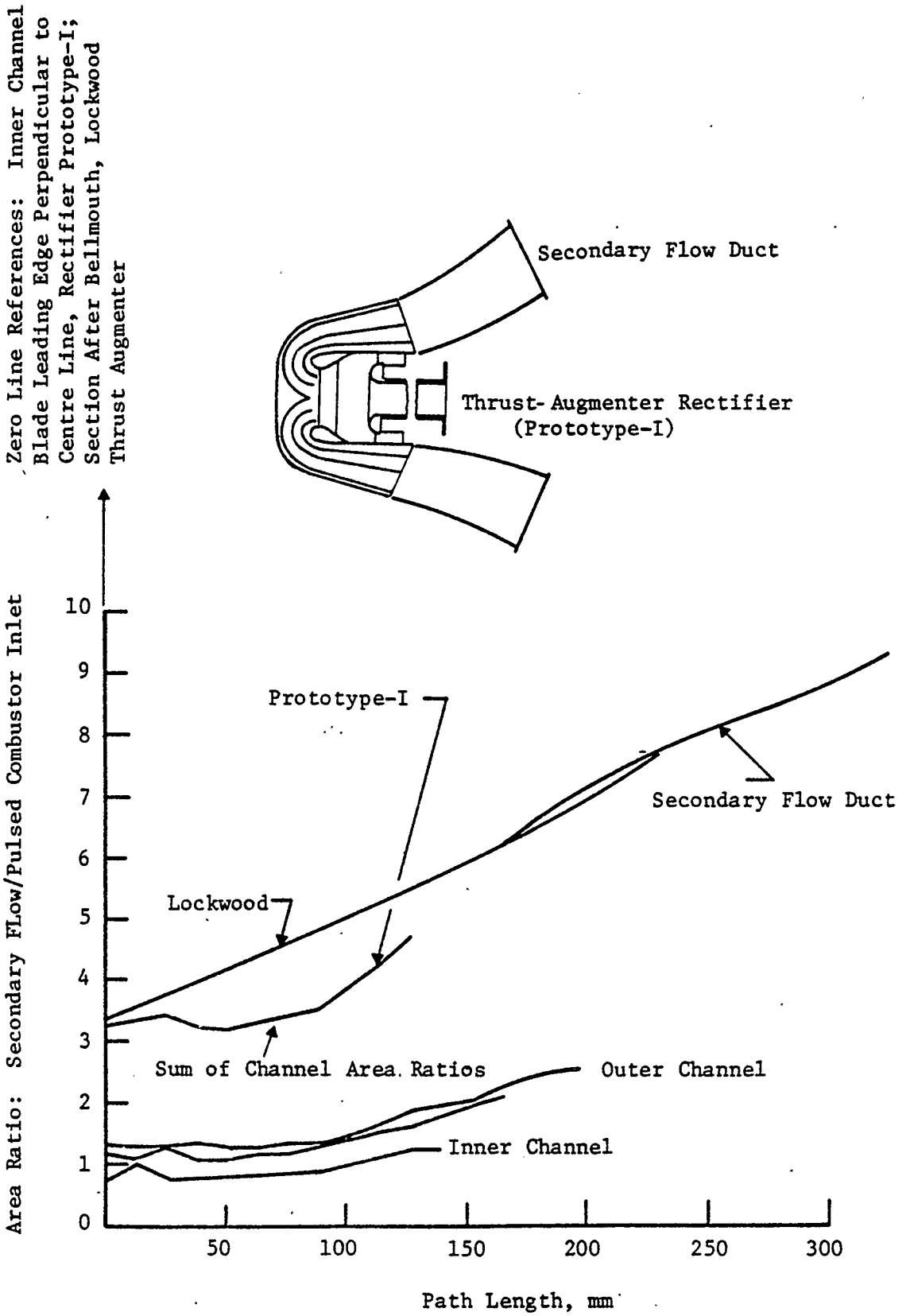

FIGURE 4.4 PROTOTYPE-I RECTIFIER UNIT - AREA RATIO DISTRIBUTION AS A FUNCTION OF PATH LENGTH

CHAPTER 5

EXPERIMENTAL PROCEEDURE AND EQUIPMENT FOR TESTING THE SECOND GENERATION SYSTEM

5.1 INITIAL TESTS: THE COMBUSTION SYSTEM IN ISOLATION

A distinct operational advantage of a pulse combustion system, as compared to a conventional combustion system, is its ability to self induce the gas flow. This allows for performance testing of the pulse system to be carried out in isolation without a separate air supply system. Once combustor startup is achieved, all that is necessary for operation is a fuel supply. Startup requires a power supply for the ignition plug and an auxiliary compressed air source to feed a starting-air jet. Set up of the test stand and combustor operation are, therefore, simple compared to the operation of the complete gas turbine system.

The performance optimization was completed on this test stand first, without the complications of a connected compressor-turbine unit and its associated auxiliary equipment. A sketch of this test stand is shown in figure 5.1. This method of optimization carries with it an important assumption: "A combustor configuration which provides optimum performance on the test stand will provide optimum performance within a gas turbine". It is believed, for testing a new system, that the benefits resulting from the ease of operation on the test stand outweigh the possible inaccuracies.

Three configurations were tested: the "Combustor Alone", the "Combustor with Secondary Flow Ducting", and the "Complete Combustion

System". These are shown in figures 5.1, 5.2 and 5.3 respectively.

Performance data found for the Combustor Alone case were used as a datum with which to compare the performance of other configurations. By comparison with previous units, it also served to check that the combustor was working properly. Three different fuel chamber nozzles were used in the combustor during such tests. Access to them was relatively convenient for this configuration.

For the Combustor with Secondary Flow Ducting case two parameters were varied. The first was the distance between the ejector and the combustor inlet opening. This is shown as distance "Y" in figure 5.4. Secondly, the secondary flow duct length was varied by adding extensions shown as distance "X" in figure 5.4.

Finally, the complete system was operated. The Exit Combining Chamber (shown in figure 4.1) shape was varied in order to determine its effect on performance. Also, the effect of the Air Inlet Plenum and its attachments was determined.

5.1.1 Performance Parameters

Thrust, fuel consumption, combustion chamber dynamic pressure, and combustor exit temperature were measured. Performance curves of "specific fuel consumption versus thrust per unit combustion zone cross sectional area" were constructed for the various test situations. Specific fuel consumption is the fuel flow rate divided by the thrust. Combustion chamber surface temperatures and combustor exhaust flow

temperatures were measured for two configurations.

5.1.2 Experimental Proceedure and Equipment

General start up and operation for all three configurations was the same as that reported by Marzouk [13]. Dynamic pressure measurements were made using a Kistler model 601B1 quartz transducer, a Kistler model 504A charge amplifier, a Tektronix model 5223 digitizing oscilloscope and an HP 7004B x-y recorder. The ignition and auxiliary air connections as well as the thrust and fuel flow measuring systems are shown in figure 5.1. They are the same as those described in detail by Marzouk [13]. Auxiliary air was provided through the building compressed air system. The ignition power was provided by a high voltage transformer (connected to a 110 volt A.C. supply) to an automotive type spark plug. Both auxiliary air and ignition were required, only during start up, until a self sustaining pulse combustion cycle was achieved. The thrust measuring system was a simple "free-mass displacement" meter, which worked on the principle of conservation of momentum. The fuel flow rate was controlled by a simple throttle valve and measured with a calibrated choked nozzle device. Figure A.1 of the appendix shows the calibration curves for two nozzles. Using these curves, the fuel flow rate was found knowing the upstream fuel pressure and temperature as well as the nozzle size. Propane fuel was used for all tests.

5.1.3 Operational Problems

It was found that the performance range was very narrow for the

combustor operating with the secondary flow ducting attached. The combustor would not operate for the higher fuel flow rates as it would when operating on its own. This problem was corrected by insulating the combustion chamber. Thermocouples were added to the highest temperature areas to detect possible overheating of the combustion chamber. A sketch of the combustion chamber showing the thermocouple locations and the ceramic fiber insulation is displayed in figure 5.5. A stainless steel shield was used to hold the insulation in place.

The Pulse Combustor completed approximately 15 hours of total running time. The system was completely disassembled for inspection twice during this period. All components showed little sign of deterioration. On the second inspection some slight distortion of the combustion chamber was detected in the area between the pressure transducer boss and the fuel chamber. This was seen as minor and no corresponding repairs were made. It should be noted that the second inspection was carried out after the operation of the system with an insulated combustion chamber.

5.2 TESTS WITH THE COMBUSTION SYSTEM CONNECTED TO THE COMPRESSOR-TURBINE UNIT

5.2.1 Performance Parameters

In the results, so called "dimensionless" groups are used. These groups are the same as those presented in Yerneni's work. This allows for direct comparison of the two sets of results. These groups were used to take into account the variation, from test to test, in the ambient pressure and temperature. They are not truely dimensionless

because variables such as the linear dimension, molecular weight, the ratio of specific heats and the absolute viscosity were omitted; nevertheless, the groups are common in gas turbine performance testing. In Yerneni's work and the present investigation, the omitted variables were assumed not to vary and would therefore have no effect on the results. A derivation of the "dimensionless" groups is shown in reference 19. These groups incorporate the following parameters: gas temperature and pressure at various stations (T and P), turbine rotor speed (N), air mass flow rate (m_a), fuel flow rate (m_f) and ambient temperature and pressure.

5.2.2 Experimental Proceedure and Equipment

The operating procedure for the Second Generation Pulse Combustor, as part of the gas turbine, was the same as that described by Yerneni [19] for the first generation system.

It is suggested by the gas turbine manufacturer that during startup the turbine inlet temperature should not exceed 750^{o}C. It was found that this limit was easier to stay within when using the second generation system compared to using the first generation system. This may be linked to the fact that the second generation system required a lower fuel flow rate during startup.

Figure 5.6 displays the gas turbine setup. The compressor outlet (station 2) and turbine inlet (station 3) pressure and temperature measurement points are shown. As can be seen from this sketch, the conventional combustor is small with only 13% of the surface area of the second generation unit.

Another view of the system presented in figure 5.7, shows the

compressor inlet (station 1) and the turbine outlet (station 4) measurement points. The system was loaded by back-pressuring the turbine by use of a butterfly valve located in the turbine exhaust duct.

Static pressures were measured at each of the four measurement stations (figure 5.7) with the use of remotely located Validyne differential pressure transducers. Temperatures at these stations were measured using type K thermocouples connected to Doric made digital readouts (^{o}C). Air flow rate was measured with a venturi type air flow meter which was connected to a water manometer. This meter was incorporated with the compressor inlet duct. The fuel flow system and the combustion chamber dynamic pressure measuring equipment are the same as those used in the isolated tests (section 5.1.2).

Noise levels for specific locations near the gas turbine installation were measured using a Bruel & Kjaer Type 2218 Integrating Sound Level Meter.

5.2.3 Operational Problems

During a total of approximately 15 hours of gas turbine operation time the combustion system was disassembled several times. On two occasions, detailed inspections were carried out.

Two major problems were reported by Yerneni [19] concerning the first generation combustion system. They include repeated material failure (burn out) of high temperature areas of the combustion chamber and tailpipe as well as insufficient propane fuel pressure. These problems were not experienced with the present system. Fuel pressure levels were always sufficient for two reasons. First of all, the test

runs for this setup were carried out during warm weather. This kept pressure levels in the outdoor tank at a high level when the fuel was flowing. Secondly, the present combustor consumed 15 to 30% less fuel than Yerneni's configuration. It is believed that the elimination of the "burn out" problem is due to the new features of the present system. Design and material changes were made to the combustion chamber and tailpipe (described in section 4.2.1). The secondary flow system provides convective cooling to the relatively high temperature areas.

There are three problems that did show up in the second generation system. First, there was persistent fuel chamber nozzle clogging due to carbon particles. This carbon would build up on the inside walls of the fuel chamber cavity (refer to figure 5.8), break off, move along with the fuel flow and get lodged in the fuel nozzles. The problem could be detected during operation when the fuel flow meter choked nozzle downstream pressure became excessive. The fuel chamber had to be taken out for removal of this carbon. This is an important problem in the sense that the combustion system has to be almost completely disassembled in order to gain access to the chamber. Such maintenance was time consuming.

Secondly, fuel chamber cracking occurred towards the end of the test series. A similar problem was reported for the first generation system (section 2.2.3). Cracked areas were welded and machined smooth. Thicker walls used in this chamber, compared to previous models, did not eliminate the cracking problems as hoped. Surface wastage of chamber areas exposed to the hot combustion gases indicated excessive material temperatures in this area. As seen in figure 5.8, the cracking occurred

in the area fartherest away from the fuel inlet where little cool fuel flows. Also, it is believed that there may be excessive thermal stresses due to the basic design in this area.

Although these fuel chamber problems have shown up in other pulse combustors, they appear to be especially acute for the second generation system. This is likely due to the unique design features of this system. The operating temperature of the fuel chamber is higher because of the relatively hot secondary flow gases that are exposed to the chamber outside surface, which is cool compared to the combustion zone. In addition, there is approximately 2 feet of tubing and connections between the fuel chamber and the outer igniter hatch (on the air inlet plenum shown in figure 4.1). About 3 inches of this connection is within the secondary flow duct and is, therefore, exposed to high temperature gases. The remaining copper tubing length is exposed to temperatures of at least 150^{o}C. The result is a preheating effect of the fuel, no doubt contributing to excessive fuel temperatures within the chamber cavity.

The third problem is one of combustion chamber warpage in the area of the transducer boss. Figure 5.9 shows this condition. The bottom picture shows how both the transducer and spark plug bosses were bent slightly from the vertical. The top photo displays the inner hatch which is held butted against the bosses by the spark plug and transducer (that the hatch allows access to). The top surface of this hatch, which can also be seen in figure 5.2, is solidly bolted on to the secondary flow equipment. It is evident that at high loads the thermal expansion

of the combustion chamber, which was fixed at the nearby inlet, was greater then that of the cooler secondary flow duct. The result was a stress that deflected the bosses and caused warpage. The combustion chamber was taken to the shop and straightened. A hatch design change was made to allow axial movement between the hatch and the combustor. Figure 5.10 shows a thin stainless steel spacer which butts up to the combustor bosses and is held in place by acting as a single washer for the spark plug and transducer. When assembled, this plate sits against the bottom of the hatch. In this bottom the spark plug and transducer holes were drilled-out to allow for movement between the combustor and the hatch. Subsequent test runs were made and no further warpage occurred.

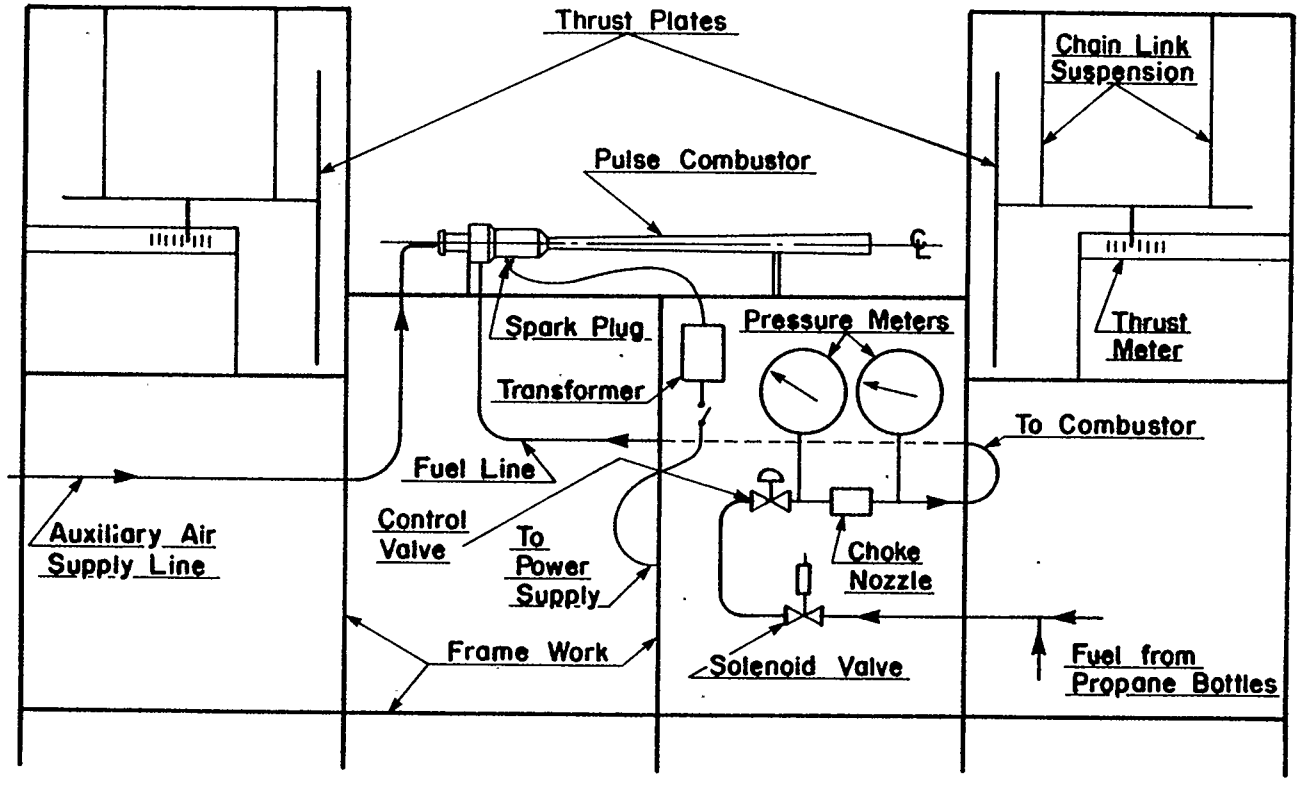

FIGURE 5.1 TEST STAND FOR OPERATING A PULSE COMBUSTOR IN ISOLATION

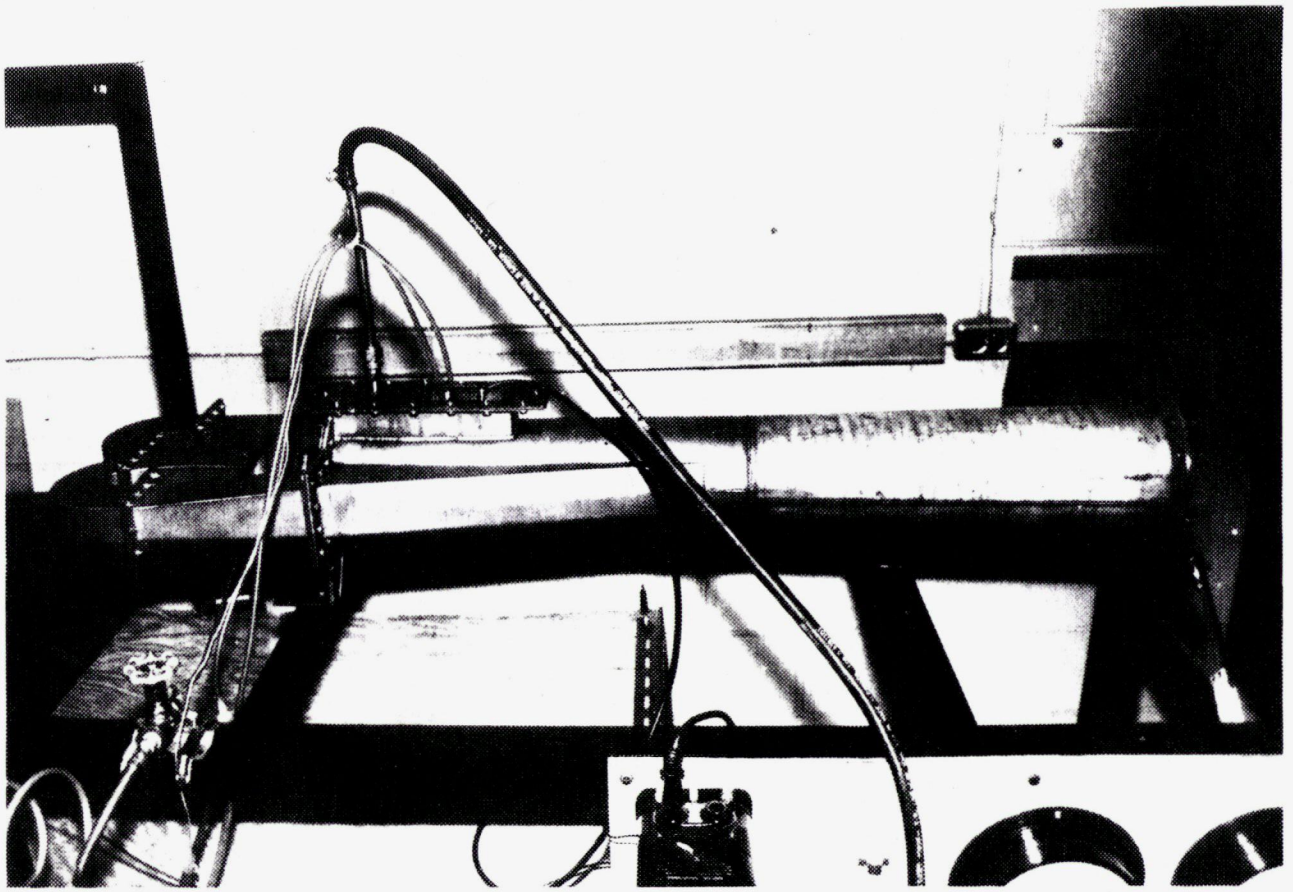

FIGURE 5.2 PULSE COMBUSTOR WITH SECONDARY FLOW SYSTEM ATTACHED (SECOND GENERATION SYSTEM)

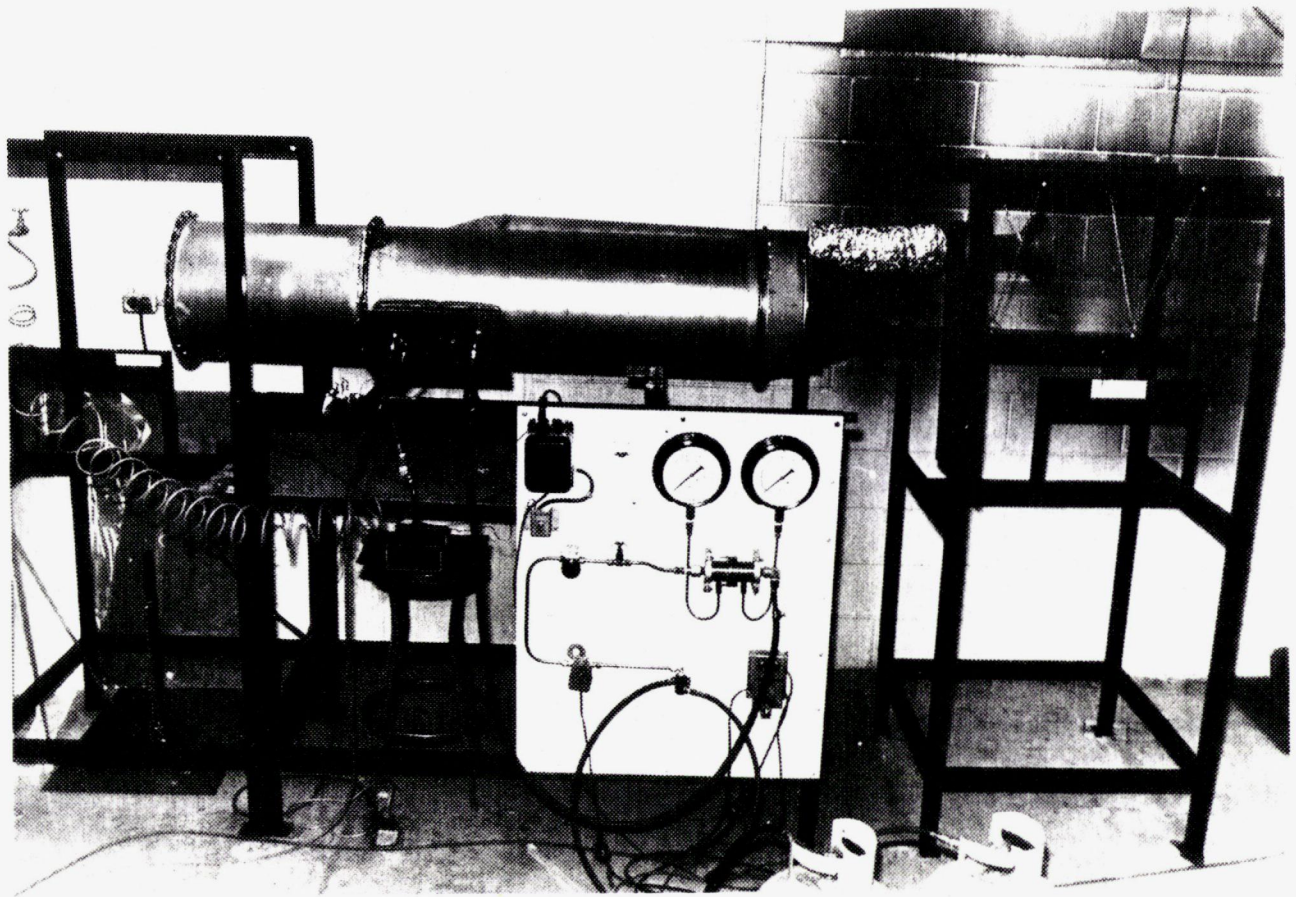

FIGURE 5.3 COMPLETE SECOND GENERATION PULSE COMBUSTION SYSTEM SETUP ON TEST STAND

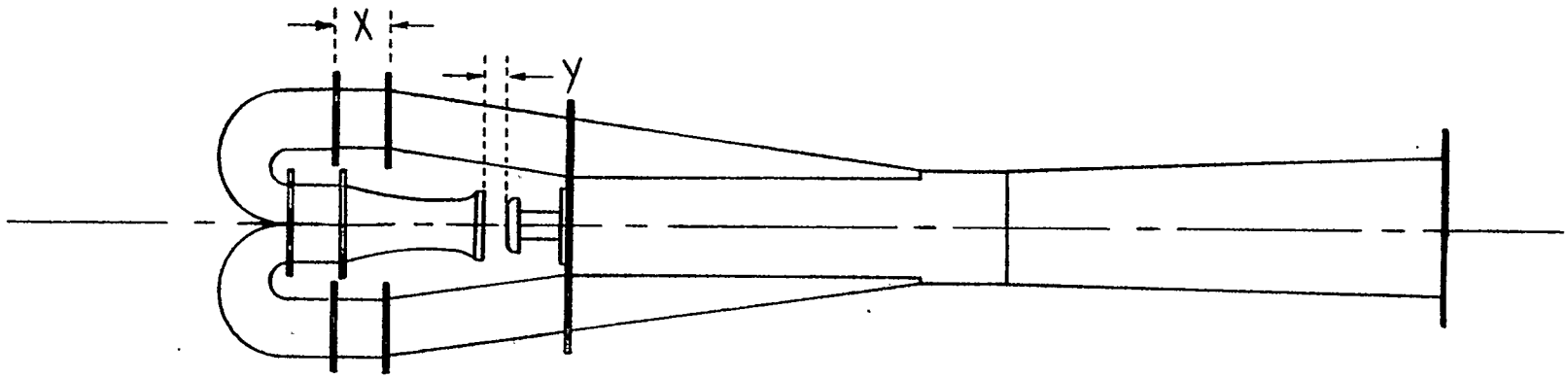

FIGURE 5.4 ADJUSTMENT OF SECONDARY FLOW DUCTING

X = secondary flow length addition

Y = distance between combustor inlet and ejector opening

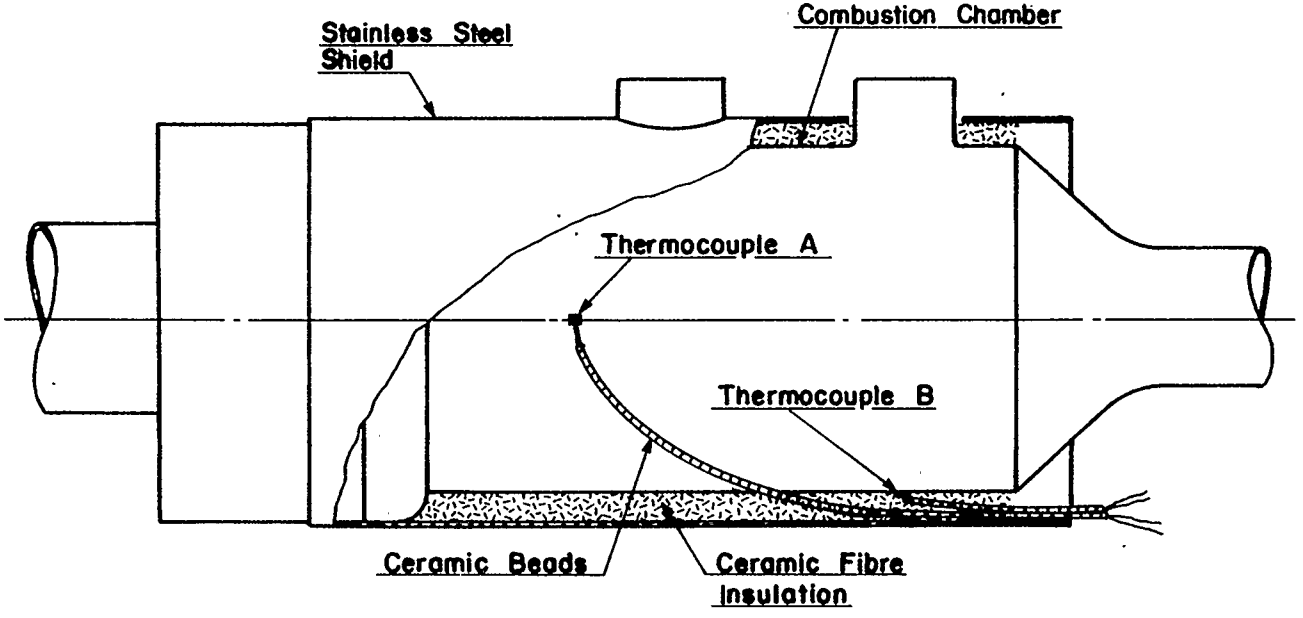

FIGURE 5.5 ADDITION OF THERMOCOUPLES AND INSULATION TO THE PULSE COMBUSTION CHAMBER

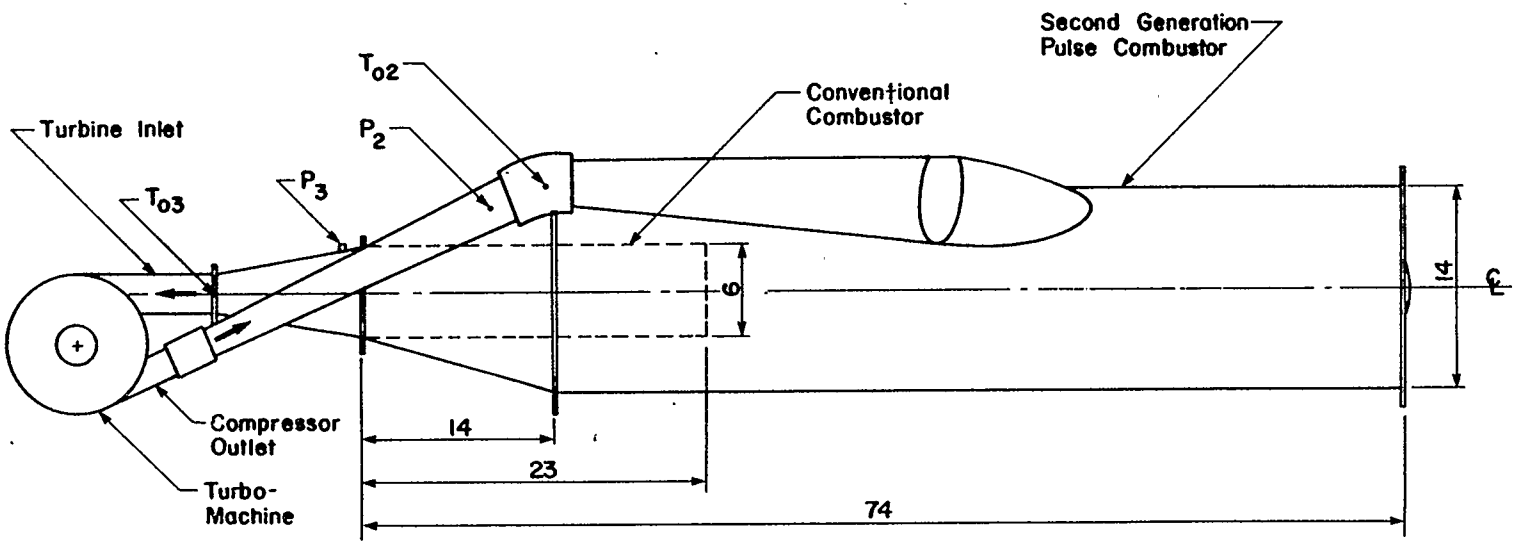

FIGURE 5.6 COMBUSTION SYSTEM - TURBO MACHINE CONNECTION
(LENGTHS SHOWN IN INCHES, 1 INCH = 25.4 mm)

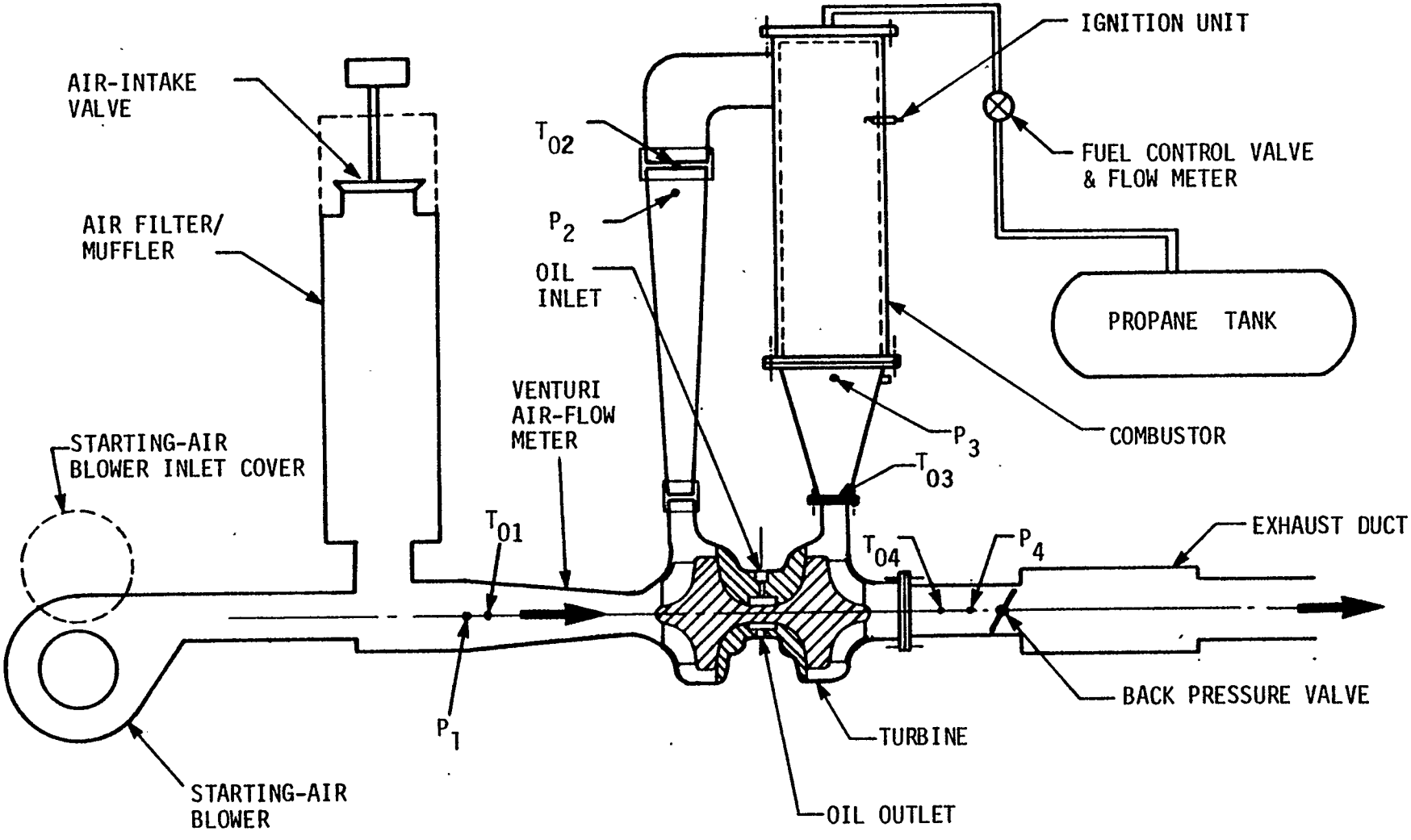

FIGURE 5.7 DIAGRAMMATIC ILLUSTRATION OF CUSSONS P.9000 GAS GENERATOR WITH CONVENTIONAL, STEADY FLOW COMBUSTOR [2]

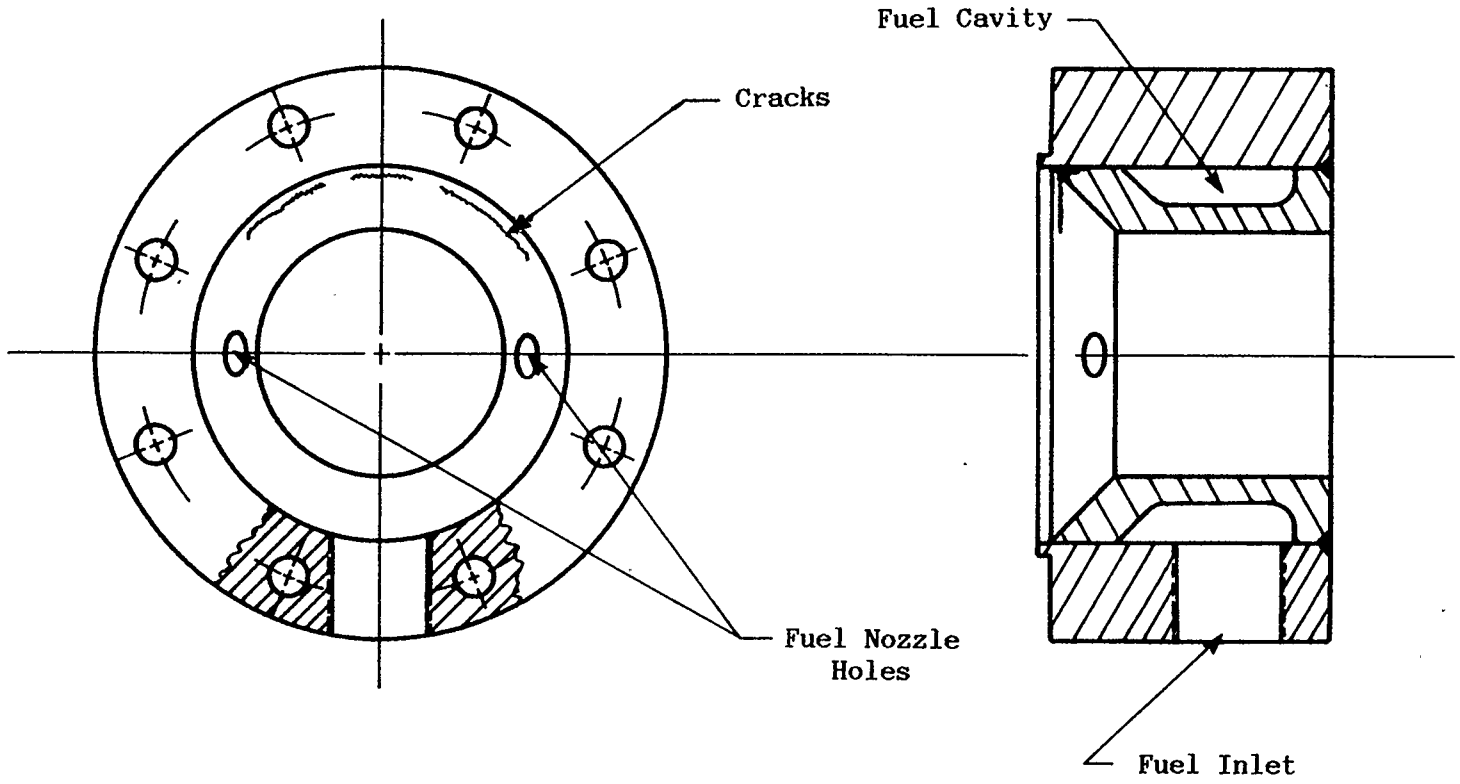

FIGURE 5.8 PULSE COMBUSTOR FUEL CHAMBER CRACKS

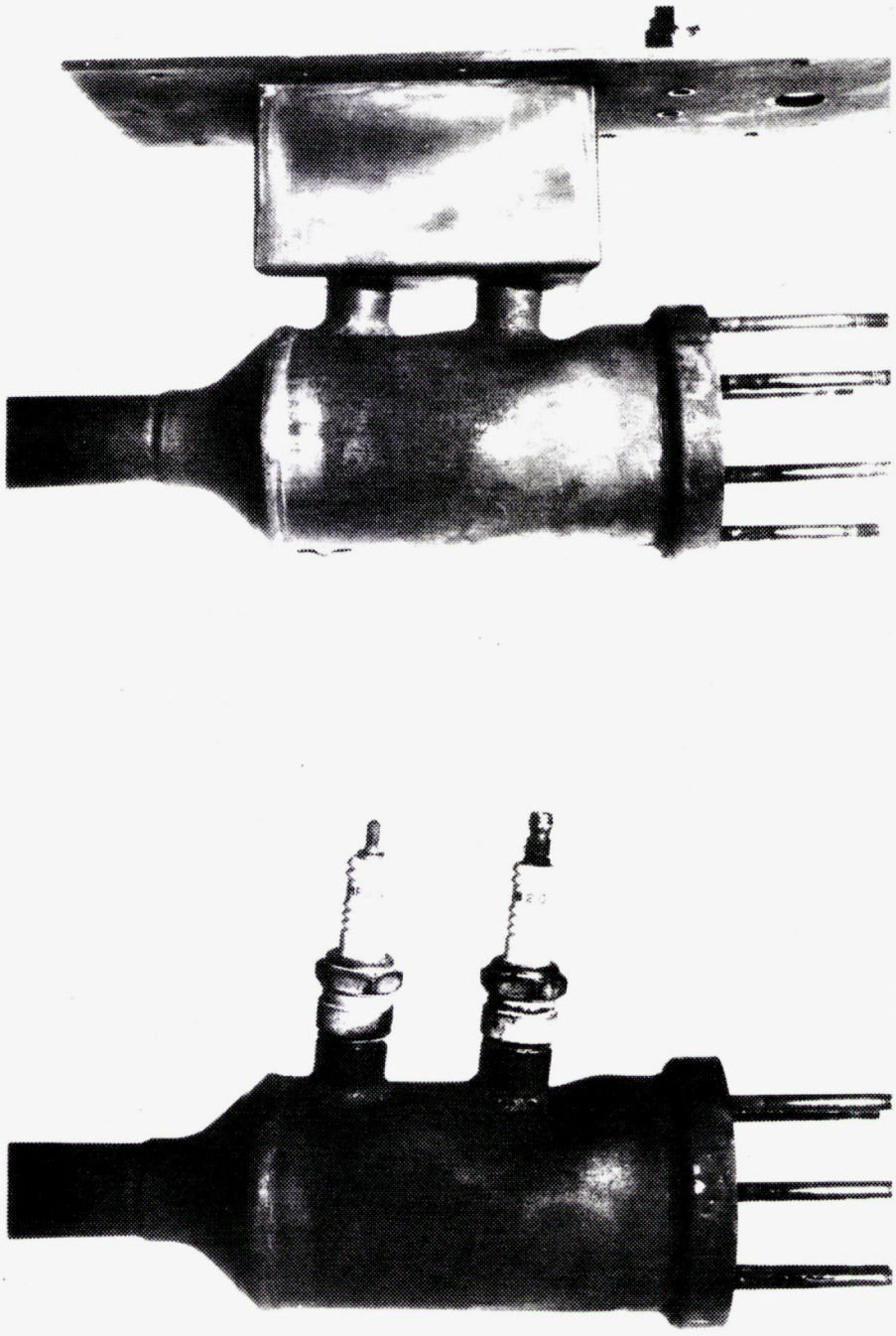

FIGURE 5.9 COMBUSTION CHAMBER WARPAGE IN SECOND GENERATION SYSTEM

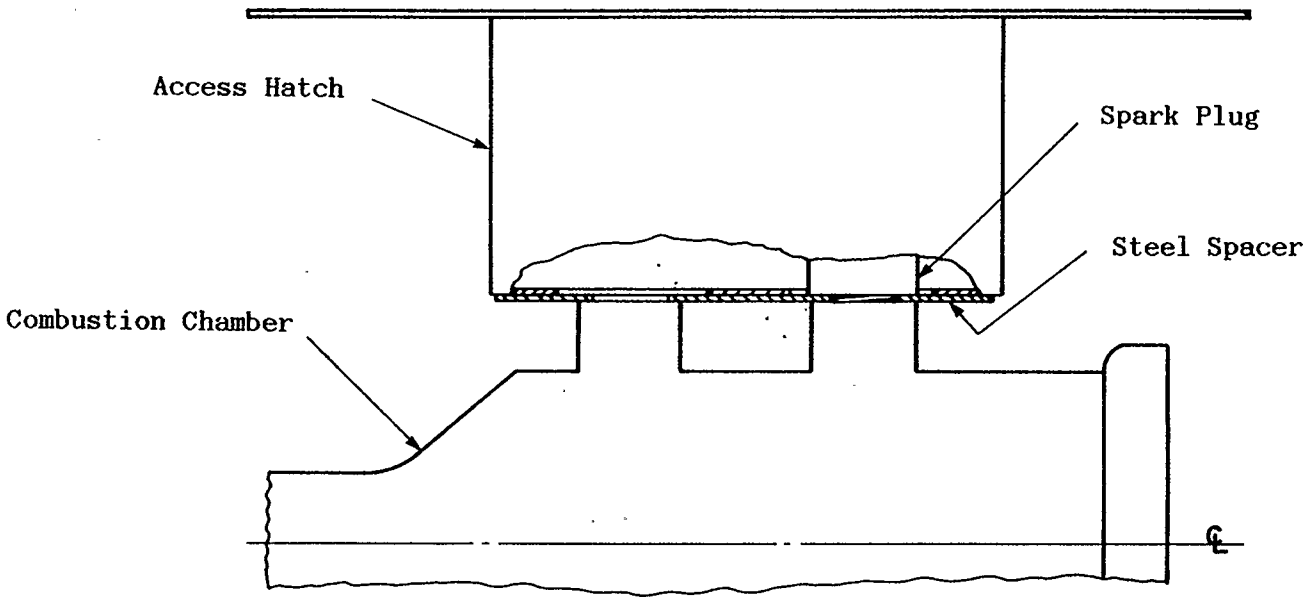

FIGURE 5.10 CONNECTION OF SECONDARY FLOW DUCT HATCH TO PULSE COMBUSTION CHAMBER

CHAPTER 6

RESULTS, ANALYSIS AND DISCUSSION

6.1 INTRODUCTION

Results are presented covering the performance of three combustion systems: the Conventional Combustor (CC), the First Generation Pulse Combustor (FGPC) and the Second Generation Pulse Combustor (SGPC). For reasons stated in section 5.1, performance tests reported in section 6.2 were carried out for the SGPC operated in isolation. Both the CC and the SGPC were operated by the author as part of the gas turbine. Results for the operation of the FGPC as part of the gas turbine were extracted from earlier work carried out by Yerneni [19]. A comparison between the gas turbine performances with these combustors is presented in section 6.3.

6.2 ISOLATED COMBUSTOR

6.2.1 Pulse Combustor Only

The performance curve for the pulse combustor operated alone is shown in figure 6.1. The "alone" operation was carried out for two reasons. First, to ensure that the combustor itself was working properly before connecting it to any attachments. Secondly, to establish a performance benchmark for comparison with other systems containing this combustor.

As can be seen in figure 6.1, the performance of the present pulse combustor is close to that of the pulse combustor used earlier within the FGPC system [4], which is 20% larger. Experimental results [9]

(shown earlier in figure 2.8) predict that the smaller combustor should have a specific fuel consumption that is about 3% greater at maximum thrust, due to size effects. Similarly, the specific thrust should be about 70% of that of the larger unit. It is apparent, therefore, that the present combustor is performing very well.

Combustion chamber dynamic pressure traces were recorded for all reported isolation setups. The operation frequency ranged between 250 and 260 Hz and was essentially independent of fuel flow rate.

6.2.2 Pulse Combustor with Axisymmetric Secondary Flow Duct Attached

The newly designed secondary flow system, consisting of a flow rectifier-thrust augmenter and a cylindrical flow duct, was attached to the present pulse combustor (refer to section 4.2 for design details).

Figure 6.2 displays the performance curves for several values of combustor inlet to ejector inlet distance, Y. They were found for a given secondary flow duct length of 59.7 inches (X = 0). A "Y" distance of 2.00 to 2.25 inches provided the best performance. For all other data reported for this system and the complete system (section 6.2.3) the distance used was 2.00 inches. Earlier work carried out by Marzouk [13] showed an optimum value for this distance to be 1.97 inches (50 mm) for the same size combustor as that used within the FGPC system.

When comparing figures 6.1 and 6.2, it can be seen that the overall performance range achievable with the combined combustor-secondary flow system is much smaller than the range achievable with the combustor

operated alone. At the higher fuel flow rates, the combustor with attached secondary flow would operate for only a fraction of a minute and then what is referred to as "premature extinction" would occur. In other words, unsteady flow stops, the thrust goes to zero and steady flow combustion begins. At this point, large yellow flames bellow from the tailpipe outlet; with the inlet air being induced only by the fuel jets. The designed purpose of the type of secondary flow ducting used in the present system is to provide convective cooling to the combustion chamber. The result is a reduction of energy losses to the ambient in this area. It was assumed that if it was performing as intended, a resulting cooler combustor operating temperature may be causing this premature extinction. The combustion chamber was then insulated as shown in figure 5.5 (section 5.1.3). Subsequent tests showed the performance range to be nearly tripled, as shown in figure 6.3.

Two thermocouples, shown in figure 5.5, were placed on the combustion chamber. Surface temperatures were measured in the above system for both cases of noninsulated and insulated combustion chambers. The temperature data for various fuel consumption rates is shown in figure 6.4. These data give an indication of the combustion chamber surface temperature that coincides with the conditions necessary to avoid premature extinction. When the maximum surface temperature was in the order of 650^{o}C, extinction occurred at a fuel flow rate of approximately 5 kg/hr. When the surface temperature was in excess of 1000^{o}C, premature extinction did not occur and the combustion system could exceed a fuel consumption of 7 kg/hr.

Figure 6.5 displays the results for the setup with an insulated

combustion chamber for two secondary flow duct lengths. The performance appears to be fairly insensitive to moderate changes in flow duct length. The longest duct, however, provides slightly better performance. In contrast, as shown in figure 6.6, the same apparatus without insulation over the combustion chamber displayed slightly better performance for the shortest secondary flow duct length. This opposite behavior would suggest that the optimum duct length depends on the operating temperature of the combustor. Combustors with higher operating temperatures seem to require a longer secondary flow for best performance.

Figure 6.7 shows overall combustor temperature ratio curves for thermocouple traverses over the radius of the combustor tailpipe-secondary flow exit. Results are shown for a fuel flow rate of 4.20 kg/hr for two secondary flow duct lengths. Operation with the longest secondary flow duct results in cooler exhaust temperatures in the region of the secondary flow exit. It is believed that this results from greater secondary flow heat losses to the ambient from the additional exposed ducting (refer to figure 5.4, section 5), and/or better flow augmentation resulting in an increased mass flow rate. Better flow augmentation means that during the part of the cycle when there is a back flow from the combustor inlet into the ejector, there is more ambient air entrained in this flow entering the ejector (which is then sent down the secondary flow channels). Improved augmentation is supported by the fact that the thrust produced was slightly greater than that for the shortest secondary duct length, for a given fuel consumption, as reported in figure 6.5.

6.2.3 Complete Combustion System

Figure 6.1 shows the best performance achieved with the complete system operated in isolation. Compared to the performance of the "pulse combustor with secondary flow" case, for a given thrust, specific fuel consumption was 10% to 20% greater. It is believed that this drop in performance is due to fluid flow losses and possibly a disturbance of the combustor inlet wave mechanics due to a "closing in" effect. Flow losses are expected to occur mainly in the compressor outlet diffuser duct shown earlier in figure 4.1. Also, it was necessary to connect to this duct a hose 25 inches long in order to clear the thrust plate. This can be seen in figure 5.3 (section 5).

Initial runs for the complete system were carried out with the combustion chamber not insulated. Also, the shortest secondary flow length of 59.7 inches was used. In this case, chamber surface temperatures ranged from 700^{o}C to 800^{o}C for the hottest areas. Premature extinction occurred at a fuel flow rate of approximately 5 kg/hr for these test runs. The above temperature range falls between the temperatures, shown in figure 6.4, for the noninsulated and insulated chamber cases of the "pulse combustor with secondary flow duct" setup (section 6.2.2). This is further evidence that conditions necessary to avoid this extinction problem correspond to surface temperatures in the hottest areas of no less then approximately 1000^{o}C.

At this point a 1/32nd inch thick stainless steel shield was placed over the combustion chamber with a 1/4th inch air space left between them. It was believed that for this case the use of insulation, described in section 6.2.2, would result in excessive chamber wall

temperatures and possible failure. Further testing showed that premature extinction was eliminated. Surface temperatures in the region of 900 to 1000^{o}C were recorded.

The remaining test work was focused largely on determining the effect of an exhaust combining chamber. The effects of shielding the combustion chamber, adding the combining chamber, and changing the combining chamber shape are shown in figure 6.8.

Performance appears to be sensitive to combining chamber shape. Both the "diverging-converging" and the "converging only" chambers, displayed in figure 6.8, had the same volume. The superior performance of the "converging only" chamber is believed to be linked with the nonsteady nature of the flow in the exhaust area. This chamber provides an abrupt four fold cross sectional flow area increase before converging to the turbine inlet duct size. The result is a pressure wave decoupling effect between the pulse combustor (with its associated secondary flow) and the turbine ducting. From a fluid loss point of view the diverging-converging chamber is expected to have superior performance. This would indicate that in this area, wave mechanics has a greater influence on performance than flow losses.

Work carried out by Cronje [4] on a larger pulse combustion system (figure 3.2, Chapter 3) shows that not only combining chamber shape, but also chamber volume has significant effects on performance. With this in mind, an extension was added to the "converging only" chamber increasing its volume by 55%. From the results, shown in figure 6.9, this larger chamber causes poorer performance than the original chamber. It may be the case that there is an optimum volume for best performance

that was surpassed. The larger surface area of this high temperature component results in greater heat losses. It also appears that the convergence angle and convergent wall to combustor outlet distance may be added factors.

The final setup chosen for use on the gas turbine was as follows: The complete combustor with, the smallest volume "converging only" combining chamber, the 59.7 inch (shortest) secondary flow duct length, and the combustion chamber without either insulation or a shield. It was believed that the higher temperature inlet conditions provided by a compressor would force the combustor to operate at a higher temperature. This would eliminate the need of a shield or insulation to be placed on the combustion chamber.

6.3 COMBUSTOR INSTALLED ON GAS TURBINE

6.3.1 Unsteady Flow Behavior

The Second Generation Pulse Combustion System (SGPC) operated in an unsteady flow manner as shown by the combustion chamber dynamic pressure traces of figures 6.10 and 6.11. These traces were recorded for the back pressure 0 load case for two fuel flow rates. The pulsation frequency was found to be independent of fuel flow rate and equal to approximately 275 Hz. The peak to trough pressure differential averages 10 psi, corresponding to a fuel flow rate of 4.80 kg/hr. In comparison, the complete combustion system operated in isolation (section 6.2.1) at the same fuel flow rate produced a 30% greater pressure differential of 13 psi and ran at a 7% lower frequency of 255 Hz. This effect is also seen in figure 6.12, which compares nearly equal amplitude pressure

traces for the two cases. In the "combustor in gas turbine" case the fuel flow was 20% greater. However, if we correct this flow rate for ambient conditions, as in figure 2.7 earlier, the effective fuel consumption is nearly the same. A similarity of combustor pressure ratios would be expected rather than a similarity of pressure excursion amplitudes. The implication is, therefore, that the combustor was working less vigorously in the gas turbine than would be expected on the basis of the tests in isolation.

The pressure traces in figure 6.12 have been lined up so that the centre peaks coincide. These peaks are nearly identical in size and shape. On either side of these peaks it can be seen that the troughs are similar in shape. However, the trace B troughs are shorter in the time axis direction. This indicates that operation of the combustor within the gas turbine affects mainly the induction part of the pulse cycle with respect to the time scale. This shows as a decrease in the proportion of induction time to the overall cycle time.

6.3.2 Fuel and Air Consumption

The fuel and air consumption characteristics of the Second Generation Pulse Combustor (SGPC) more closely match those of the Conventional Combustor (CC) then those of the First Generation Pulse Combustor (FGPC).

Fuel and air consumption curves are shown in figures 6.13 through 6.18 for the gas turbine loads corresponding to back pressure settings of 0, 1 and 2. It should be kept in mind that the back pressure setting 0 implies only the inherent back pressure associated with the exhaust

kinetic energy loss and frictional loss.

Initial test runs for the SGPC were carried out with its external surface exposed to the ambient. For this case, the SGPC fuel consumption was 5 to 8%, 6 to 9% and 8 to 12% greater for the back pressure 0, back pressure 1 and back pressure 2 settings respectively, as compared to the CC. For a given back pressure, the first quoted percentage corresponds to the smallest difference, which occurs at a low to midrange compressor-turbine rotor speed. The second percentage corresponds to the greatest difference, which always occurs at the maximum shown rotor speed. The SGPC has greater surface area and operates with a higher outside surface temperature than CC. With the information from thermocouples (visible in figure 6.28) placed on the exposed surface, it was estimated that approximately 8% of the energy entering the system was lost to the ambient (refer to section 6.3.5 for a detailed explanation). The SGPC was then covered with a layer of ceramic fiber insulation approximately one inch thick. Further testing showed a 3 to 6% reduction in fuel consumption for this insulated combustor. Fuel consumption curves (figures 6.13 to 6.15) for this case show that the insulated second generation pulse combustor (ISGPC) has nearly identical fuel consumption to that of the CC for back pressure 0 and back pressure 1 load settings in the lower half of the rotor speed range. For the back pressure 2 setting and the upper half of the rotor speed range of any load, the fuel consumption for the ISGPC was greater than that of the CC to a maximum of approximately 5%.

As compared to the First Generation Pulse Combustor (FGPC) the fuel consumption for the ISGPC is, on average, 22%, 19%, and 17% lower for

the back pressure 0, back pressure 1 and back pressure 2 load settings respectively. The FGPC was poorly matched to the compressor-turbine in that it was too large and was therefore forced to operate in the low end of its performance spectrum (refer to section 3.2.1). Also, and more importantly, this combustor had areas such as the combustion chamber and the secondary flow ducts which were exposed to the ambient, resulting in large energy losses.

Figures 6.16, 6.17 and 6.18 show the air mass flow characteristics of the three combustion chambers for the three back pressure loads. The compressor air inflow rate for the first and second generation pulse combustors is as much, or more, than for the CC for all running conditions. The FGPC shows the highest air consumption of the three combustors. The two pulse combustors display opposite behaviours with respect to load. As the back pressure is increased, the FGPC is characterised by an increasing air flow compared with the CC. In contrast, the behavior of the SGPC tends to converge with that of the CC as load is increased. At the load setting 0 condition the SGPC air flow is approximately 4% more for a given rotor speed. At maximum load, the air flows are virtually the same.

In earlier work by Yerneni [19], from which the data for the FGPC was obtained, it is stated that the high air flow is likely due to a relatively poor compressor efficiency resulting from a high compressor operating temperature. As shown earlier in fig 2.2, the FGPC has an exposed combustor and secondary flow system, causing a higher laboratory room temperature. Also an additional conical exhaust duct, not used on the CC, was located close to the compressor-combustor connection duct.

The result was a higher compressor casting temperature. The SGPC has much lower heat losses than the FGPC; 8% compared to 30%. The SGPC also uses the conical exhaust duct. However, in this case, the compressor-combustor connection duct was insulated.

It should be noted that the Insulated Second Generation Pulse Combustor (ISGPC) has vitrually identical air consumption to that of the uninsulated SGPC.

6.3.3 Pressure Gain Characteristics

Combustor Pressure Ratio curves are shown for three back pressure settings in figures 6.19 to 6.21. The Second Generation Pulse Combustor produces a stagnation pressure gain ranging from 1.1% to a maximum of 1.6% during normal operation. This is approximately four times higher than the 0.25% to 0.45% stagnation pressure gain range of the First Generation Pulse Combustor (FGPC). The Conventional Combustor (CC) produced a stagnation pressure loss ranging from -1.0% to -2.0%. It is believed that the superior pressure gain performance of the SGPC, over that of the FGPC, is due to better combustor size component matching and reduced energy and fluid flow losses inherent in the SGPC design (refer to sections 3.2, 4.1 and 4.2.2).

The shape of the pressure ratio curves over the rotor speed range can provide information about the respective combustion chambers. The negatively sloped curves of the CC reflect the fact that total pressure losses due to the "fundamental loss" and fluid friction increase with additional energy added and increasing flow velocities. In contrast, the curve slopes for the pulse combustors are more horizontal for the

FGPC curves and even positive for parts of the SGPC curves. These slope characteristics display the natural ability of the SGPC combustor to effectively overcome increasing pressure drops associated with these losses that exist in all combustors. Note that fundamental losses result in only about 5% to 10% of the total losses for a combustor operating in its temperature ratio range (refer to section 6.3.4) and can therefore be ignored in the above argument [3].

The pressure gain curve shapes provide information about where a pulse combustor is operating within its own performance range. Figure 2.7 displays the pressure gain curve for a pulse combustor in isolation under ambient conditions. The shape of this curve is similar to that of the pressure gain curve for the SGPC operated within the gas turbine at a back pressure 2 load setting (figure 6.21). This curve shows a maximum in its shape. This indicates that the combustor is running in the upper half of its operating range. The pressure gain peak value for the isolation case occurs near the maximum fuel consumption value. In the design stage (section 3.2.2), the SGPC was sized with the intention that the combustor would operate in the higher end of the performance spectrum where the pressure gain is the greatest. It appears that this objective has been achieved. Also, the larger combustor used in the FGPC provided a lower pressure gain. This shows, as might be expected, that the larger combustor was running in the lower part of its operating range where the pressure gain is small.

The pressure gain values shown in figures 6.19 to 6.21, referred to earlier, are the minimum ones obtained for the SGPC. During a minority of test runs, stagnation pressure gain values as high as 2.1% were

measured for back pressure 0 and back pressure 1 load cases. The results are presented in figure 6.22. The combustor operates in what appears to be two distinct modes. There was one mode that the combustor operated in most of the time, during which the lower pressure gain was achieved. The second mode corresponds to performance that resulted in higher pressure gain. These modes could be distinguished by sound pitch. For certain test runs this change in mode occurred during operation. In these cases the combustor produced high pressure gain until about half the way through the test, when the apparatus was thoroughly warmed up. At this point the sound would change and the pressure gain would drop to the lower values. The reason for this behaviour is unknown. It is believed, however, that fine tuning the combustor design could force it to consistently operate in either one mode or the other. This fine tuning, which was not carried out in the present investigation, is suggested for future work (section 7.2). Note that only a small amount of data were gathered for the high pressure gain mode of operation. All other results for the SGPC, except for those shown in figure 6.22, correspond to the lower pressure gain mode of operation.

6.3.4 Temperature and Pressure Ratios

Results for the compressor and turbine pressure ratios for the CC and the SGPC are shown in figures 6.23 to 6.27. For each loading condition, the pressure ratios for the SGPC and the CC are very close. Because of pressure gain, one would expect that the stagnation pressure in the turbine exit duct (P_{04}) would be greater for the SGPC than for

the CC for a given load and turbine rotor speed. This idea is supported by the fact that the turbine power must be sufficient to drive the compressor and overcome frictional losses. The P_{04} measurements, indeed, show this to be true. This behaviour is an important factor in the calculations presented in section 6.3.7.

Cycle temperature ratio curves, displayed in figures 6.26 and 6.27, show that turbine inlet temperature increases with increasing back pressure. This temperature ratio ranges from a minimum of about 2.65 to a maximum of nearly 3.25.

The turbine inlet temperature was calculated using a heat balance that included the combustor inlet temperature, the fuel to air ratio, specific heat, and the heat losses (see appendix, page 129). Using estimated combustor surface temperatures and areas, the heat losses were calculated to be 2% and 0.5% of the input energy for the insulated SGPC (ISGPC) and the CC respectively. It was also assumed that both combustors have the same combustion efficiency of 100%. The measured turbine inlet temperature values were not used because they were believed to be inaccurate. The protected thermocouple used for this measurement had its tip located approximately one third the way across the duct cross section. Temperature gradients in the gases resulted in readings that did not reflect the mass average temperature. This was especially so with the CC, where the turbine inlet temperature was actually "measured" to be lower than the turbine outlet temperature! Due to better fluid mixing of the unsteady flow, the turbine inlet readings for the SGPC were found to be closer to the calculated values.

This same problem is described in earlier work carried out by Yerneni [19] and is one that should be corrected in future work with this system.

6.3.5 Component Surface Temperatures

Thermocouples were placed at various locations on the SGPC to measure the temperatures of the combustor outside surface and the highest temperature areas of the combustion chamber surface shown in figures 6.28 and 5.5 (section 5) respectively. The combustion chamber surface temperatures were found to reach a maximum of approximately 950^{o}C for back pressure 0 conditions near maximum rotor speed and fuel flow rate of 5.84 kg/hr. In comparison, for approximately the same fuel flow rate, this system reached a maximum of about 850^{o}C when operated in isolation (refer to section 6.2). It is believed that the difference is due mainly to the fact that the compressor delivers the air to the combustor at a temperature that is about 80^{o}C higher than ambient. These temperature values are acceptable, with respect to at least short term durability, when one considers that the SGPC was operated safely in the isolated state with its combustion chamber insulated. In this case a maximum temperature of 1127^{o}C was reached without significant damage. Over a total of roughly 15 hours of operation with this combustion system connected to the compressor–turbine unit, the combustion chamber did not fail.

In order to estimate the heat loss through the outside plenum and the exhaust chamber of the SGPC to the ambient, five thermocouples were placed on these exposed surfaces of the uninsulated combustor at various

locations. Figure 6.28 shows these locations along with the corresponding temperatures for a given fuel consumption. Using these temperature data and surface area values, the energy loss was calculated to be approximately 8% of the energy entering the system. This calculation took into account both convection and radiation.

6.3.6 Noise Level

Noise level readings were carried out for both the CC and the insulated SGPC. They were taken from two specific locations. One was taken inside the laboratory at approximately four feet away from the combustor area, and the other taken outside the laboratory at two feet away from the turbine exhaust exit.

For a rotor speed of about 75000 rpm, with the gas turbine under "load 0" conditions, the inside noise level was 100 dB for the insulated SGPC compared to 91 dB for the CC. The exhaust noise level for this case was 96 dB for the ISGPC and 93 dB for the CC. The fact that the difference in noise level at the exhaust is much less than the difference inside indicates that the turbine is effective at damping out a great deal of the pressure pulsations and thus the noise.

6.3.7 Gas Generator Performance Comparison

The performance of the turbo-machine operated with the Conventional Combustor (CC), compared to that of operation with the Insulated Second Generation Pulse Combustor (ISGPC), can be assessed from a gas generator point of view. Such a study concerns the conditions of the gas flow exiting the gas generator turbine. This point of view considers the

combined effect of air and fuel mass flow rate, and turbine exit pressure and exit temperature.

The earlier examination of performance for the two combustion systems, in sections 6.3.2 to 6.3.4, involves a comparison of single parameters such as fuel and air mass flow rate for a given turbine rotor speed.

The gas generator performance, η, can be considered a function of $\dot{m}_{gas}$, $\dot{m}_{fuel}$, P_{04}, T_{04}, and the pressure drop across the back pressure valve, ΔP_v. The comparison is made by considering the work output of a fictitious back pressure turbine. Applying isentropic relations and knowing that the gas generator exit pressure is much greater than the pressure drop across the back pressure valve, the following can be written:

$$\frac{\eta_{pc}}{\eta_{cc}} = \frac{\dot{m}_{air,pc}}{\dot{m}_{air,cc}} \times \frac{P_{04,cc}}{P_{04,pc}} \times \frac{T_{04,pc}}{T_{04,cc}} \times \frac{\dot{m}_{fuel,cc}}{\dot{m}_{fuel,pc}} \times \frac{\Delta P_{v,pc}}{\Delta P_{v,cc}} \qquad (6.1)$$

where, $$\frac{\dot{m}_{gas,pc}}{\dot{m}_{gas,cc}} \simeq \frac{\dot{m}_{air,pc}}{\dot{m}_{air,cc}}$$

since, $\dot{m}_{gas} = \dot{m}_{air} + \dot{m}_{fuel}$, and, $\dot{m}_{air} >> \dot{m}_{fuel}$. Also, T_{01} and P_{01} (ambient) are the same for both cases. Note that equation 6.1 is written assuming that the fictitious turbine will have the same efficiency for both cases.

Two other important parameters to consider in this comparison are turbine rotor speed and turbine inlet (cycle maximum) temperature. It was found that for a given "dimensionless" rotor speed the turbine inlet temperature was often different between operation for the two combustors. The comparison can therefore be considered in one of two ways; for a given rotor speed, or for a given turbine inlet temperature.

Figure 6.29 shows the gas generator performance comparison over the rotor speed range. For the back pressure 0 and back pressure I load settings the ISGPC provided better performance than the CC over the full range of rotor speed. The maximum performance increase is in the region, for this very low pressure ratio unit, of 40%. However, for the high rotor speed range and the back pressure II setting, ISGPC operation provided a slightly poorer performance to a maximum decrement of nearly 4%.

Table 6.1 shows the data for the "equal turbine rotor speed" comparison. This shows that the air mass flow rate and the pressure drop across the back pressure valve (exit delta pressure) are consistantly higher for the ISGPC operation. In this sense the ISGPC out-performs the CC. This, however, is counteracted, to varying degrees, by the greater fuel flow rate, lower turbine exit temperature and higher turbine exit pressure for the ISGPC. The difference between the turbine inlet temperature for the two combustors is also shown in the table and is plotted in figure 6.30. The ISGPC provides "cooler" operation for the lower half of the back pressure and rotor speed ranges. This interestingly corresponds roughly to the ranges for which the ISGPC performance (η_{pc}) is the best, compared to CC performance.

The measured turbine exit temperatures used in the above analysis are somewhat suspect. As discussed in section 6.3.4, there appears to be larger temperature gradients across the turbine inlet duct for the CC then for the ISGPC, due to mixing affects. It is possible that the same behaviour is occurring in the turbine exit duct. It is likely, however, that it would happen to a lesser extent in this case, because of the mixing which the turbine would provide. There is an indication that measured turbine exit temperatures for the ISGPC are artifically low compared to those for the CC. This is evident mainly for the maximum back pressure load setting (II), where the turbine inlet temperatures are equal for both combustors but the turbine outlet temperatures are about 4 to 8% lower for the ISGPC (for given turbine rotor speeds). For this reason it is believed that the predicted performance of the ISGPC is artificially low for high loads. With this in mind, the above performance analysis was recalculated using an estimated turbine exit temperature ratio, also shown in table 6.1, which follows the behaviour of the turbine inlet temperature ratio (see appendix, page 129). It must be kept in mind that the turbine inlet temperatures were calculated using a heat balance, as stated in section 6.3.4., and are assumed to be more accurate than measured temperatures. The recalculated results, shown in figure 6.31, differ significantly from the earlier results (figure 6.29) only for the back pressure II load setting. This indicates that the ISGPC performes better than the CC for all load conditions over nearly the entire rotor speed range. With respect to load and rotor speed, both sets of performance calculations above show similar trends to the fuel comsumption comparison made earlier in

section 6.3.2. Overall, however, this analysis shows that the ISGPC performs more favourably than the fuel consumption alone would indicate. In short, more fuel was being put into the ISGPC but more gas power was being put out of the gas generator.

Table 6.2 shows data for the performance analysis based on "equal turbine inlet temperatures". This comparison indicates that the ISGPC performes better for back pressure 0 and back pressure I load settings, in the higher rotor speed range, and poorer for the lower range. In contrast, the "equal turbine rotor speed" analysis (table 6.1) predicts poorest ISGPC relative performance for the higher rotor speed range. It should be kept in mind that this comparison is dependent on the turbine inlet temperature characteristics of each combustor which show quite different behaviours.

Yerneni [19] made predicitons, based on simple theory, of gas generator performance for various combustor pressure ratios, as referred to in chapter 1 (section 1.2.1). These predictions, shown in figure 1.4, were made assuming the turbine and compressor isentropic efficiencies to be both equal to 85%. It is believed that the system tested has turbine and compressor isentropic efficiencies of approximately 85% and 70% respectively. For the given compressor temperature rise it is predicted, from figure 1.4, that the ISGPC would provide a thermal efficiency of approximately 14.0% compared to 13.0% for the CC.

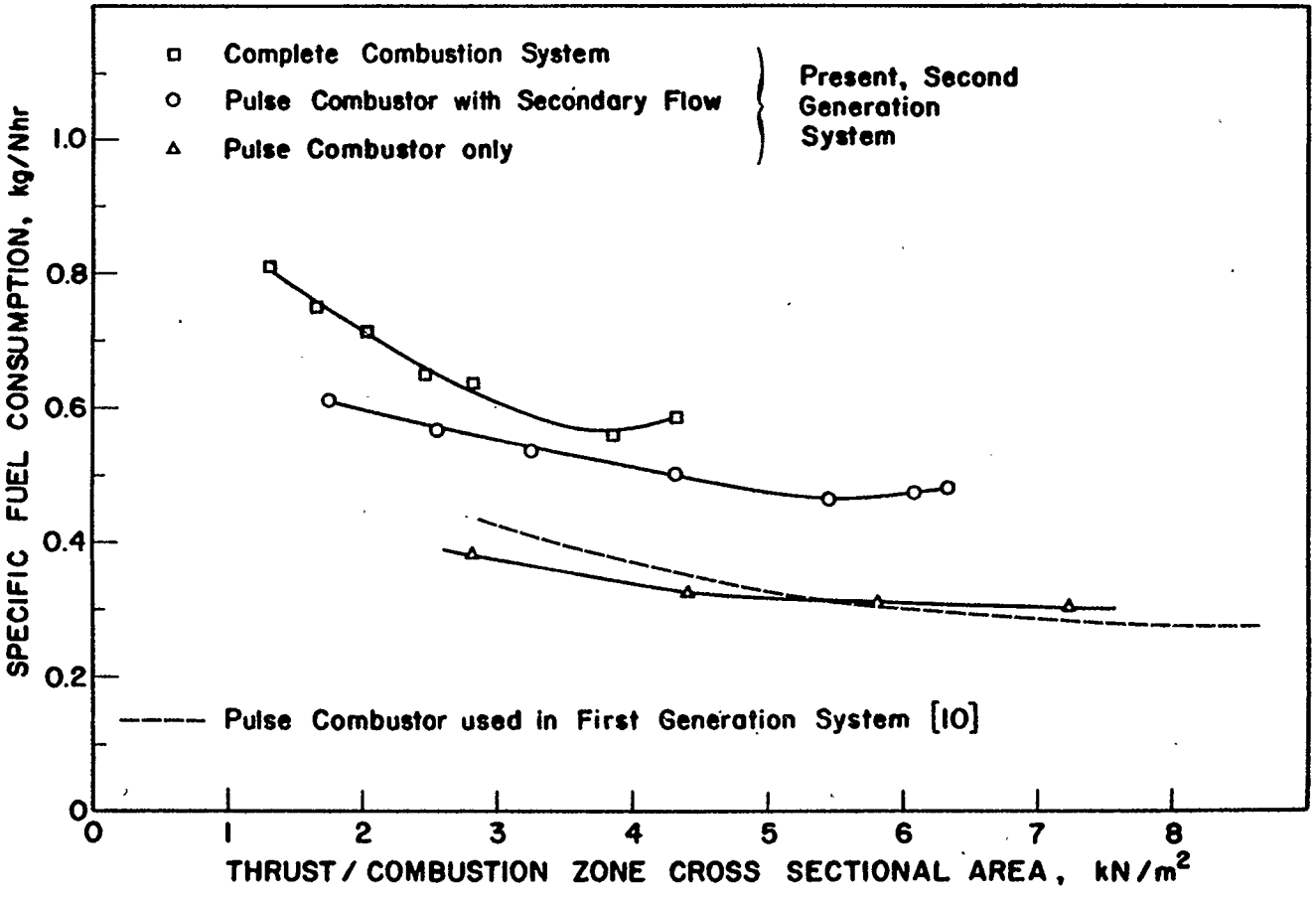

FIGURE 6.1 PERFORMANCE OF SECOND GENERATION SYSTEM OPERATED IN ISOLATION FOR VARIOUS CONFIGURATIONS

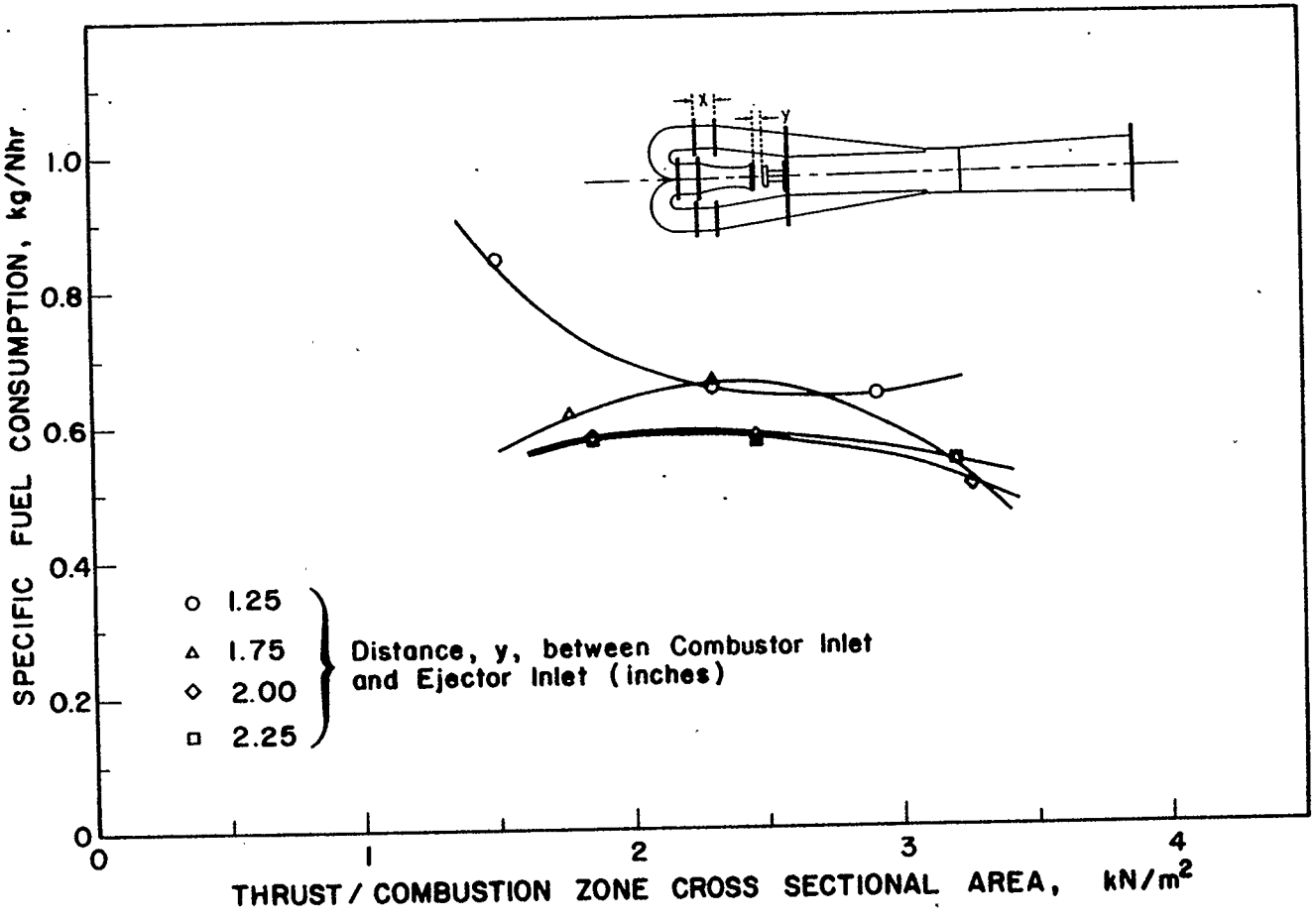

FIGURE 6.2 PERFORMANCE OF PULSE COMBUSTOR WITH SECONDARY FLOW SYSTEM ATTACHED (SECOND GENERATION SYSTEM), X = 0

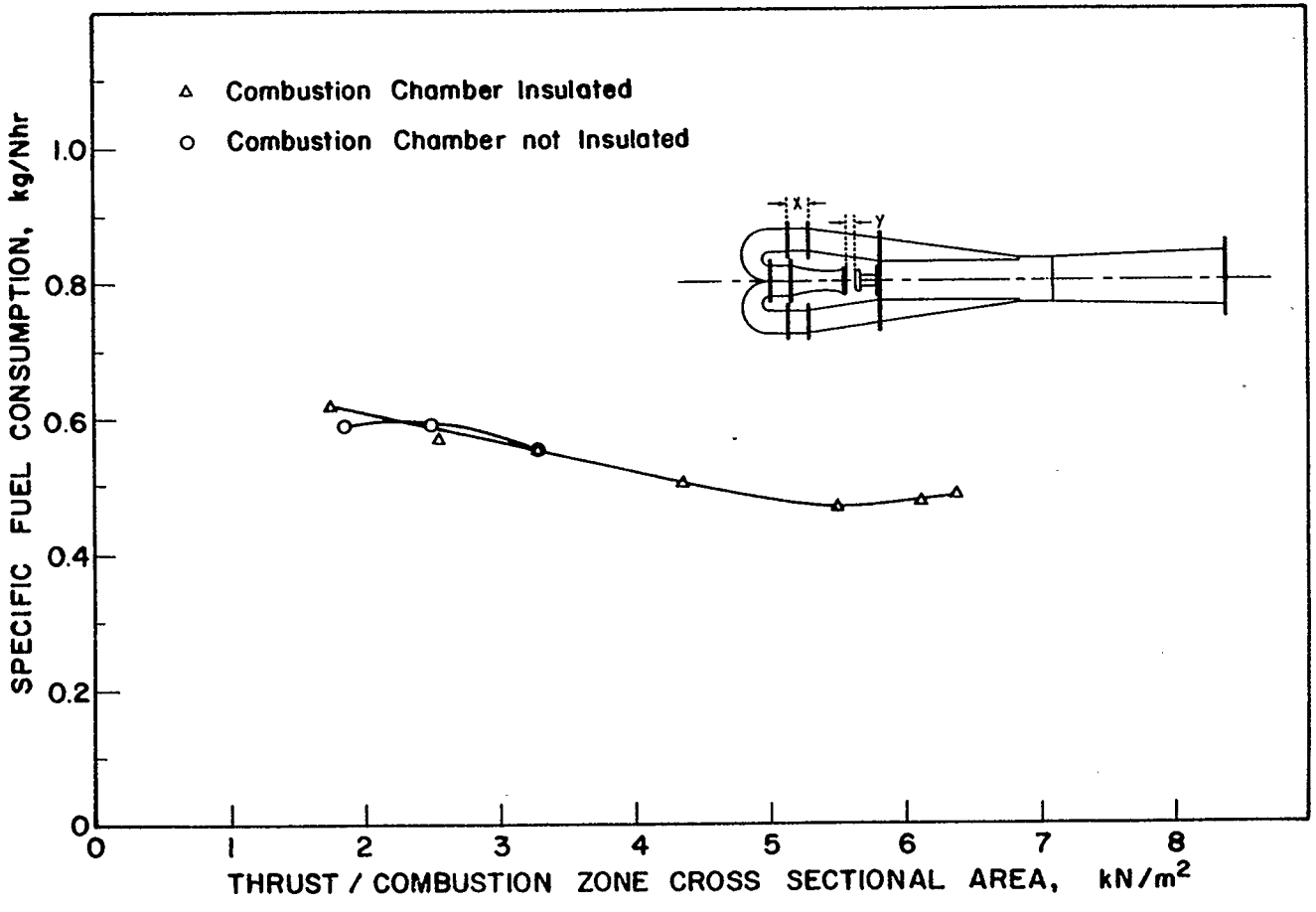

FIGURE 6.3 THE EFFECT OF INSULATING THE PULSE COMBUSTION CHAMBER, X = 0, Y = 2 inches

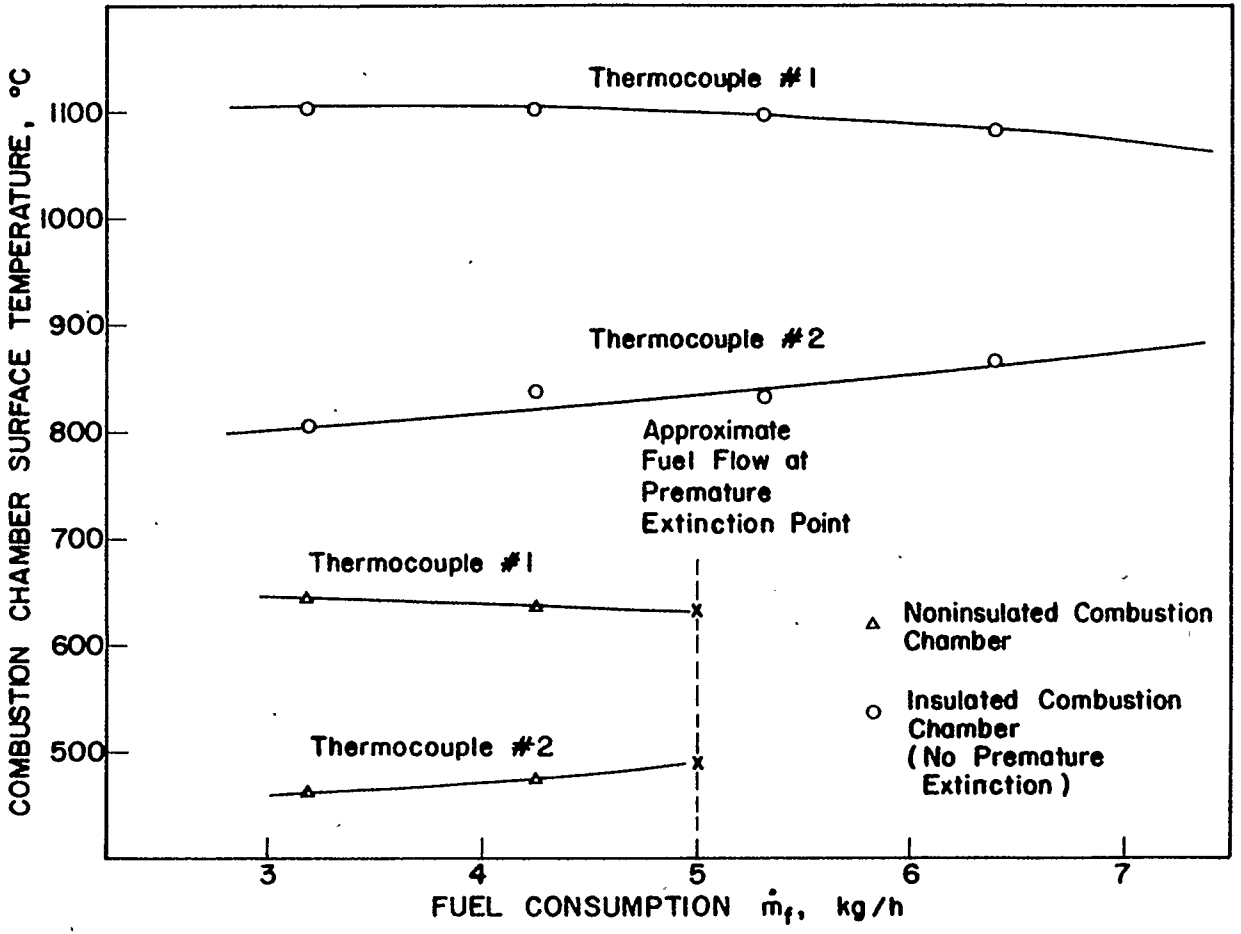

FIGURE 6.4 **COMBUSTION CHAMBER SURFACE TEMPERATURES FOR THE SECOND GENERATION COMBUSTION SYSTEM (MEASURED IN TWO LOCATIONS)**

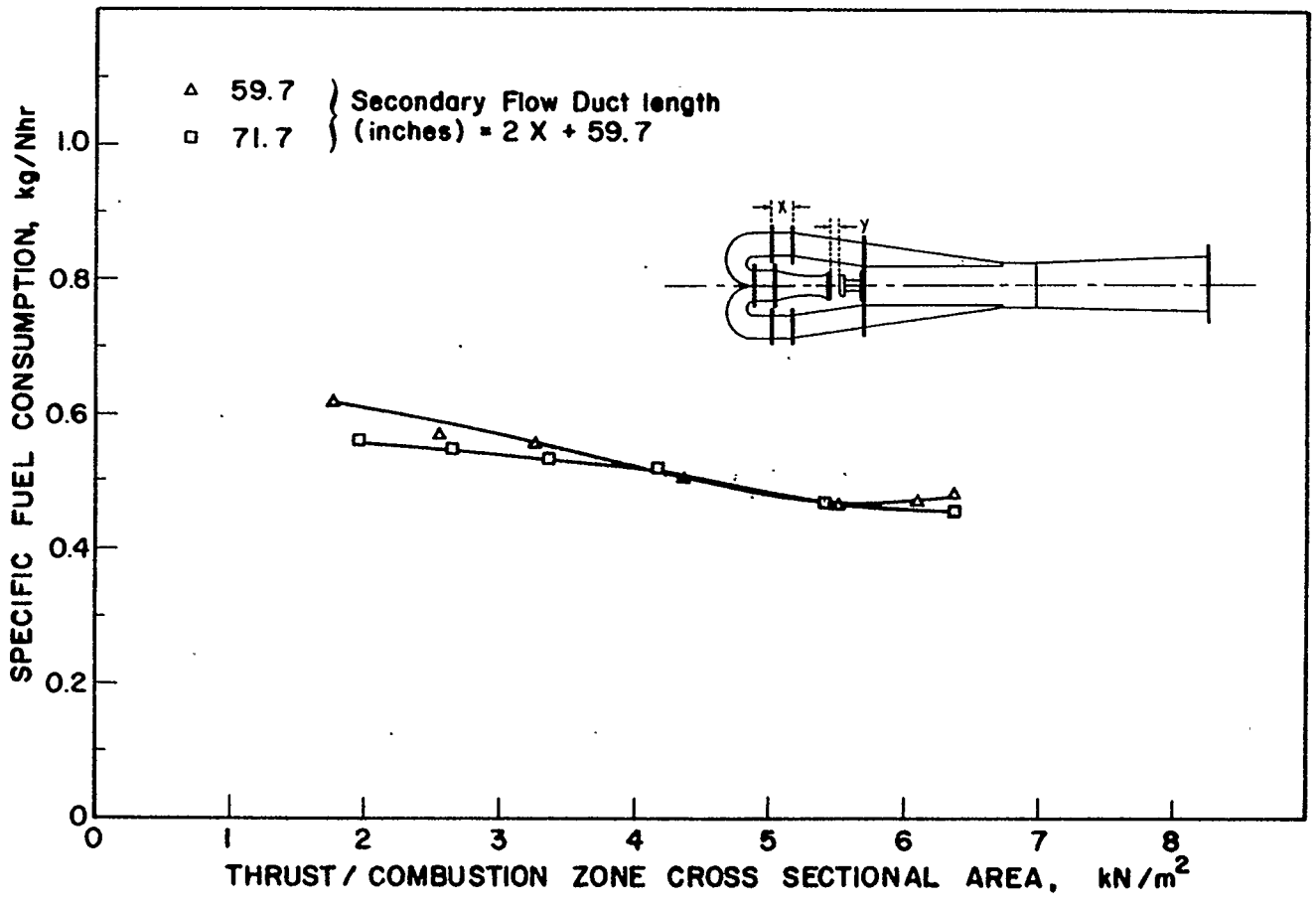

FIGURE 6.5 EFFECT OF SECONDARY FLOW DUCT LENGTH ON PERFORMANCE – COMBUSTION CHAMBER INSULATED, Y = 2 inches

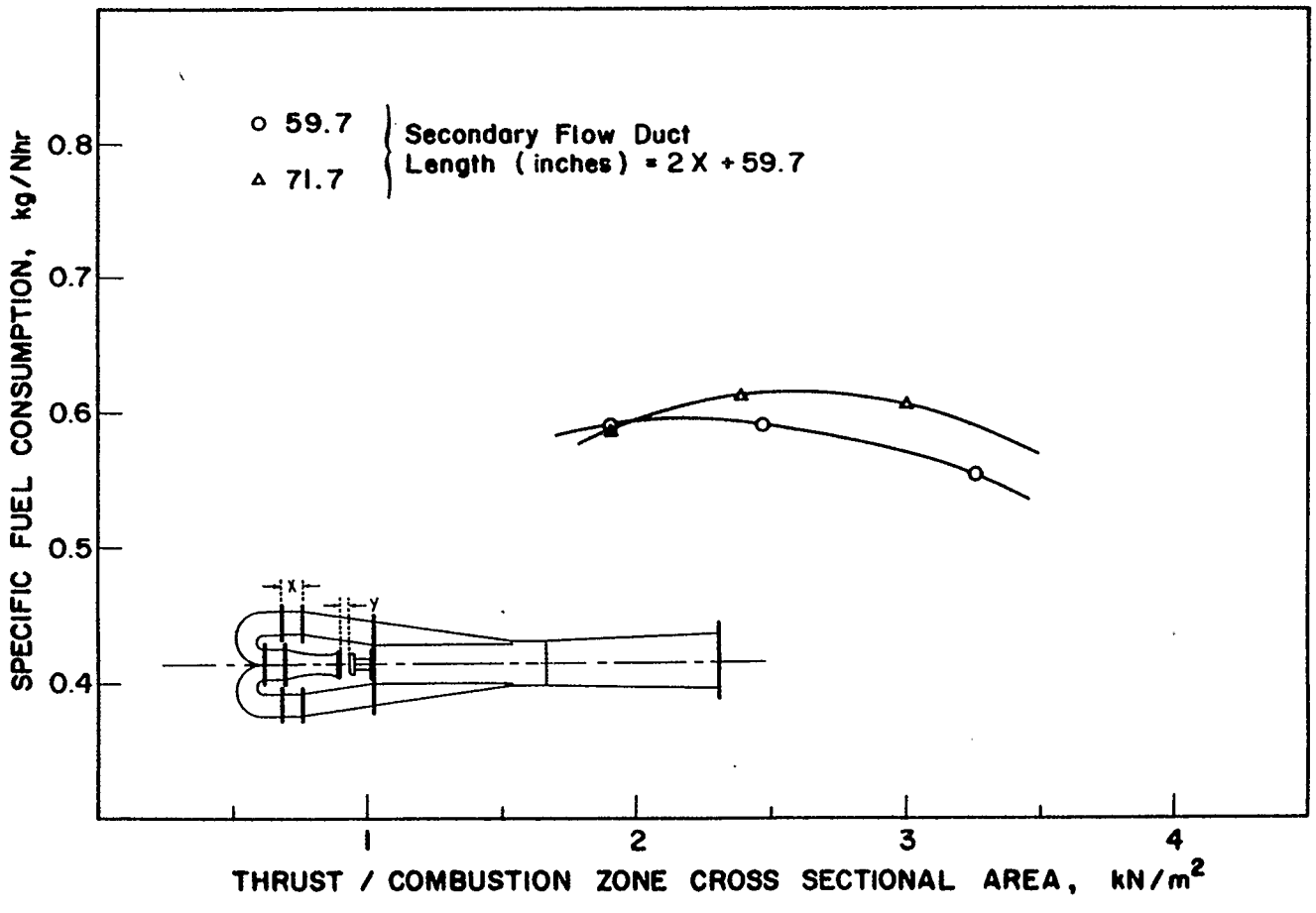

FIGURE 6.6 EFFECT OF SECONDARY FLOW DUCT LENGTH ON PERFORMANCE - COMBUSTION CHAMBER NOT INSULATED, Y = 2 inches

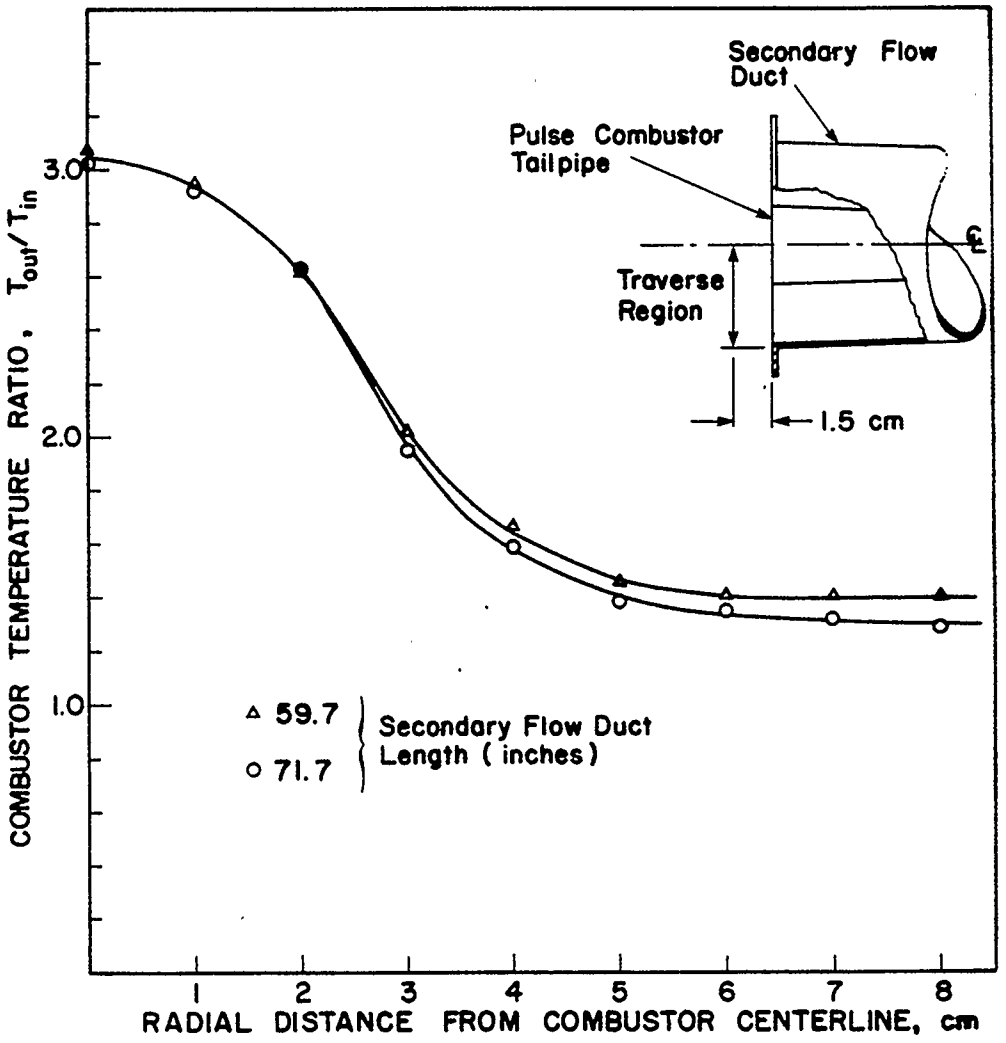

FIGURE 6.7 **OVERALL TEMPERATURE RATIO - COMBUSTOR WITH SECONDARY FLOW SYSTEM ATTACHED (INSULATED COMBUSTION ZONE)**

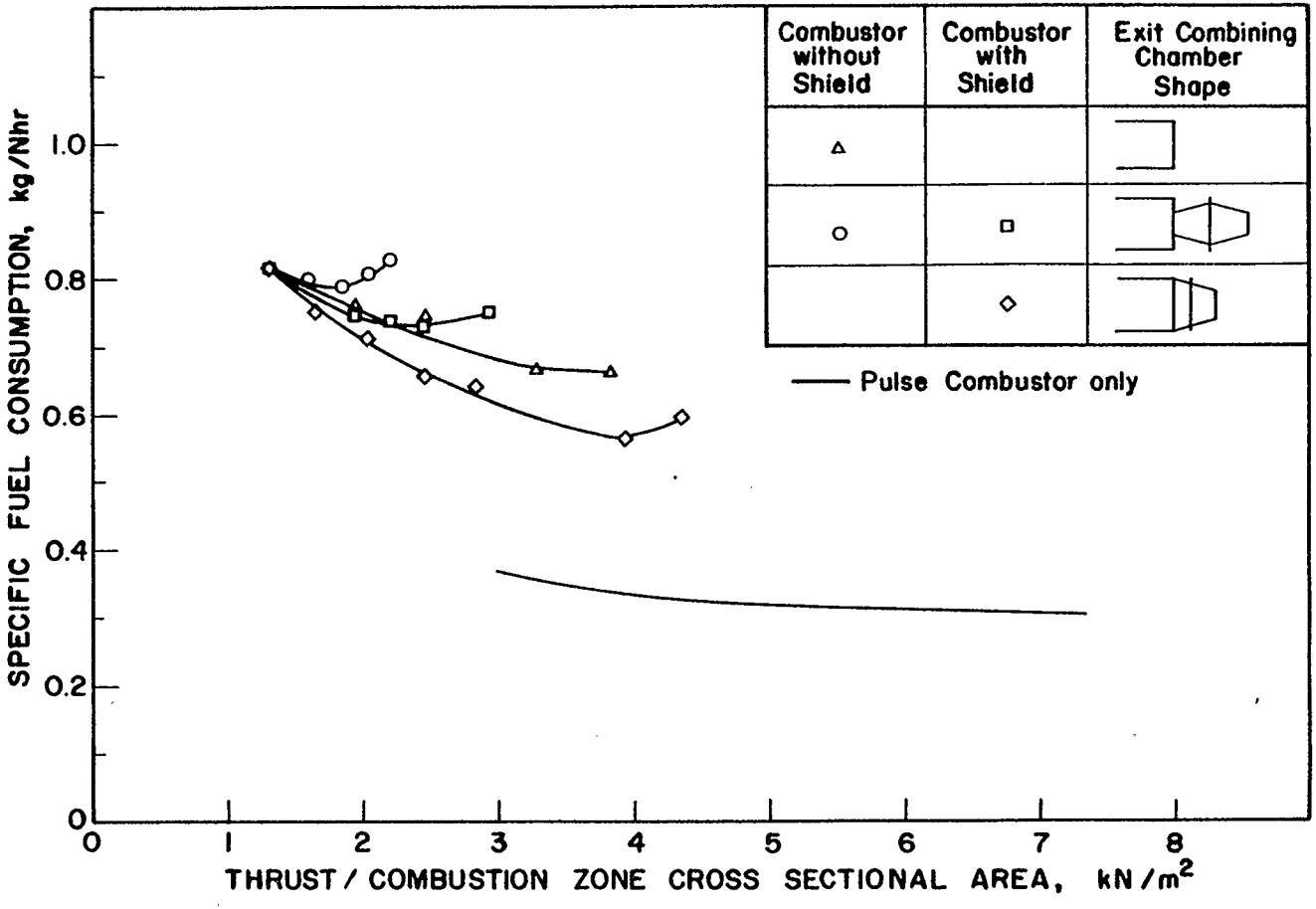

FIGURE 6.8 EFFECT OF EXIT COMBINING CHAMBER SHAPE ON PERFORMANCE OF, ISOLATED, COMPLETE SECOND GENERATION SYSTEM

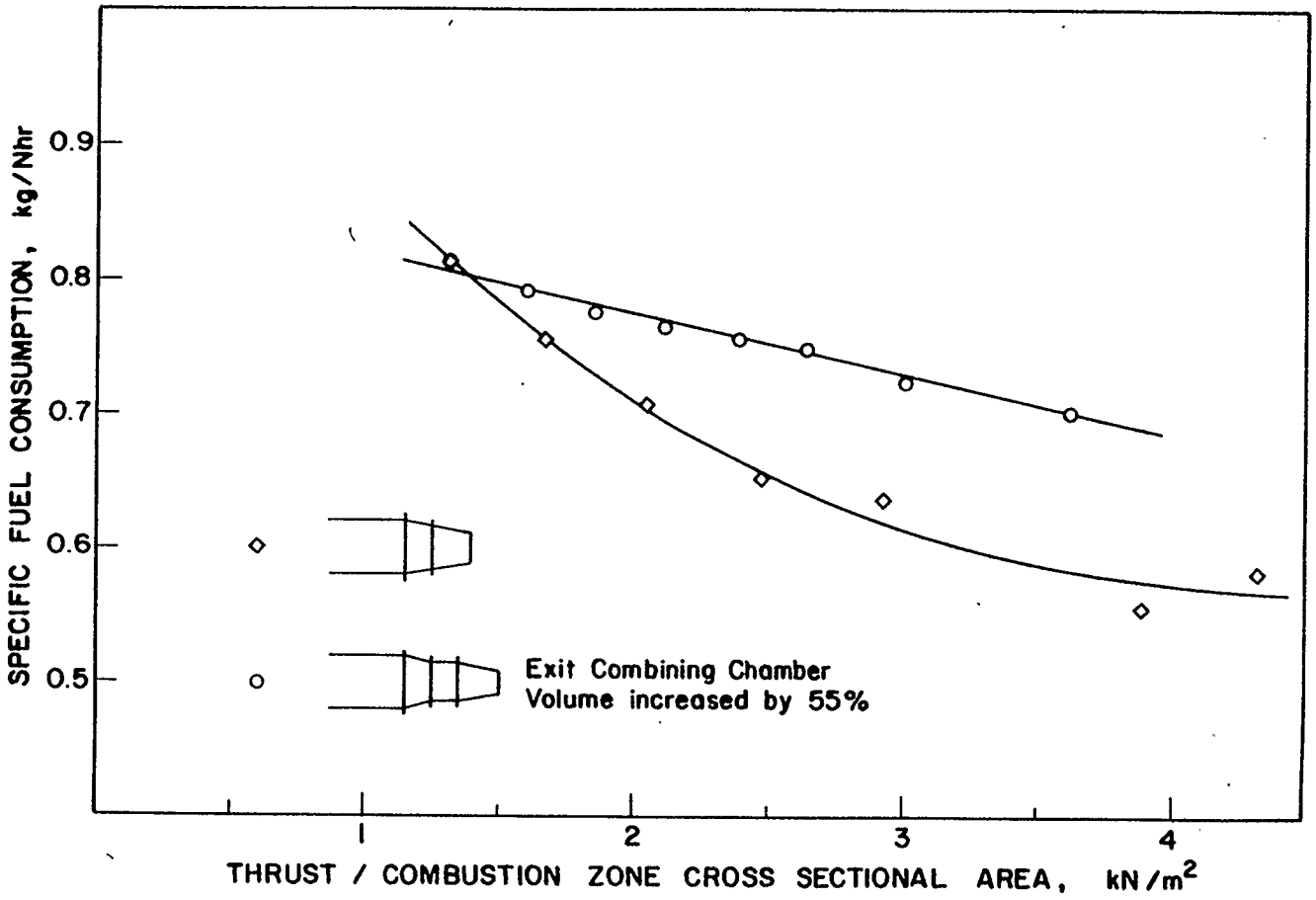

FIGURE 6.9 EFFECT OF EXIT COMBINING CHAMBER VOLUME ON PERFORMANCE OF, ISOLATED, COMPLETE SECOND GENERATION SYSTEM

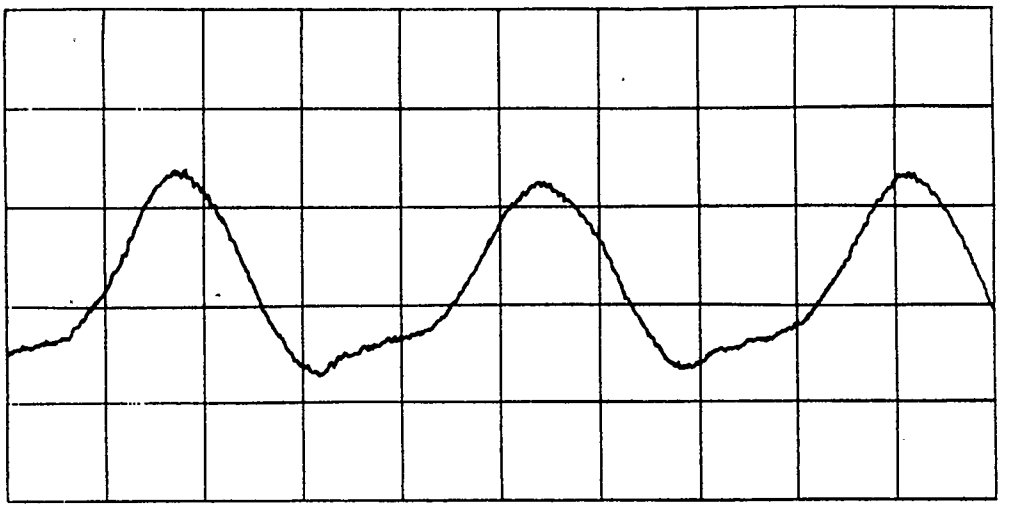

X axis: 1 ms/div Y axis: 5 psi/div

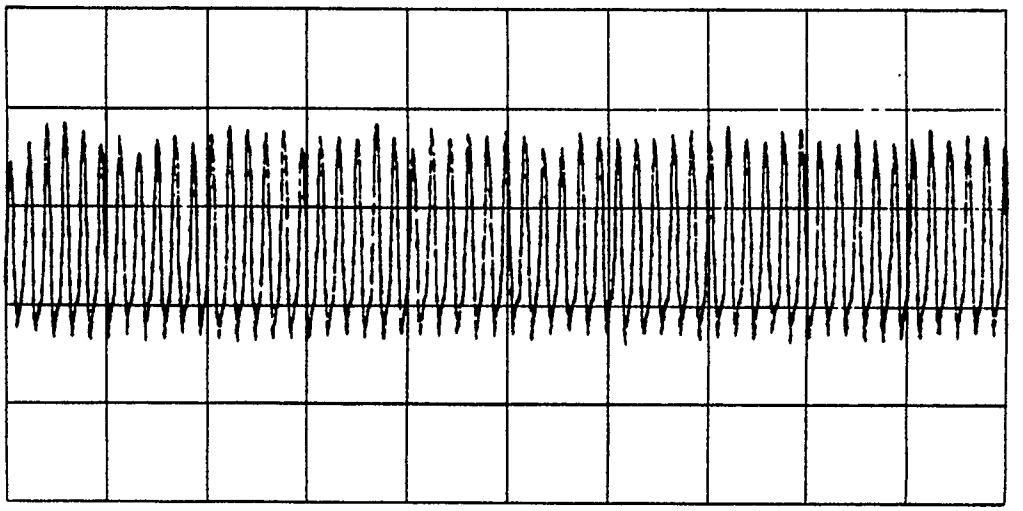

X axis: 20 ms/div Y axis: 5 psi/div

FIGURE 6.10 COMBUSTION CHAMBER DYNAMIC PRESSURE - BACK PRESSURE 0
LOADING - FUEL FLOW RATE = 4.80 kg/h

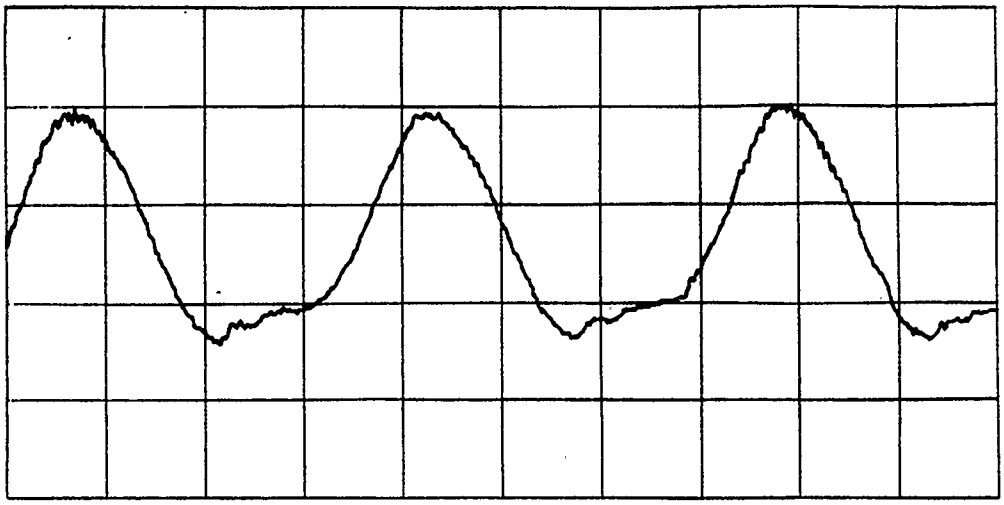

X axis: 1 ms/div Y axis: 5 psi/div

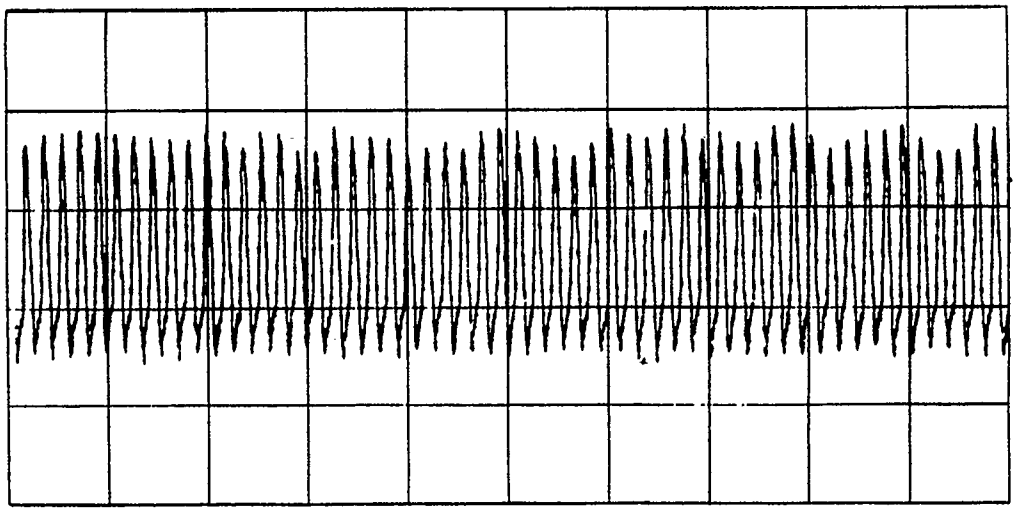

X axis: 20 ms/div Y axis: 5 psi/div

FIGURE 6.11 COMBUSTION CHAMBER DYNAMIC PRESSURE - BACK PRESSURE 0 LOADING - FUEL FLOW RATE = 5.11 kg/h

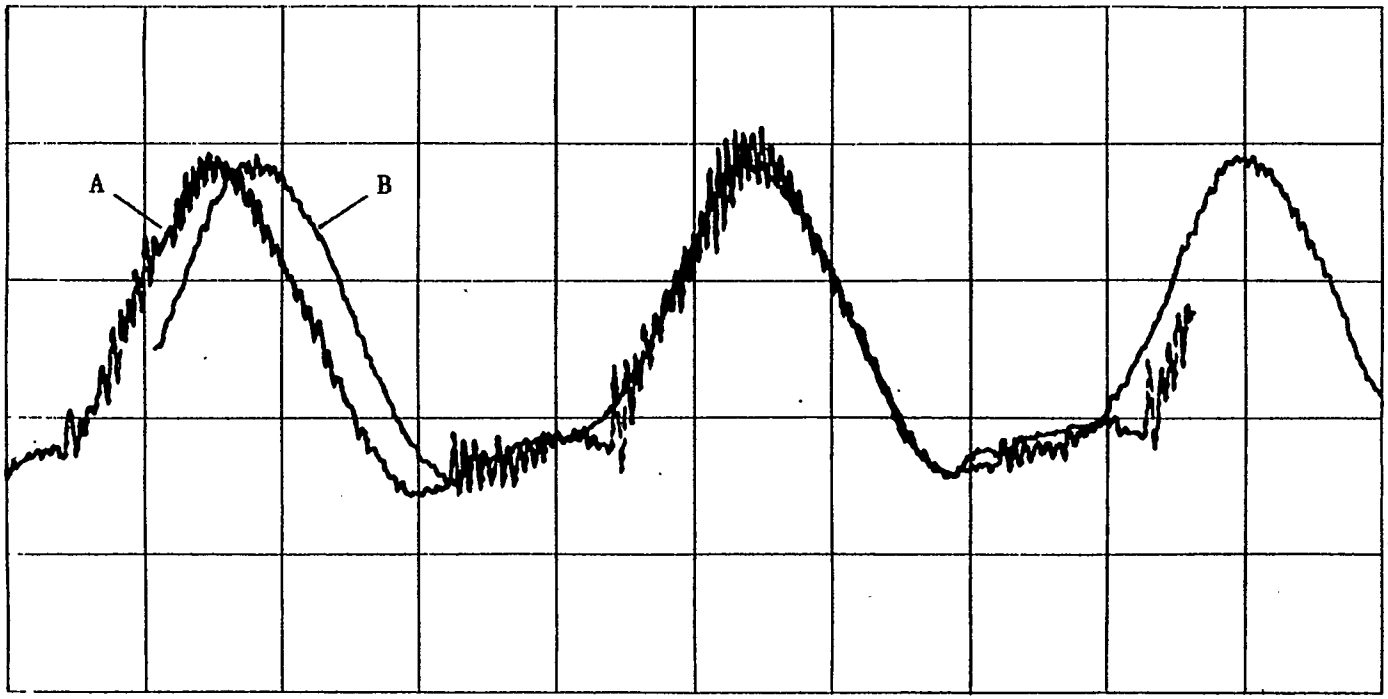

X axis: 1 ms/div Y axis: 5 psi/div

Trace A: Combustor in Isolation, $\dot{m}_f$ = 4.26 kg/h

Trace B: Combustor in Gas Turbine, $\dot{m}_f$ = 5.11 kg/h

FIGURE 6.12 COMPARISON OF COMBUSTION CHAMBER DYNAMIC - PRESSURE TRACES

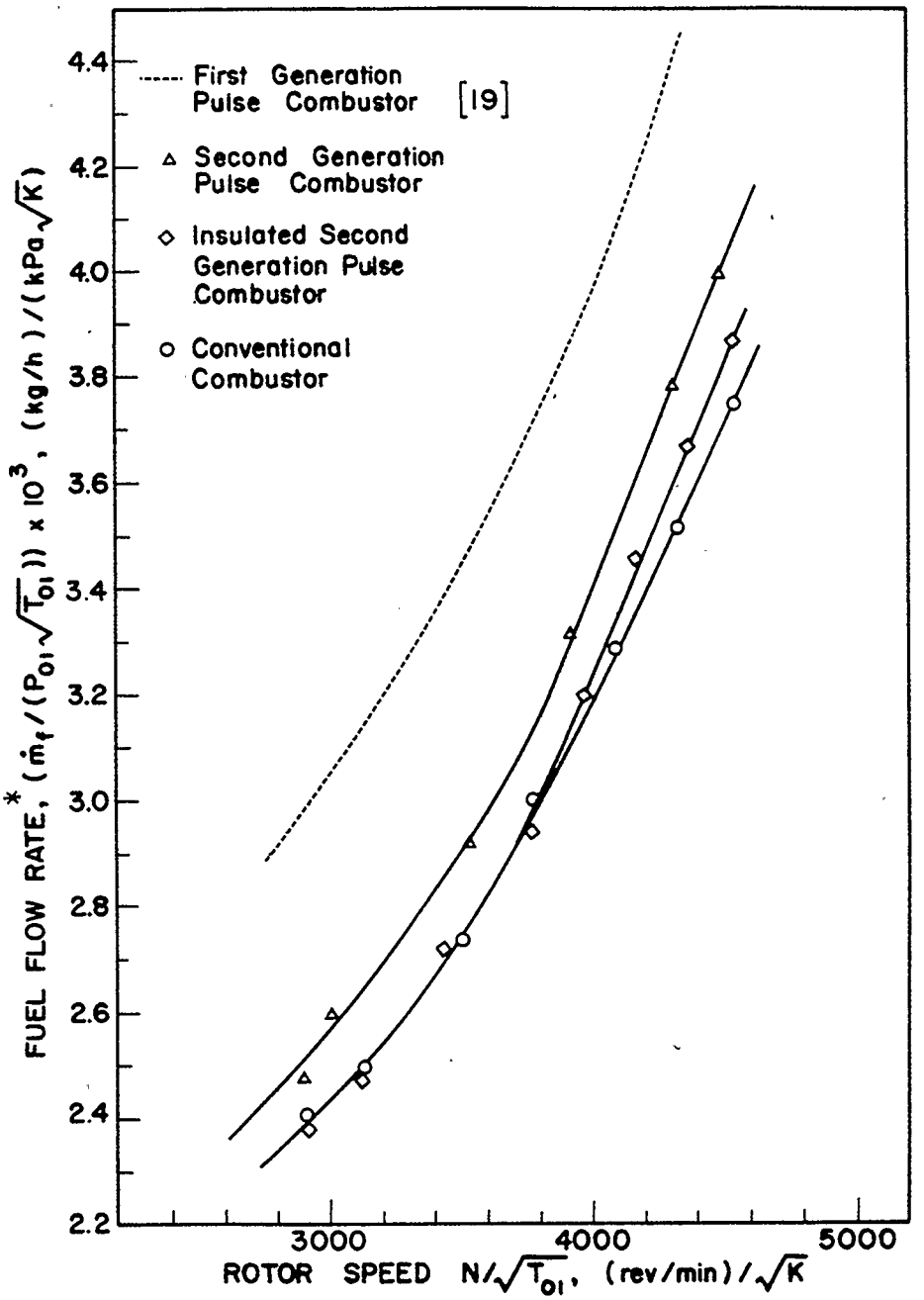

FIGURE 6.13 FUEL CONSUMPTION RATES FOR THE THREE COMBUSTION SYSTEMS OPERATED WITHIN THE GAS TURBINE
- BACK PRESSURE 0 LOADING

* Note: To obtain flow rate divide the number shown by 10^3

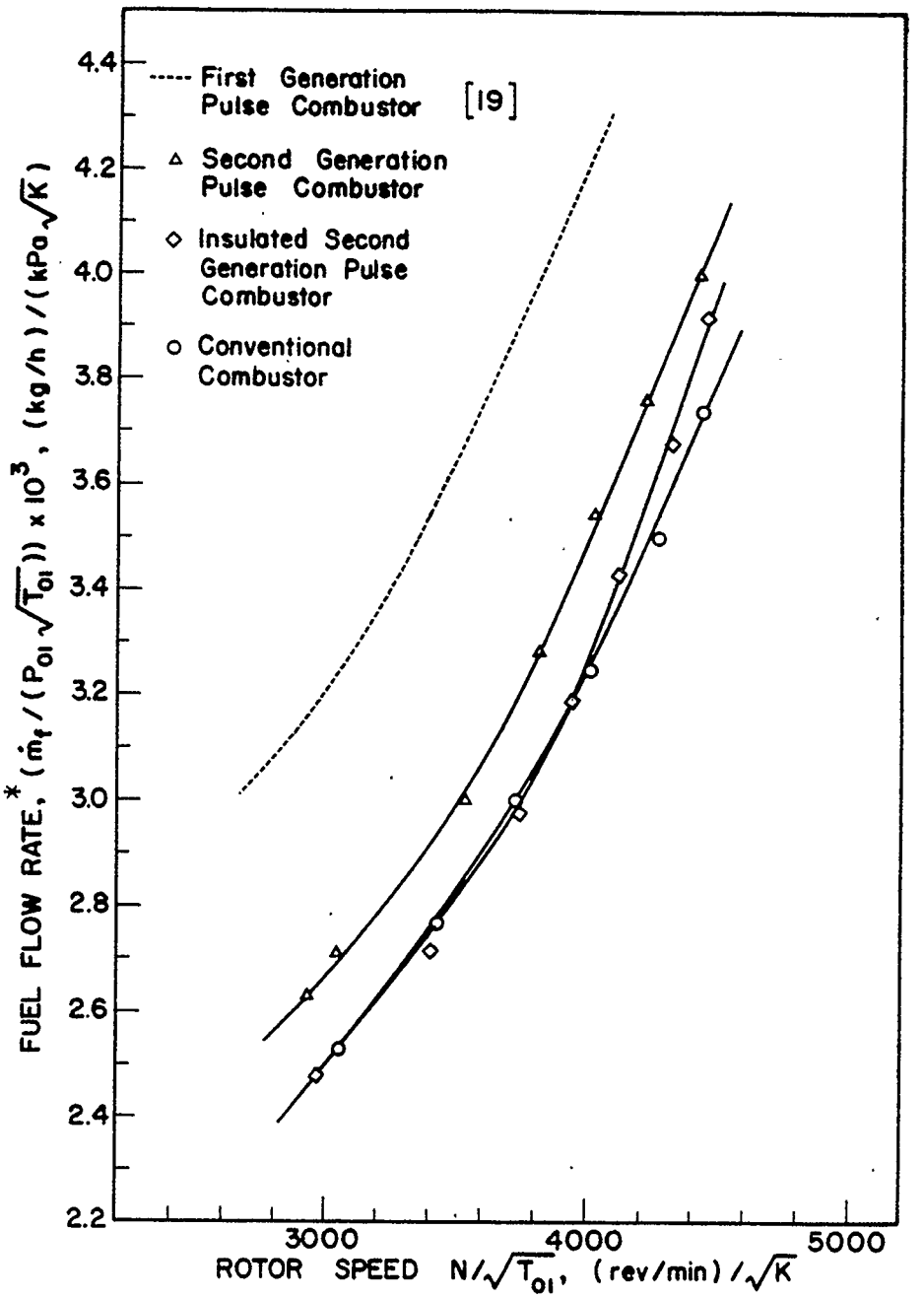

FIGURE 6.14 FUEL CONSUMPTION RATES FOR THE THREE COMBUSTION SYSTEMS OPERATED WITHIN THE GAS TURBINE - BACK PRESSURE 1 LOADING

* Note: To obtain flow rate divide the number shown by 10^3

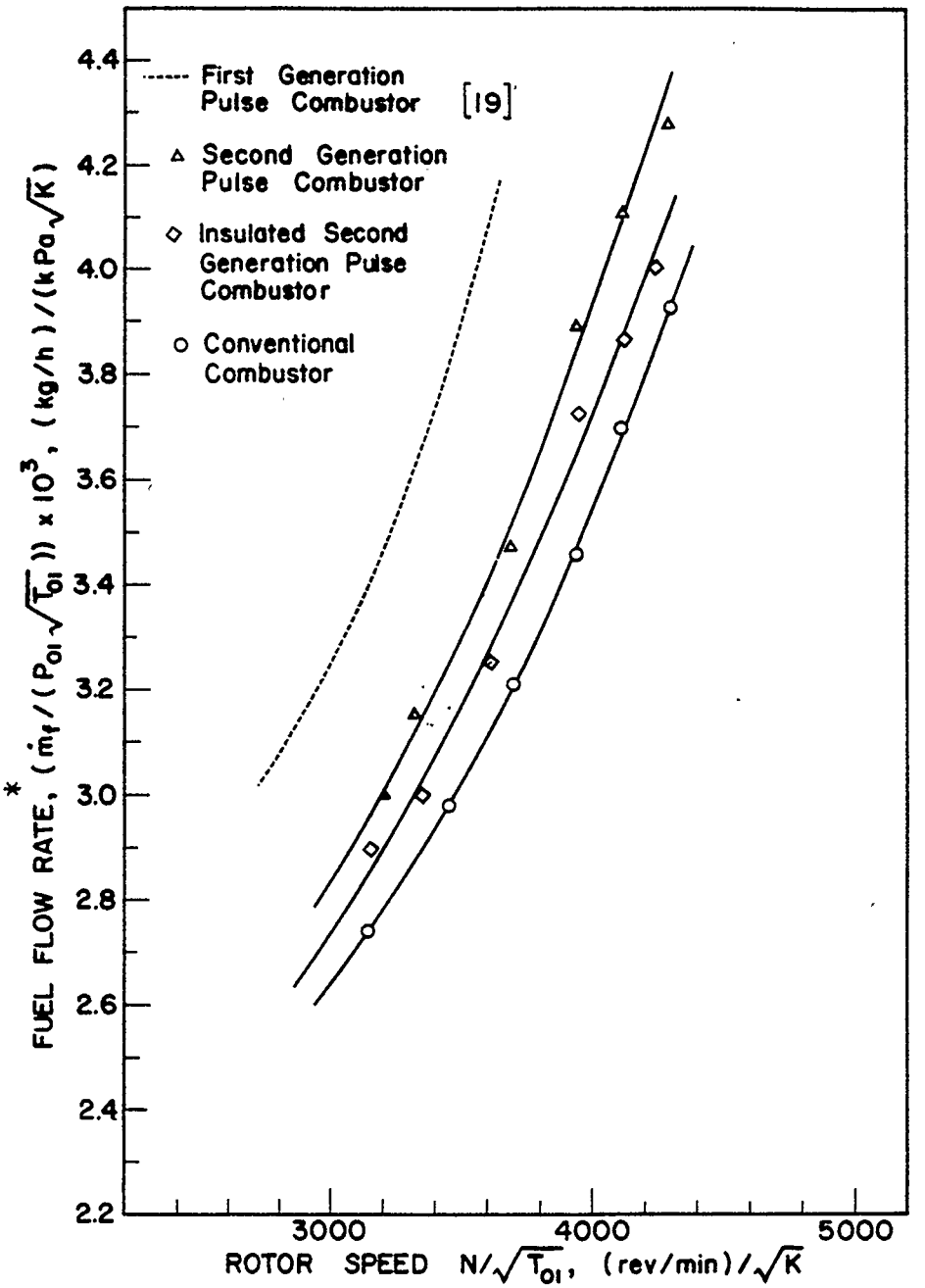

FIGURE 6.15 FUEL CONSUMPTION RATES FOR THE THREE COMBUSTION SYSTEMS OPERATED WITHIN THE GAS TURBINE - BACK PRESSURE 2 LOADING

* Note: To obtain flow rate divide the number shown by 10^3

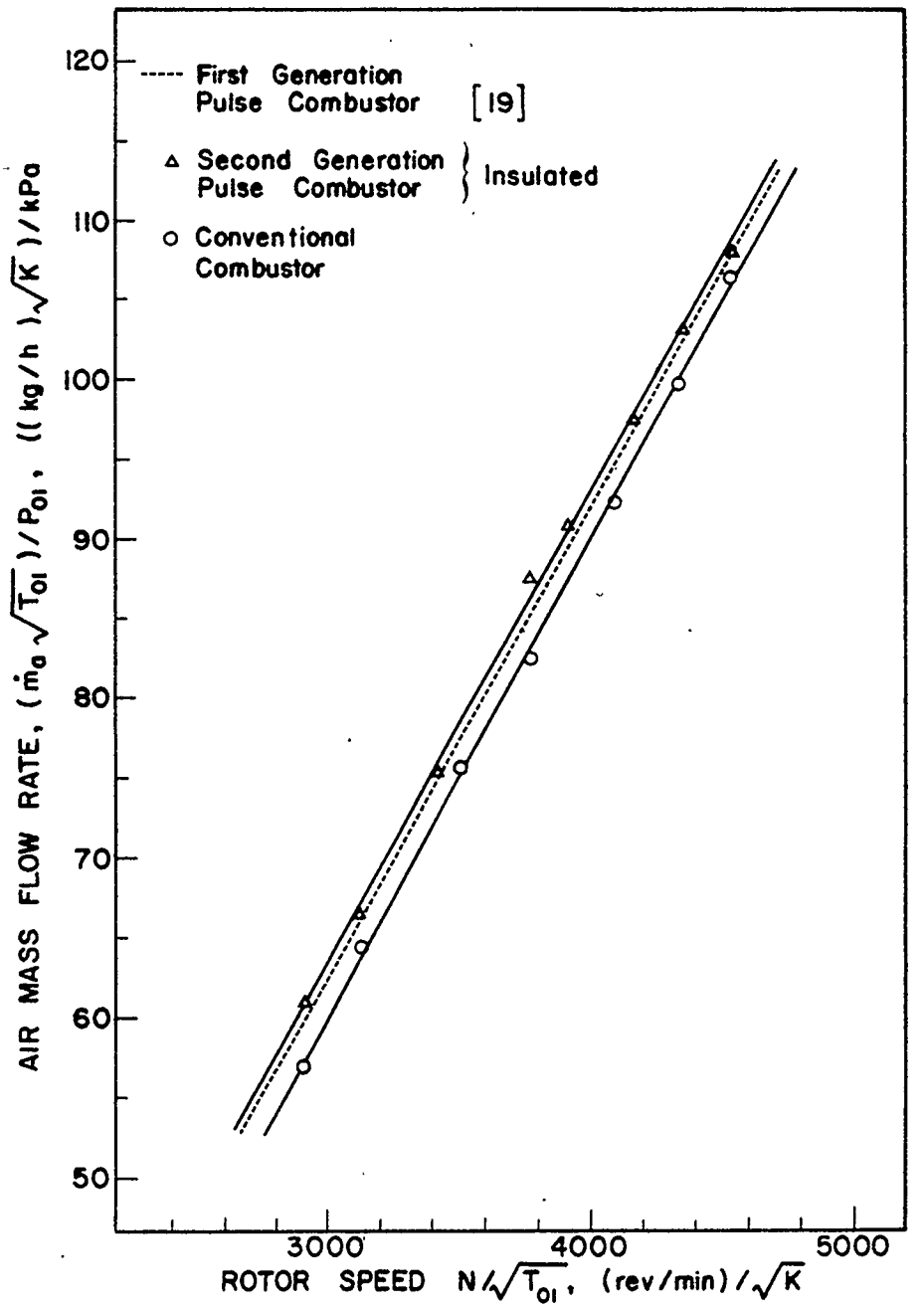

FIGURE 6.16 AIR MASS FLOW RATES FOR THE THREE GAS TURBINE COMBUSTION SYSTEMS - BACK PRESSURE 0 LOADING

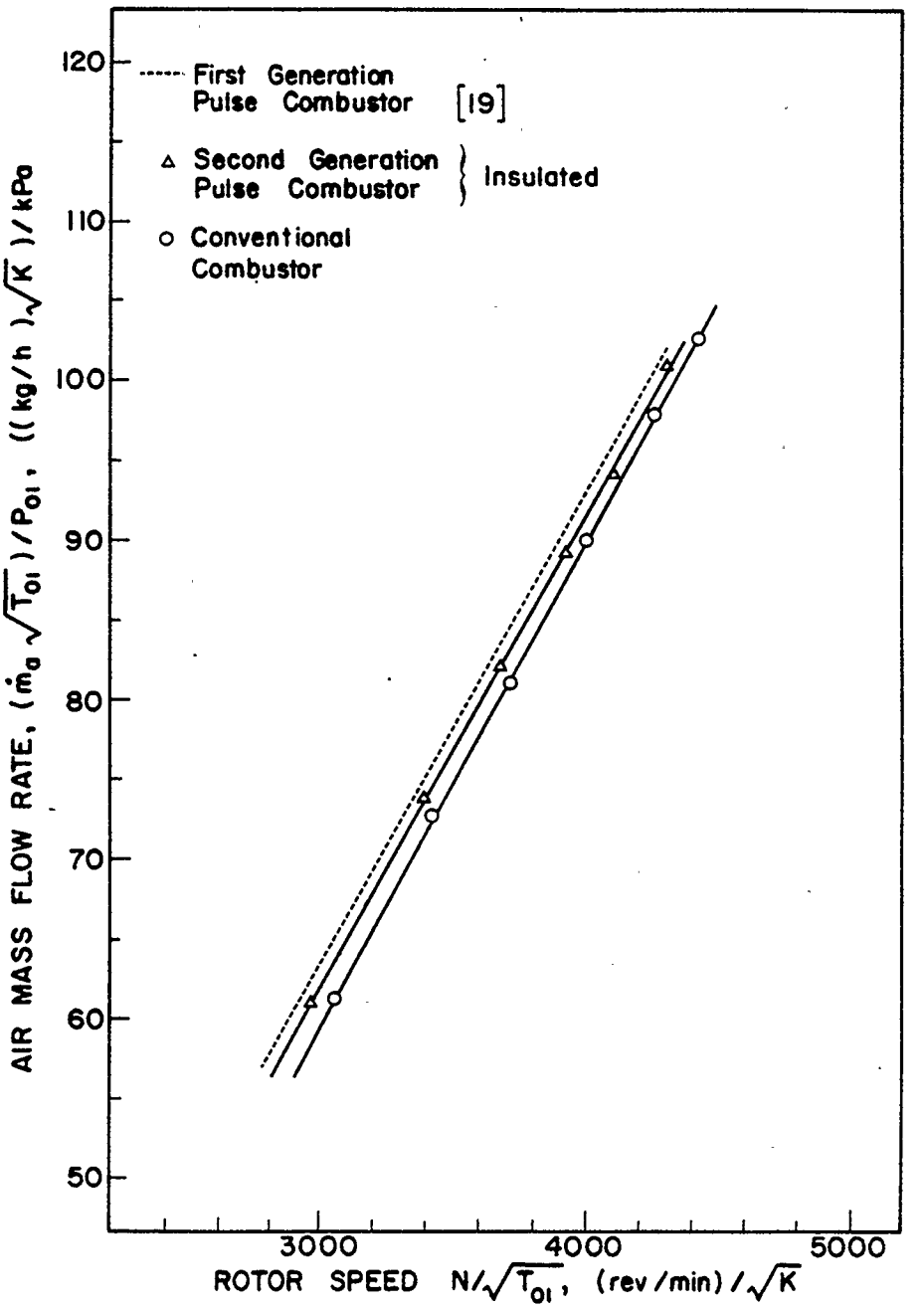

FIGURE 6.17 AIR MASS FLOW RATES FOR THE THREE GAS TURBINE COMBUSTION SYSTEMS - BACK PRESSURE 1 LOADING

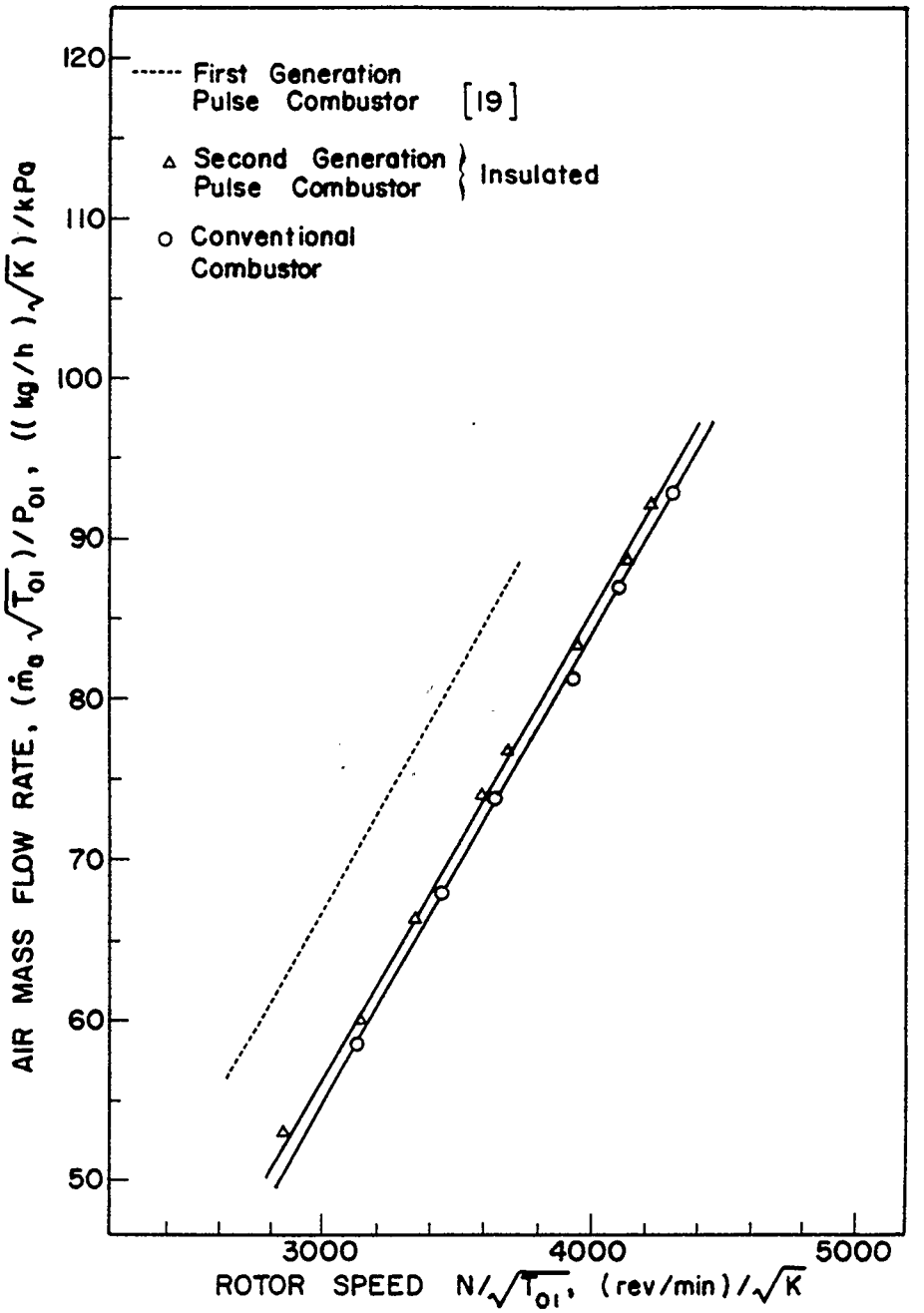

FIGURE 6.18 AIR MASS FLOW RATES FOR THE THREE GAS TURBINE COMBUSTION SYSTEMS - BACK PRESSURE 2 LOADING

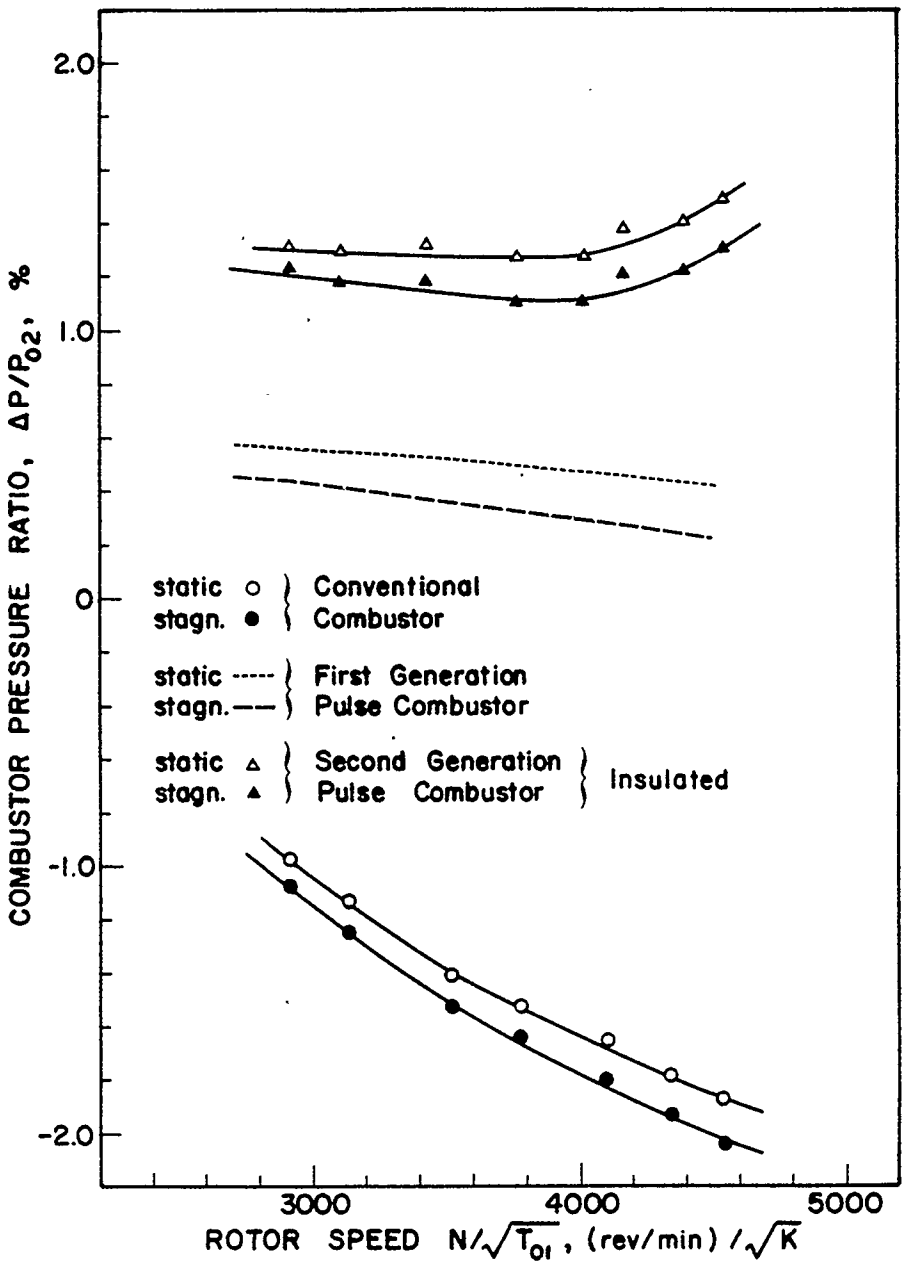

FIGURE 6.19 COMPARISON OF GAS TURBINE COMBUSTOR PRESSURE RATIOS - BACK PRESSURE 0 LOADING

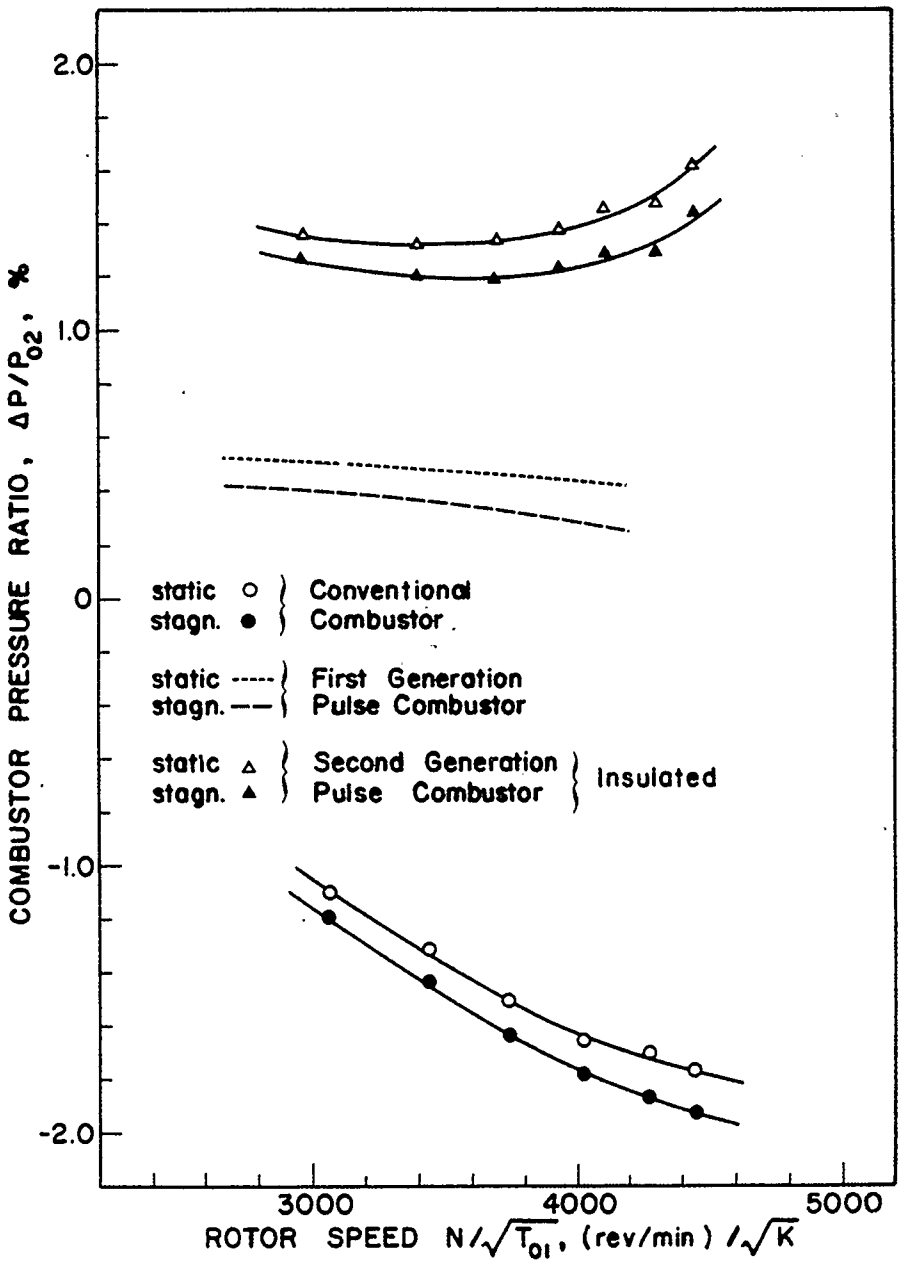

FIGURE 6.20 COMPARISON OF GAS TURBINE COMBUSTOR PRESSURE RATIOS - BACK PRESSURE 1 LOADING

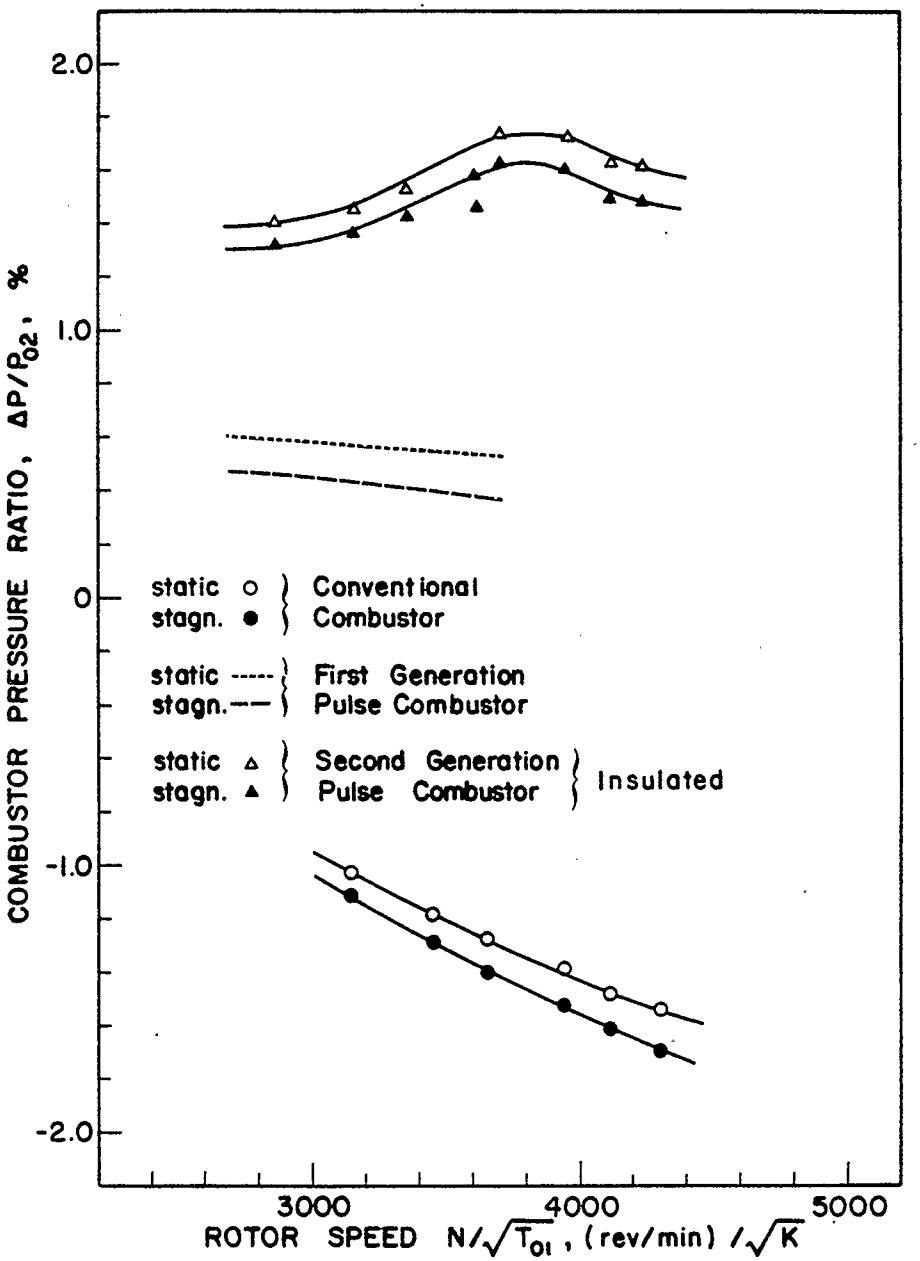

FIGURE 6.21 COMPARISON OF GAS TURBINE COMBUSTOR PRESSURE RATIOS - BACK PRESSURE 2 LOADING

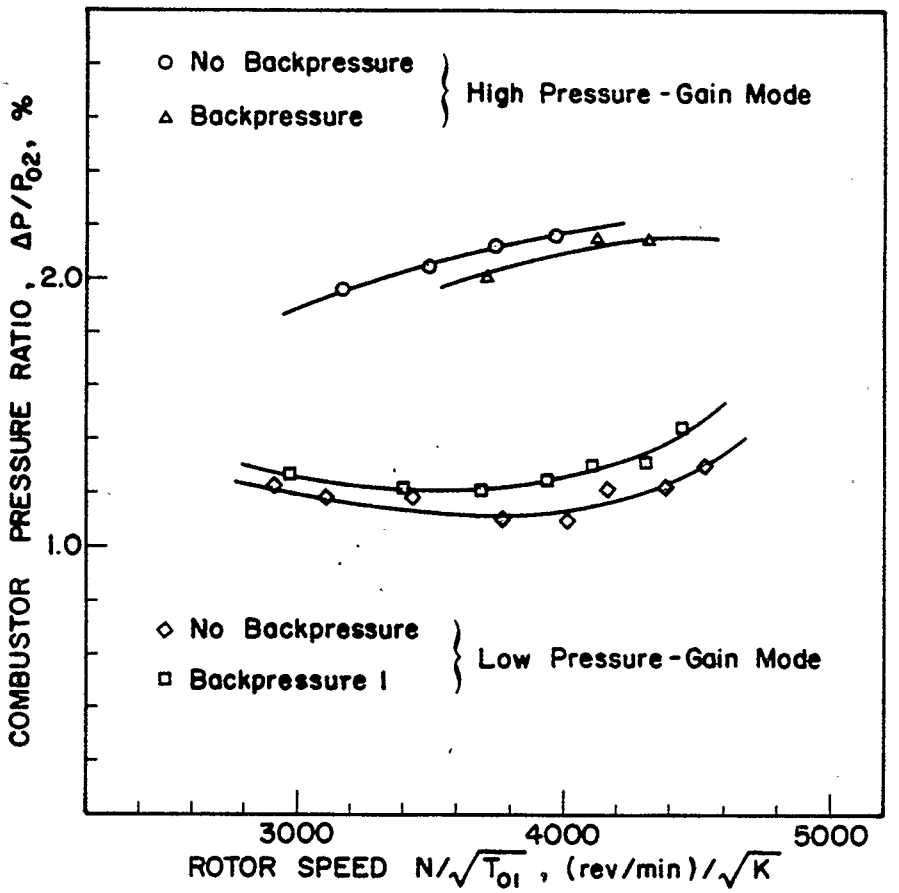

FIGURE 6.22 MAXIMUM STAGNATION PRESSURE RATIOS ACHIEVED BY THE SECOND GENERATION PULSE COMBUSTOR OPERATED WITHIN THE GAS TURBINE

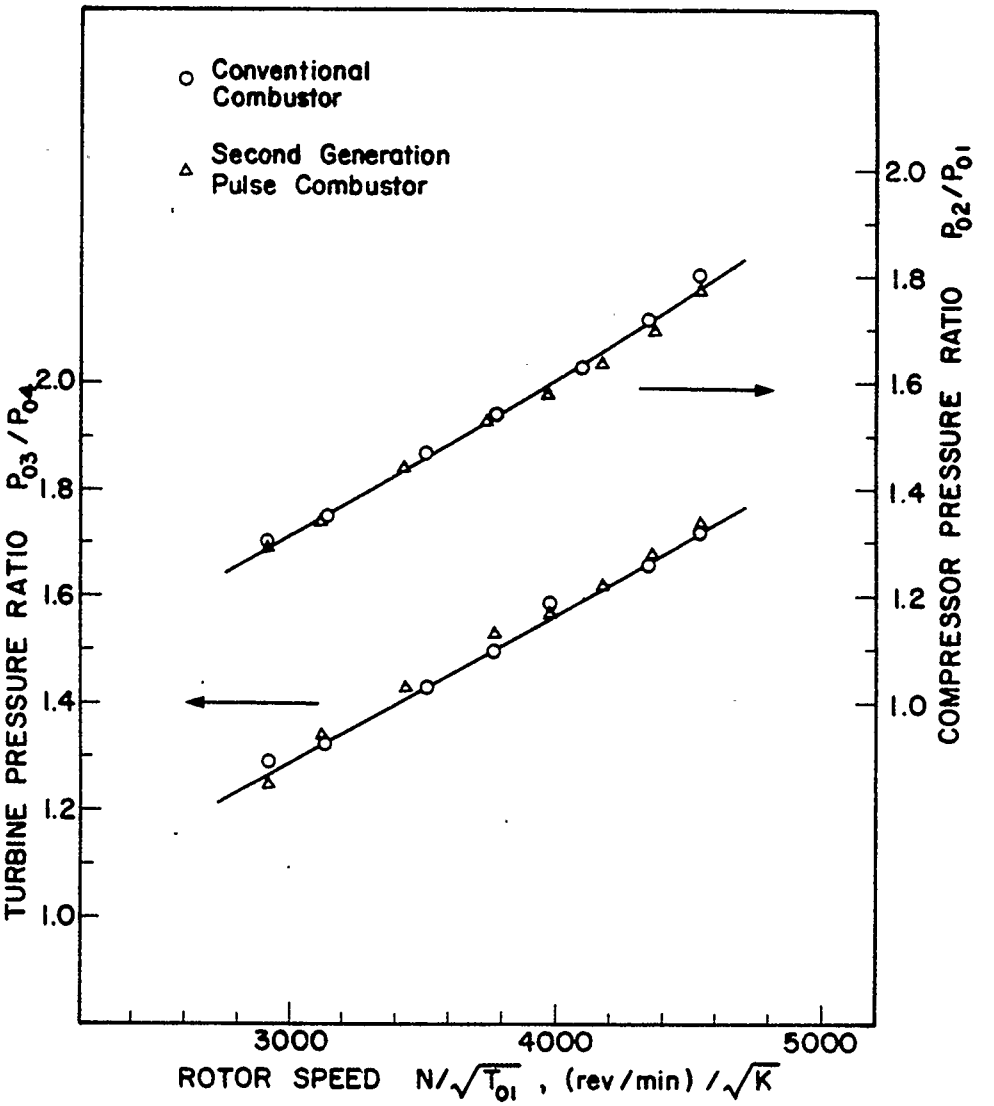

FIGURE 6.23 COMPARISON OF COMPRESSOR AND TURBINE PRESSURE RATIOS - BACK PRESSURE 0 LOADING

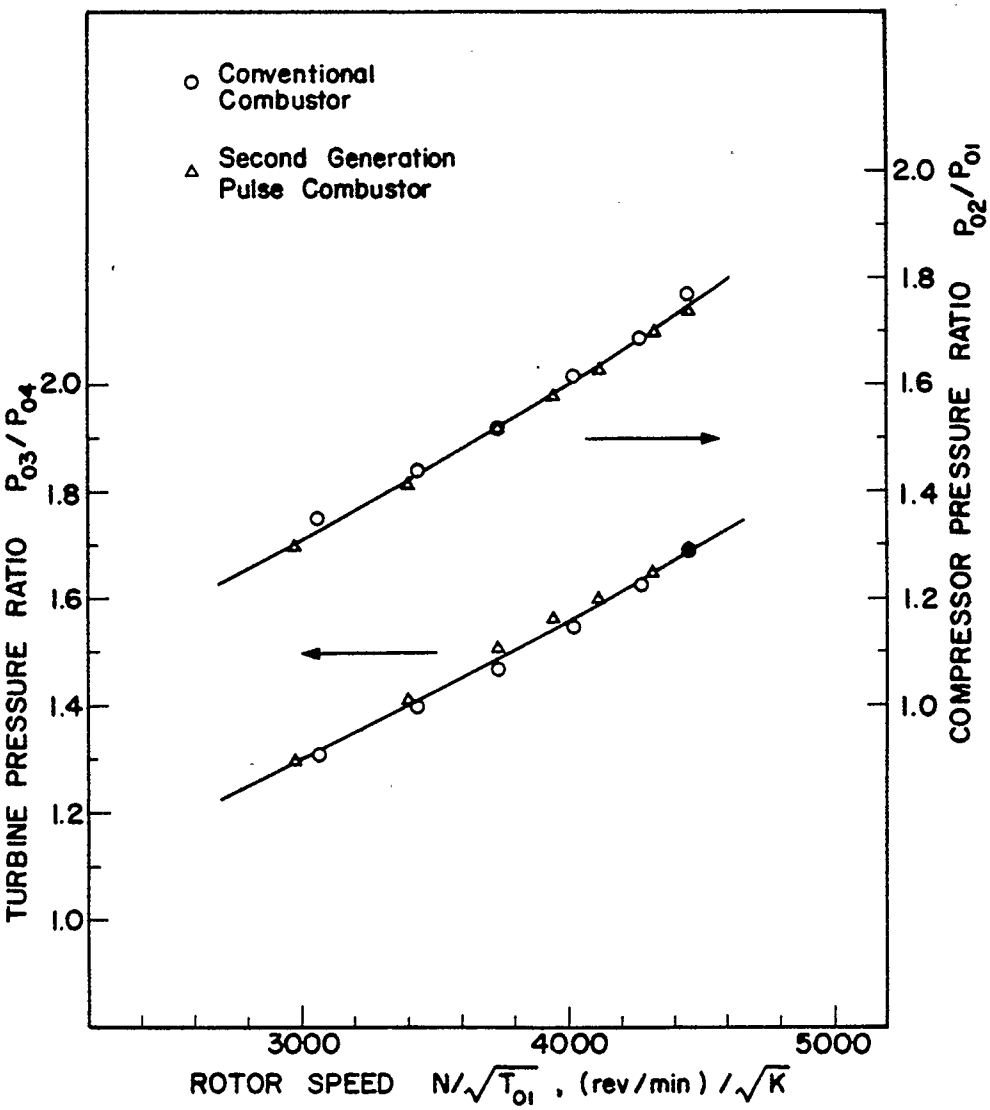

FIGURE 6.24 COMPARISON OF COMPRESSOR AND TURBINE PRESSURE RATIOS - BACK PRESSURE 1 LOADING

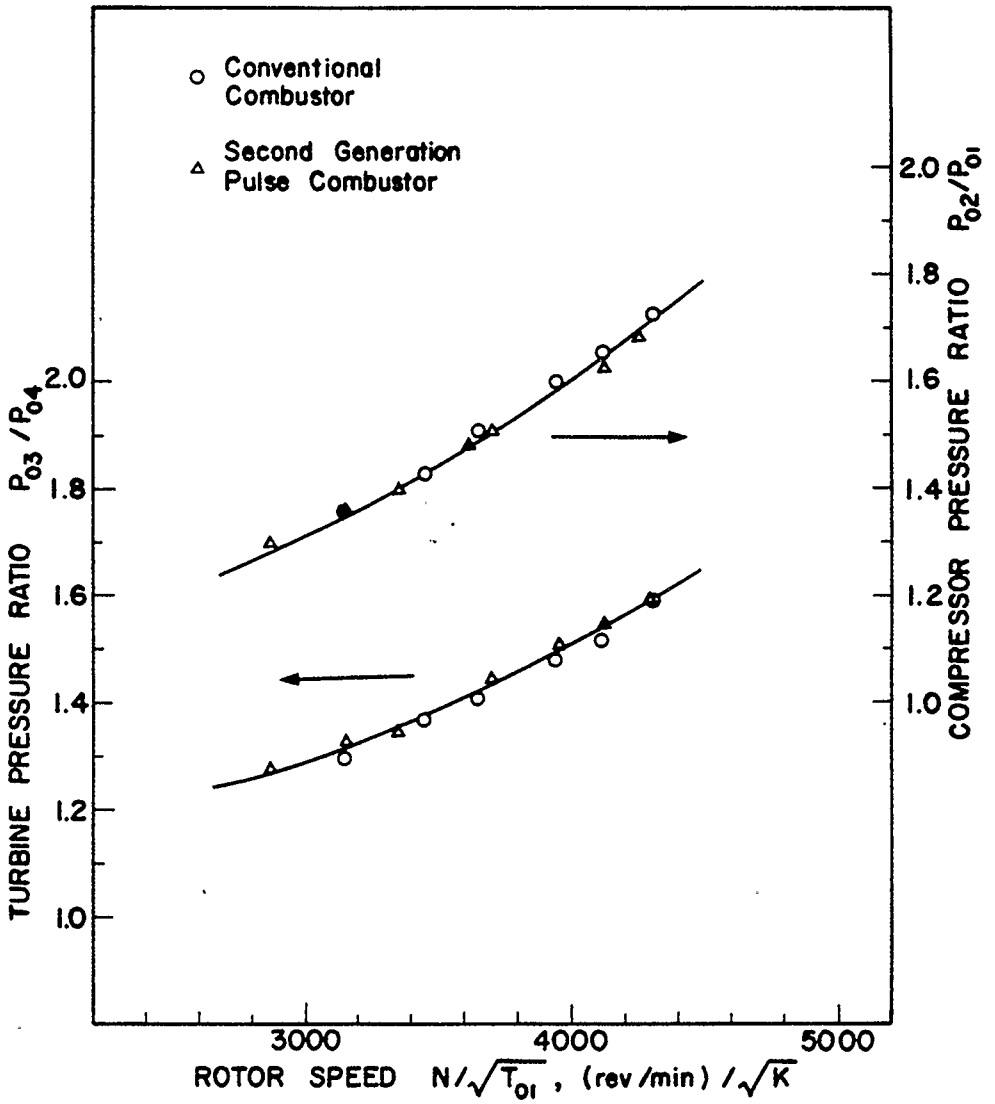

FIGURE 6.25 COMPARISON OF COMPRESSOR AND TURBINE PRESSURE RATIOS - BACK PRESSURE 2 LOADING

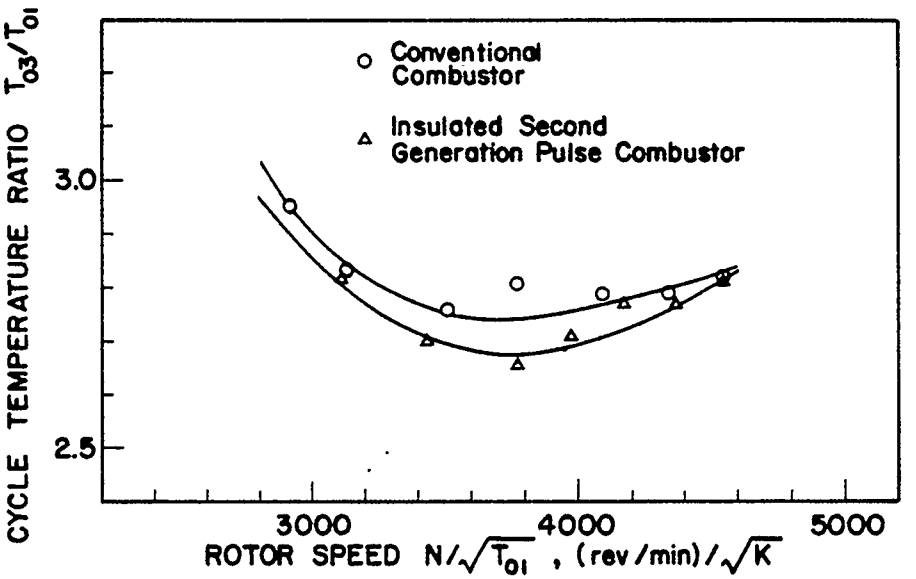

FIGURE 6.26 COMPARISON OF CYCLE TEMPERATURE RATIOS - BACK PRESSURE 0 LOADING

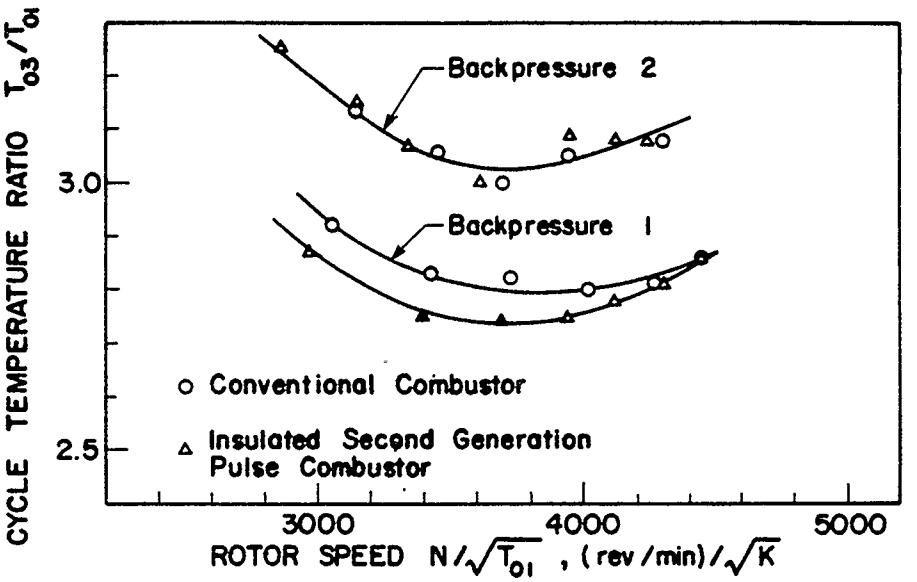

FIGURE 6.27 COMPARISON OF CYCLE TEMPERATURE RATIOS - BACK PRESSURE 1 AND 2 LOADINGS

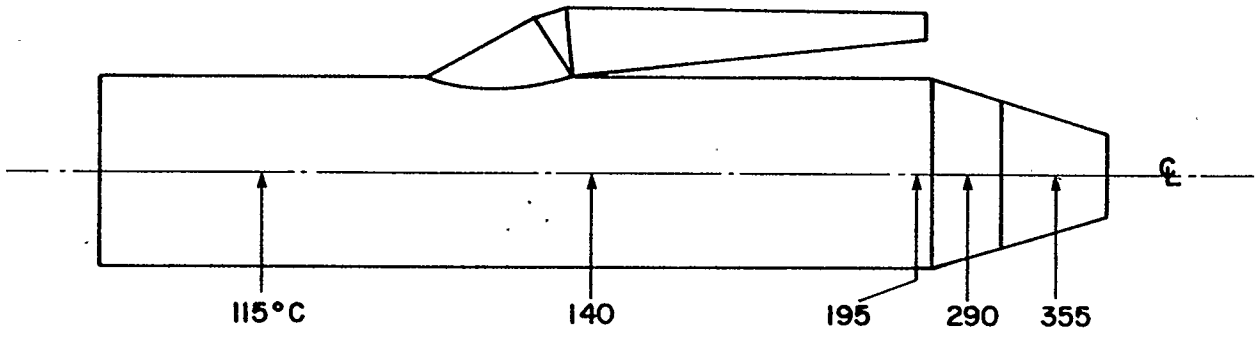

FIGURE 6.28 SURFACE TEMPERATURES FOR THE SECOND GENERATION PULSE COMBUSTOR
- BACK PRESSURE 0 LOADING - FUEL FLOW RATE = 4.74 kg/h
- HEAT LOSS = 8% (NOT INSULATED)

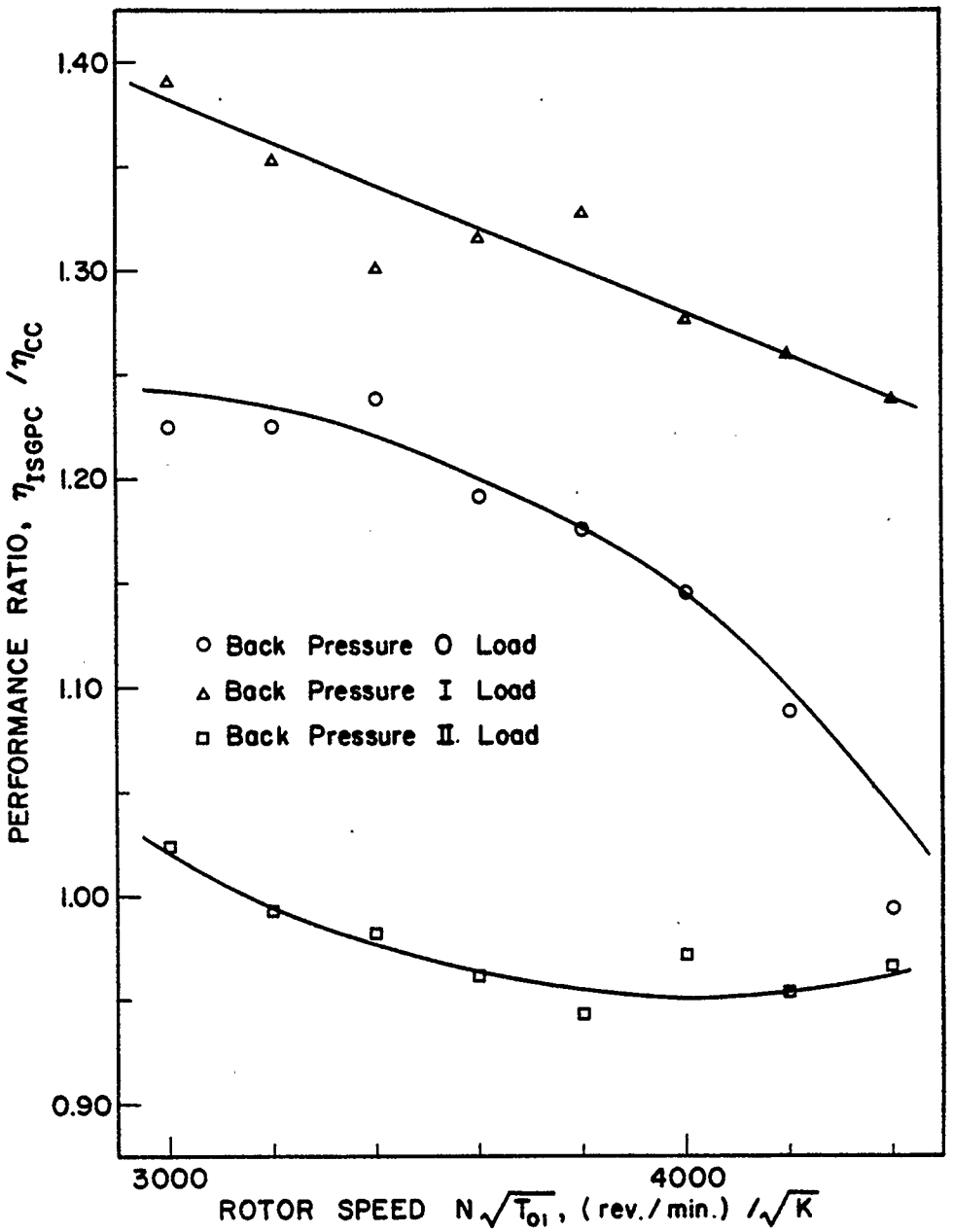

FIGURE 6.29 GAS GENERATOR PERFORMANCE COMPARISON BETWEEN THE CONVENTIONAL COMBUSTOR AND THE INSULATED SECOND GENERATION PULSE COMBUSTOR

GAS GENERATOR ANALYSIS BASED ON "EQUAL TURBINE ROTOR SPEEDS"

TURBINE SPEED	B P LOAD SETTING	AIR FLOW RATIO PC/CC	TURB. INLET TEMP. DIFF. PC-CC K	TURB. INLET TEMP. PC and CC LOAD II, K	FUEL FLOW RATIO PC/CC	EXIT PRES. RATIO PC/CC KPa	EXIT TEMP. RATIO PC/CC	EXIT DELTA PRESSURE RATIO PC/CC	PERFOR. RATIO PC/CC	INCR. IN PERFOR. PC %	BASED ON ESTIMATED TEMPERATURE RATIO EST. EXIT TEMP. RATIO PC/CC	PERFOR. RATIO PC/CC	INCR. IN PERFOR. PC %
3000	0	1.055	-28		1.000	1.002	0.954	1.218	1.225	22.5	0.980	1.258	25.8
	I	1.041	-21		1.000	1.004	0.964	1.393	1.391	39.1	0.980	1.415	41.5
	II	1.029	0	974	1.034	1.003	0.939	1.100	1.025	2.5	1.000	1.091	9.1
3200	0	1.052	-20		1.000	1.002	0.967	1.206	1.225	22.5	0.980	1.241	24.1
	I	1.026	-23		1.000	1.005	0.965	1.373	1.352	35.2	0.980	1.374	37.4
	II	1.025	0	953	1.040	1.003	0.940	1.074	0.993	-0.7	1.000	1.056	5.6
3400	0	1.054	-12		1.000	1.002	0.980	1.201	1.239	23.9	0.980	1.239	23.9
	I	1.020	-21		1.000	1.005	0.968	1.326	1.302	30.2	0.980	1.319	31.9
	II	1.024	0	939	1.048	1.003	0.943	1.069	0.982	-1.8	1.000	1.041	4.1
3600	0	1.038	-7		1.000	1.002	0.985	1.167	1.192	19.2	0.980	1.185	18.5
	I	1.029	-19		1.000	1.006	0.974	1.322	1.317	31.7	0.980	1.325	32.5
	II	1.019	0	934	1.048	1.003	0.939	1.057	0.962	-3.8	1.000	1.025	2.5
3800	0	1.036	0		1.000	1.002	0.988	1.152	1.176	17.6	0.980	1.167	16.7
	I	1.036	-6		1.000	1.007	0.979	1.316	1.327	32.7	0.980	1.328	32.8
	II	1.018	0	936	1.051	1.002	0.941	1.039	0.944	-5.6	1.000	1.003	0.3
4000	0	1.033	0		1.022	1.002	0.992	1.145	1.146	14.6	0.980	1.132	13.2
	I	1.018	5		1.009	1.007	0.987	1.292	1.277	27.7	0.980	1.268	26.8
	II	1.015	0	941	1.051	1.004	0.954	1.058	0.972	-2.8	1.000	1.019	1.9
4200	0	1.029	0		1.033	1.002	0.993	1.102	1.089	8.9	0.980	1.075	7.5
	I	1.018	5		1.029	1.008	0.995	1.291	1.260	26.0	0.980	1.242	24.2
	II	1.013	0	947	1.050	1.002	0.966	1.024	0.953	-4.7	1.000	0.986	-1.4
4400	0	1.030	0		1.033	1.000	0.991	1.007	0.994	-0.6	0.980	0.983	-1.7
	I	1.017	13		1.033	1.008	1.000	1.269	1.239	23.9	0.980	1.215	21.5
	II	1.011	0	954	1.044	1.001	0.983	1.016	0.966	-3.4	1.000	0.983	-1.7

NOTES: PC represents the Insulated Second Generation Pulse Combustor
CC represents the Conventional Combustor

Refer to analysis based on "EQUAL TURBINE INLET TEMPERATURES" for LOAD 0 and LOAD I turbine inlet temperature values.

TABLE 6.1 DATA FOR A GAS GENERATOR PERFORMANCE COMPARISON BETWEEN THE CONVENTIONAL COMBUSTOR AND THE INSULATED SECOND GENERATION PULSE COMBUSTOR, BASED ON "EQUAL TURBINE ROTOR SPEEDS"

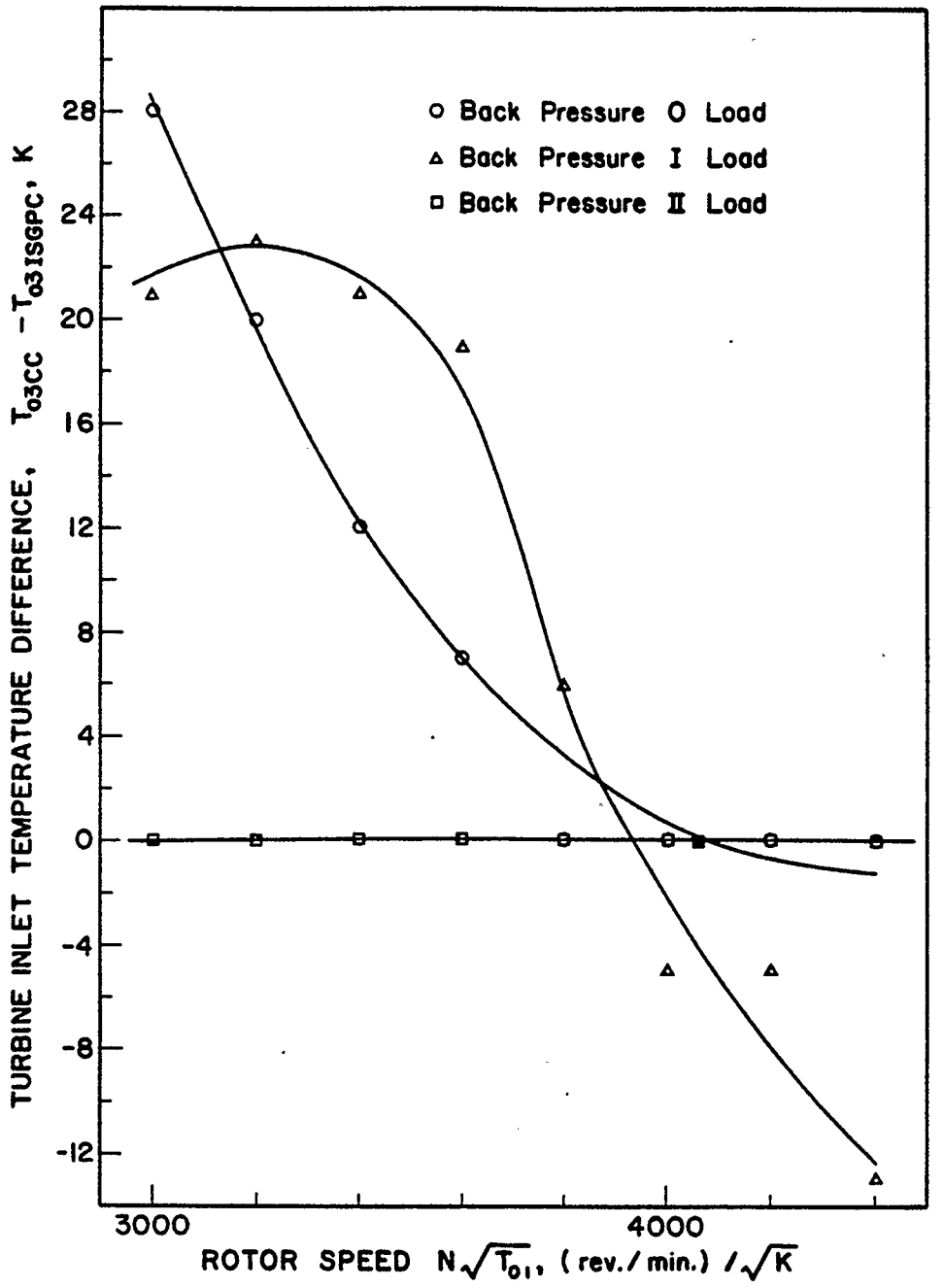

FIGURE 6.30 TURBINE INLET TEMPERATURE COMPARISON BETWEEN THE CONVENTIONAL COMBUSTOR AND THE INSULATED SECOND GENERATION PULSE COMBUSTOR

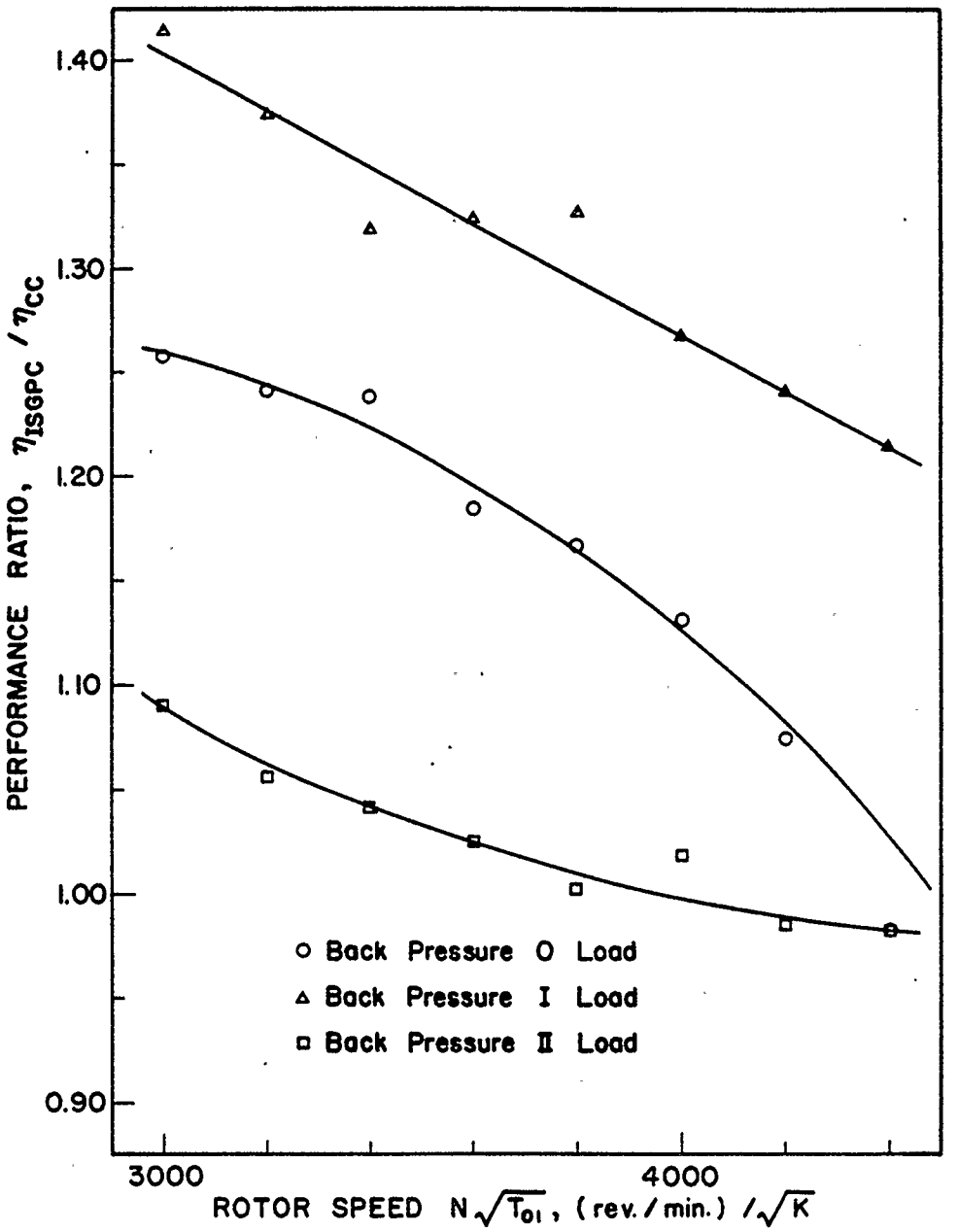

FIGURE 6.31 GAS GENERATOR PERFORMANCE COMPARISON BETWEEN THE CONVENTIONAL COMBUSTOR AND THE INSULATED SECOND GENERATION PULSE COMBUSTOR, BASED ON AN ESTIMATED TURBINE EXIT TEMPERATURE RATIO

GAS GENERATOR ANALYSIS BASED ON 'EQUAL TURBINE INLET TEMPERATURES'

LOAD	TURBINE INLET TEMP, K	TURBINE SPEED PC	TURBINE SPEED CC	AIR FLOW RATIO PC/CC	FUEL FLOW RATIO PC/CC	EXIT PRES. RATIO PC/CC	EXIT DELTA PRESSURE RATIO PC/CC	EXIT TEMP. RATIO PC/CC	PERFOR. RATIO PC/CC	INCR. IN PERFOR. PC, %
0	860	2740	3230	0.836	0.899	0.997	0.896	1.003	0.838	-16.2
	855	2850	3300	0.836	0.908	0.998	0.878	1.001	0.811	-18.9
		4500	4500	1.025	1.038	1.002	1.104	0.991	1.078	7.8
	850	3000	3400	0.884	0.910	0.999	0.898	1.001	0.874	-12.6
		4420	4420	1.026	1.036	1.002	1.116	0.992	1.095	9.5
	845	3120	3500	0.896	0.912	0.999	0.906	0.999	0.890	-11.0
		4300	4300	1.028	1.000	1.001	1.114	0.992	1.135	13.5
	840	3300	3680	0.901	0.900	0.999	0.892	0.995	0.890	-11.0
		4180	4060	1.070	1.071	1.004	1.223	0.995	1.211	21.1
I	890	2820	3060	0.923	0.949	1.001	1.152	0.977	1.095	9.5
	880	2930	3180	0.923	0.950	1.001	1.121	0.980	1.065	6.5
	870	3040	3320	0.916	0.937	1.001	1.068	0.982	1.024	2.4
		4340	4480	0.971	0.987	1.005	1.155	0.992	1.121	12.1
	860	3140	3500	0.886	0.963	1.000	0.980	0.986	0.889	-11.1
		4220	4350	0.976	0.983	1.005	1.184	0.993	1.161	16.1
	855	3200	3670	0.852	0.891	1.000	0.919	0.990	0.870	-13.0
		4160	4250	0.990	0.997	1.006	1.220	0.992	1.195	19.5
	840	3260	4000	0.776	0.820	0.991	0.763	0.993	0.723	-27.7
		4080	4000	1.047	1.050	1.005	1.370	0.991	1.347	34.7

NOTES: For LOAD II the TURBINE INLET TEMPERATURE is approximately equal for both combustors, for a given turbine speed. Refer to the analysis based on 'EQUAL TURBINE ROTOR SPEEDS' for LOAD II case.

PC represents the Insulated Second Generation Pulse Combustor
CC represents the Conventional Combustor

TABLE 6.2 DATA FOR A GAS GENERATOR PERFORMANCE COMPARISON BETWEEN THE CONVENTIONAL COMBUSTOR AND THE INSULATED SECOND GENERATION PULSE COMBUSTOR, BASED ON "EQUAL TURBINE INLET TEMPERATURES"

CHAPTER 7

CONCLUSIONS AND RECOMMENDATIONS

7.1 CONCLUSIONS

The following conclusions concerning the development of Pulse Combustion as applied to a gas turbine can be made:

1. In comparison to the first application of pulse combustion (First Generation Pulse Combustor) to a gas turbine, the second generation system showed improvements in:

   a. **Performance:** Fuel consumption was reduced by approximately 20%. The pressure gain was increased substantially, to over 2% in some cases.

   b. **Reliability:** Design and material changes improved the longevity of high temperature components.

2. Pulse combustion, as applied to a small gas turbine, has been developed to the point where the gas generator performance provided is better than that provided by a conventional combustor over the majority of the operating range.

3. Shortcomings in the present system still exist in the areas of:

   a. **Reliability:** Such problems primarily concern the fuel chamber.

   b. **Performance:** Pressure gain capabilities are still much lower than expected.

   c. **Instrumentation:** Inaccurate temperature measurement

7.2 RECOMMENDATIONS

It is believed that the existing systems should be developed

further by carring out the suggestions summarized under the following headings:

1. **Improve Pressure Gain Performance:** Several so called "fine tuning" changes should be carried out. The secondary flow duct length can be easily changed, as explained in section 6.2.2, for the combustor operated in isolation. Such changes should be made to the combustion system when operated as part of the gas turbine.

The ejector shape should be varied to determine an optimum shape for best performance. This unit can be seen in figure 4.1. It is felt that the ejector inlet opening has a cross sectional area which is too small. On the two ejector surfaces in the plane of the drawing (figure 4.1), relatively high surface temperatures were evident from the darker metal colour in these areas. The ejector opening may be needlessly restricting the flow of gases. A cross sectional shape that is more square or even circular towards the ejector opening may provide better flow characteristics. Larger bellmouth radii shown in the side view (figure 4.3) may provide better performance. Several new ejectors can be easily made and each one simply bolted on and tested as a substitute for the original one.

Test results for the combustion system operated in isolation (section 6.2.3) indicate that the combining chamber significantly effects combustor performance. The evidence displayed in figures 6.8 and 6.9 indicates that combining chamber shape may be a more important factor than volume. Various chambers should be constructed and each tested on the existing system. It should be kept in mind that this is

the highest temperature area of the outside surface. Energy losses to the ambient may also be a factor in chamber design.

2. **Reduce Heat and Flow Losses:** The second generation pulse combustion system has approximately 8 times the outside surface area then the conventional combustor it replaces. The result is inherently greater heat losses. In this study, heat losses were reduced by insulating the outside surface. Insulating the smaller surface area of the secondary flow ducting (figure 4.1) may be more effective.

Outside surface area and overall size can be reduced by shortening the flanged cylindrical attachment which contains the safety bursting disc. Depending on the secondary flow duct length chosen, the overall length can be reduced by 3 to 9 inches, reducing the outside surface area by about 5 to 13%. However, it should be kept in mind that such a change could infuence the operation of the combustor by virtue of decreasing the combustor inlet plenum volume.

There is an abrupt cross sectional change where the combustor inlet pipe and the fuel chamber connect, as seen in figure 2.1. This area is exposed to the secondary flow within the second generation system. Fluid flow losses can be reduced by installing a metal shield, which can be secured to the fuel chamber, that "smooths out" the shape in this area.

3. **Eliminate Fuel Chamber Problems:** Problems associated with the fuel chamber, described in section 5.2.3, are particularly important because of the extensive disassembly required to access this area. Repeated repairs therefore become time consuming, slowing down overall development. Cracking problems may be reduced by the following changes:

The use of a type 310 stainless steel instead of the type 316 stainless steel, used in the present chamber, will likely increase the material durability. The use of several single-hole nozzles, instead of two multiple-hole nozzles, may provide more even cooling of the nozzle area by the fuel.

As outlined in section 5.2.3, there were severe fuel nozzle carbon clogging problems which were especially acute with the second generation system. It is believed that this problem is due to excessive fuel chamber and fuel connection line operating temperatures. To lower these temperatures, both the outside surfaces of the fuel chamber and the connection line could be insulated. It may be possible to incorporate the chamber insulation with the metal shield (used for flow loss reduction) suggested earlier in this section. This may also help to reduce the cracking problems described above.

Before a new fuel chamber is constructed it is suggested that the original one be operated until carbon build up occurs, and then removed and carefully cut open to determine exactly where the carbon is collecting. Such information could possibly indicate what additional design changes should be made to improve this part.

4. **Improve Instrumentation:** It is important in future investigations to better understand how pulse combustion works in comparison to conventional combustion. More accurate performance data is required to understand specific affects. Such information can provide clues to design changes that will improve performance and best utilize the benifits of pulse combustion.

As seen in section 6.3.4, the measurement of gas temperature at

various locations is inaccurate. New temperature measurement equipment and/or techniques should be used that will accurately measure the mass average gas temperature inside a duct. For example, multiple thermocouples or traversing thermocouples can be employed. Such information would allow a more comprehensive comparison to be made between the performance of a conventional combustor and that of a pulse combustor, as applied to a gas turbine cycle. Such information would allow the calculation of turbine efficiency and show how it is affected, in practice, by unsteady flow.

A comprehensive gas turbine exhaust gas analysis should be carried out for both combustor applications. This would provide information for a comparison between the combustor efficiencies.

A more sophisticated method of noise measurement will allow noise spectra to be obtained from the system.

REFERENCES

1. Adams, C.W., "Performance Results of the Lennox Pulse-Combustion Furnace Field Trials", Symposium on Pulse Coombustion Application, Gas Research Institute, Atlanta, Ga., 1982.

2. Atlas Stainless Steels, "Technical Data", Reo Algoma Limited, Ontario, Canada, 1984.

3. Cohen, H., Rogers, C., Saravanamutto, H., "Gas Turbine Theory", Longman Group Limited, London, Second Edition, 1972.

4. Cronje, J.S., "An Experimental and Theoretical Study Including Frictional and Heat Transfer Effects, of Pulse Pressure-Gain Combustion", Ph.D. Thesis, The University of Calgary, Alberta, Canada, 1979.

5. "Design Guidelines for the Selection and use of Stainless Steel" A Designers' Handbook Series, Committee of Stainless Steel Products, American Iron and Steel Institute, Washington D.C., April 1977.

6. Ibrahim, G.M.S., "An Investigation of the Performance of a Carbureted, Liquid Fuelled, Valveless, Pulse Combustor", M.Sc. Thesis, The University of Calgary, Alberta, Canada, 1979.

7. Kentfield, J.A.C., "Thrust Augmenting Fluid Rectifier for a Pulsed Combustor", Canadian Patent No. 1034508, June 1976.

8. Kentfield, J.A.C. and O'Blenes, M., "Methods for Achieving a Combustion-Driven Pressure-Gain in Flow Process: A Review", Presented at the 1986 Spring Technical Meeting for the Combustion Institute in Banff, Alberta - April 27-30, 1986.

9. Kentfield, J.A.C., Rehman, A. and Cronje, J., "The Performance of Pressure-Gain Combustors Without Moving Parts", American Institute of Aeronautics and Astronautics Journal of Energy, Vol. 4, No. 2, March-April 1980, pp. 56-63.

10. Kentfield, J.A.C., Rehman, M. and Marzouk, E.S., "A Simple Pressure-Gain Combustor for Gas Turbines", ASME Journal of Engineering for Power, Vol. 99, No 2, April 1977, pp. 153-158.

11. Kentfield, J.A.C. and Yerneni, P., "Pulsating Combustion Applied to a Small Gas Turbine", The American Society of Mechanical Engineers, New York, Presented at the Gas Turbine Conference and Exhibit Houston, Texas - March 18-21, 1985, ASME Paper 85-GT-52.

12. Lockwood, R.M., "Guidelines for Design of Pulse Combustion Devices, Particularly Valveless Pulse Combustors", Paper No. 14, Proceedings Vol. 1, Symposium on Pulse Combustion Applications, Gas Research Institute, Atlanta, Ga., 1982.

13. Marouk, E.S., "A Theoretical and Experimental Investigation of Pulsed Pressure Gain Combustion", Ph.D. Thesis, The University of Calgary, Calgary, Alberta, Canada, 1974.

14. Olorunmaiye, J.A., "Numerical Simulation and Experimental Studies of Highly-Loaded Valveless Pulsed Combustors", Ph.D thesis, The University of Calgary, Calgary, Alberta, Canada, 1984.

15. Read, M.A., "An Investigation of the Performance of Two Gas Dynamically-Coupled Valveless Pulsed Combustors", M.Sc. Thesis, University of Calgary, Calgary, Alberta, Canada, 1977.

16. Rehman, A., "A Theoretical and Experimental Study of the Affect of Size on Liquid Fuelled Carbureted Valveless Pulsed Combustors", M.Sc. Thesis, The University of Calgary, Calgary, Alberta, Canada, 1978.

17. Rehman, M., "A Study of a Multiple-Inlet Valveless Pulsed-Combustor", Ph.D. Thesis, University of Calgary, Calgary, Alberta, Canada, 1976.

18. Sran, B.S., Kentfield, J.A.C., "Twin Valveless Pulse Combustors Coupled to Operate in Antiphase", Paper No. 3, Proceedings Vol. 1, Symposium on Pulse Combustion Application, Gas Research Institute, Atlanta, Ga., 1982.

19. Yerneni, V.N., "Pulsating Combustion Applied to a Small Gas Turbine", M.Sc. Thesis, The University of Calgary, Calgary, Alberta, Canada, 1984.

APPENDIX

Calibration curves for fuel flow measurements using choked nozzles, figure A.1.

Technical data for stainless steels, tables A.1 and A.2.

Turbine inlet temperature (T_{03}) calculation

Estimated turbine exit temperature ratio ($T_{04,ISGPC}/T_{04,CC}$)

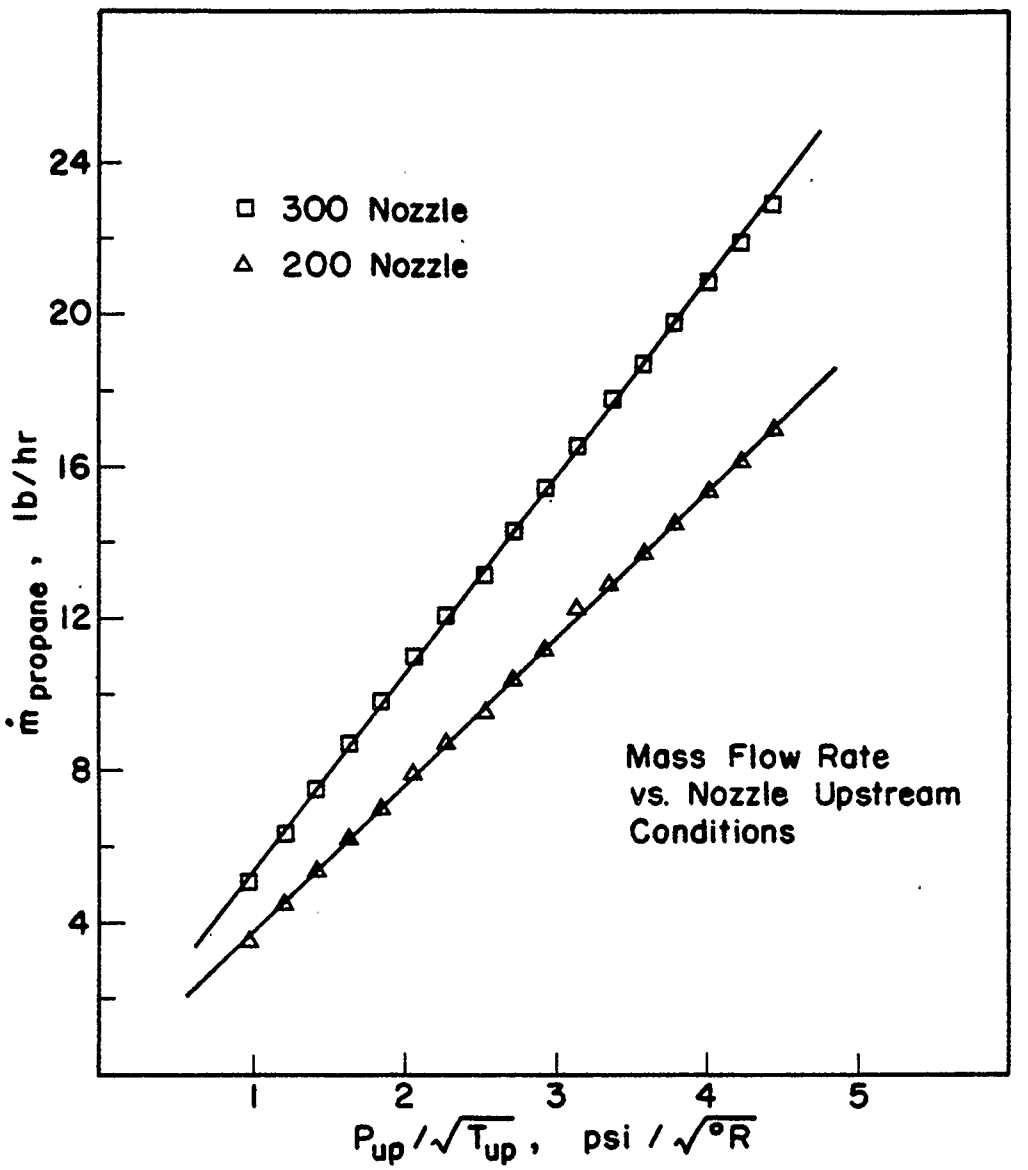

FIGURE A.1 CALIBRATION CURVES FOR CHOKED NOZZLES USED IN FUEL FLOW MEASUREMENTS

Stainless Steel Type (ATLAS)	Yield Strength psi.	Ultimate Strength psi.	Oxidation Resistance At High Temperatures
310	45000	95000	Good in intermittent service to 1900°F and continuous service to 2100°F
316	42000	84000	Good in intermittent service to 1600°F and continuous service to 1700°F

TABLE A.1 PROPERTIES OF STAINLESS STEEL [2]

RUPTURE AND CREEP CHARACTERISTICS OF CHROMIUM-NICKEL STAINLESS STEELS

Type	Testing temperature °F	Testing temperature °C	Stress: Rupture Time: 100 hr ksi	100 hr MPa	1000 hr ksi	1000 hr MPa	10,000 hr ksi	10,000 hr MPa	Stress: Creep Rate: 0.01% hr. ksi	0.01% hr. MPa	Extroplated elogation at rupture in 10,000 hr, %
302	1600	871	4.70	33	2.80	19	1.75	12	2.50	17	150
	1800	982	2.45	17	1.55	11	0.98	7	1.30	9	30
	2000	1093	1.30	9	0.76	5	0.46	3	.62	4	18
309S	1600	871	5.80	40	3.20	22	—	—	3.50	24	—
	1800	982	2.60	18	1.65	11	1.00	7	1.00	7	105
	2000	1093	1.40	10	0.83	6	0.48	3	.76	5	42
310S	1600	871	6.60	45	4.00	28	2.50	17	4.00	28	30
	1800	982	3.20	22	2.10	15	1.35	9	1.75	12	60
	2000	1093	1.50	10	1.10	7	0.76	5	.80	6	60
314	1600	871	4.70	32	3.00	21	1.95	13	2.30	16	110
	1800	982	2.60	18	1.70	12	1.10	8	1.00	7	120
	2000	1093	1.50	10	1.12	7	0.85	6	.90	6	82
316	1600	871	5.00	34	2.70	19	1.40	10	2.60	18	30
	1800	982	2.65	18	1.25	9	0.60	4	1.20	8	35
	2000	1093	1.12	8	0.36	2	—	—	4.00	28	—

TABLE A.2 TEST RESULTS FOR STAINLESS STEEL [5]

TURBINE INLET TEMPERATURE (T_{o3}) CALCULATION

The turbine inlet temperature was calculated using the following energy balance equation:

$$(1-h_1)fQ_{lower}\eta_c = C_p(T_{03}-T_{02})$$

where,

h_1 ≡ Heat losses from the combustor outside surface, % of input energy (estimated using thermocouples)

f ≡ Fuel to air ratio (measured)

Q_{lower} ≡ Lower calorific value of the propane fuel

η_c ≡ Combustor efficiency (≃ energy conversion efficiency)

C_p ≡ Specific heat at constant pressure (depends on temperature)

T_{02} ≡ Combustor inlet temperature (measured)

T_{03} ≡ Turbine inlet temperature

ESTIMATED TURBINE EXIT TEMPERATURE RATIO ($T_{04,ISGPC}/T_{04,CC}$)

The estimation of the turbine exit temperature ratio was carried out using the following expression:

$$\frac{T_{04,ISGPC}}{T_{04,CC}} \simeq \frac{T_{03,ISGPC}}{T_{03,CC}}$$

Where $T_{03,ISGPC}$ and $T_{03,CC}$ are found from the above energy balance.

This estimation is based on the assumption that the power required to operate the compressor will be the same for the gas turbine employed with either the conventional combustor or the insulated second generation pulse combustor. This applies for a given turbine rotor speed and back pressure load setting.

It should be kept in mind that this is simply an estimation and significantly affects only the data reported for the back pressure load setting II (compare figures 6.29 and 6.31; the data are shown in table 6.1)